

Für Hans & Karin



# **The role of ephrinB signaling during synaptic plasticity**

**Dissertation der Fakultät für Biologie  
der Ludwig-Maximilians-Universität München**

**Angefertigt am Max-Planck-Institut für Neurobiologie, Martinsried  
in der Arbeitsgruppe „Signal Transduction“**

**Clara Luise Essmann  
aus Freiburg i. Br.**

**München \* 16. Dezember 2008**

1. Gutachter: Prof. Dr. Rüdiger Klein
2. Gutachter: Prof. Harry MacWilliams

Tag der mündlichen Prüfung: 16. Juli 2009

The work presented in this thesis was performed in the laboratory of Dr. Amparo Acker-Palmer, Junior Group – Signal transduction, at the Max-Planck-Institute of Neurobiology, Martinsried, Germany.

## Erklärung

Ich versichere hiermit, dass ich die vorgelegte Dissertation „The role of ephrinB signaling during synaptic plasticity“ selbständig und ohne unerlaubte Hilfe angefertigt habe. Ich habe mich dabei keiner anderen als der von mir ausdrücklich bezeichneten Hilfen und Quellen bedient.

Hiermit erkläre ich, dass ich mich nicht anderweitig einer Doktorprüfung ohne Erfolg unterzogen habe. Die Dissertation wurde in ihrer jetzigen oder ähnlichen Form bei keiner anderen Hochschule eingereicht und hat noch keinen sonstigen Prüfungszwecken gedient.

München, den .....

.....

(Unterschrift)



# Table of Contents

<b>1</b>	<b>Publications .....</b>	<b>9</b>
<b>2</b>	<b>Abbreviations.....</b>	<b>11</b>
<b>3</b>	<b>Summary .....</b>	<b>15</b>
<b>4</b>	<b>Introduction .....</b>	<b>17</b>
4.1	<b>Synaptogenesis .....</b>	<b>17</b>
4.2	<b>Postsynaptic density.....</b>	<b>20</b>
4.3	<b>Dendritic spines .....</b>	<b>22</b>
4.4	<b>From filopodia to spines.....</b>	<b>23</b>
4.5	<b>Synaptic plasticity .....</b>	<b>26</b>
4.5.1	LTP and LTD .....	27
4.6	<b>AMPA receptors .....</b>	<b>30</b>
4.6.1	AMPA-receptor trafficking .....	32
4.7	<b>PDZ-proteins.....</b>	<b>35</b>
4.7.1	Glutamate receptor interacting protein (GRIP) .....	37
4.8	<b>The Eph receptors and ephrin ligands.....</b>	<b>39</b>
4.8.1	Classification and structure .....	40
4.8.2	Eph/ephrin interaction .....	46
4.8.3	Eph/ephrin signaling outside the nervous system .....	50
4.8.4	Eph/ephrin signaling in the nervous system.....	50
<b>5</b>	<b>Results.....</b>	<b>55</b>
5.1	<b>Grb4 and GIT1 transduce ephrinB reverse signals modulating spine morphogenesis and synapse formation.....</b>	<b>55</b>
5.1.1	EphrinB-reverse signaling promotes spine morphogenesis .....	55
5.1.2	Interference with ephrinB-reverse signaling impairs spine formation .....	57
5.1.3	Spine morphogenesis downstream of ephrinB mediated via Grb4 and GIT1 .....	62
5.2	<b>Serine phosphorylation of ephrinB2 regulates trafficking of synaptic AMPA receptors .....</b>	<b>68</b>
5.2.1	EphrinB2 reverse signaling regulates AMPA-receptor trafficking .....	68
5.2.2	Lack of ephrinB2 leads to enhanced AMPA-receptor internalization and reduced synaptic transmission .....	73
5.2.3	GRIP molecules link ephrinB ligands to AMPA receptors .....	78
5.2.4	GRIP molecules are required for ephrinB ligand-mediated AMPA-receptor stabilization....	80
5.2.5	GRIP binding to ephrinB ligands is regulated by activation through EphB receptors .....	85
5.2.6	Serine phosphorylation in ephrinB ligands regulates PDZ-interactions.....	86
5.2.7	Serine phosphorylation of ephrinB ligands regulates AMPA-receptor internalization .....	90

---

<b>6</b>	<b>Discussion .....</b>	<b>95</b>
<b>6.1</b>	<b>Grb4 and GIT1 transduce ephrinB reverse signals modulating spine morphogenesis and synapse formation.....</b>	<b>95</b>
6.1.1	EphrinB ligands induce spine morphogenesis .....	95
6.1.2	Grb4 and GIT1 transduce ephrinB reverse signals .....	98
<b>6.2</b>	<b>Serine phosphorylation of ephrinB2 regulates trafficking of synaptic AMPA receptors .....</b>	<b>100</b>
6.2.1	GRIP as the bridging molecule.....	103
6.2.2	PICK1 as a ephrin-AMPA receptor linker .....	105
6.2.3	GRIP binding to ephrinB regulated via serine phosphorylation .....	106
6.2.4	Serine phosphorylation of ephrinB ligands .....	107
6.2.5	How does ephrinB2 exert its function during synaptic plasticity? .....	108
6.2.6	Concluding remarks .....	109
<b>7</b>	<b>Material and methods.....</b>	<b>111</b>
<b>7.1</b>	<b>Material .....</b>	<b>111</b>
7.1.1	Chemicals, Reagents, Commercial Kits & Enzymes .....	111
7.1.2	Antibodies .....	113
7.1.3	Consumable Material .....	115
7.1.4	Equipment .....	116
7.1.5	Oligonucleotides .....	119
7.1.6	Plasmids .....	121
7.1.7	Cell lines and bacteria .....	123
7.1.8	Primary cells and tissue.....	123
7.1.9	Media and standard solutions.....	124
7.1.10	Solutions and buffers for Western Blot analysis.....	131
<b>7.2</b>	<b>Methods.....</b>	<b>135</b>
7.2.1	Molecular Biology .....	135
7.2.2	Cell culture .....	140
7.2.3	Biochemistry .....	143
7.2.4	Postsynaptic density fractionation .....	149
7.2.5	Tandem affinity purification (TAP) and mass spectrometry .....	149
7.2.6	Electrophysiology-patch-clamp recordings .....	149
7.2.7	Data analysis .....	150
<b>8</b>	<b>Acknowledgements .....</b>	<b>153</b>
<b>9</b>	<b>Curriculum Vitae .....</b>	<b>155</b>
<b>10</b>	<b>Bibliography .....</b>	<b>157</b>

# 1 Publications

Publications from the work presented in this thesis

Inmaculada Segura\*, Clara L. Essmann\*, Stefan Weinges\* and Amparo Acker-Palmer

"Grb4 and GIT1 transduce ephrinB reverse signals modulating spine morphogenesis and synapse formation."

Nat Neurosci **10** (3): 301-10 (2007)

\* equal contribution

Clara L. Essmann, Elsa Martinez, Julia C. Geiger, Manuel Zimmer, Matthias H. Traut, Valentin Stein, Rüdiger Klein and Amparo Acker-Palmer

"Serine phosphorylation of ephrinB2 regulates trafficking of synaptic AMPA receptor."

Nat Neurosci **11** (9): 1035-43 (2008)



## 2 Abbreviations

<b>(m)EPSP</b>	(miniature) Excitatory postsynaptic potential
<b>°C</b>	Degree Celsius
<b>μ</b>	Micro
<b>A</b>	Alanin
<b>ABP</b>	AMPA receptor binding protein
<b>ACSF</b>	Artificial cerebrospinal fluid
<b>ADAM</b>	A-Disintegrin-And-Metalloprotease
<b>Amp</b>	Ampicillin
<b>AMPA</b>	(S)- $\alpha$ -Amino-3-hydroxy-5-methylisoxazole-4-propionic acid
<b>AP</b>	Alkaline phosphatase
<b>ATP</b>	Adenosine-5'-triphosphate
<b>BAR domain</b>	Bin/amphiphysin/Rvs domain
<b>bp</b>	Base pairs
<b>BSA</b>	Bovine serum albumin
<b>Ca</b>	Calcium
<b>CA1 / CA3</b>	Cornu ammonis; literally 'Amun's horns'
<b>CAM</b>	Cell adhesion molecule
<b>CaMKII</b>	Ca <sup>2+</sup> /calmodulin-dependent kinase
<b>Cdc42</b>	Cell division cycle 42
<b>cDNA</b>	Complementary DNA
<b>CFP</b>	Cyan fluorescent protein
<b>CMV</b>	Cytomegalovirus
<b>CNQX</b>	6-Cyano-7-nitroquinoxaline-2,3-dione
<b>CNS</b>	Central nervous system
<b>C-terminus</b>	Carboxy terminus
<b>DG</b>	Dentate gyrus
<b>DIV</b>	<i>Days in vitro</i>
<b>DMEM</b>	Dulbecco's modified Eagle's medium
<b>DNA</b>	Desoxyribonucleic acid
<b>E</b>	Embryonic day
<b>E</b>	Glutamic acid

---

<b>eB2KO</b>	ephrinB2 knockout
<b>ECL</b>	Enhanced chemiluminescence
<b>EDTA</b>	Ethylenediamine-tetra acetic acid
<b>Eph</b>	Erythropoietin-producing hepatocellular
<b>Ephexin</b>	Eph-interacting exchange protein
<b>ephrin</b>	Eph receptor interacting
<b>F</b>	Phenylalanine
<b>FAK</b>	Focal adhesion kinase
<b>FBS</b>	Fetal bovine serum
<b>Fc</b>	Fragment crystallizable, constant part of the antibody
<b>GEF</b>	Guanine nucleotide exchange factor
<b>GFP</b>	Green fluorescent protein
<b>GIT1</b>	G-protein coupled receptor kinase-interacting protein 1
<b>GluR1-4</b>	Glutamate receptor subunit
<b>GPI</b>	Glycosylphosphatidylinositol
<b>Grb4</b>	Growth-factor-receptor-bound protein 4
<b>GRIP</b>	Glutamate receptor interacting protein
<b>GTP, GDP</b>	Guanosine triphosphate; guanosine diphosphate
<b>GTPase</b>	Enzyme that hydrolyses GTP
<b>HBSS</b>	Hank's balanced salt solution
<b>HEK</b>	Human embryonic kidney
<b>HeLa</b>	Henrietta Lacks
<b>Hepes</b>	(hydroxyethyl)-piperanzine-ethane sulfonic acid
<b>HRP</b>	Horse reddish peroxidase
<b>HS</b>	Horse serum
<b>IF</b>	Immunofluorescence
<b>Ig</b>	Immunoglobulin
<b>IP</b>	Immunoprecipitation
<b>JNK</b>	c-Jun N-terminal kinases
<b>Kan</b>	Kanamycin monosulfate
<b>kb</b>	kilo base
<b>kD</b>	kilo Dalton
<b>l</b>	Liter

<b>LB</b>	Luria-bertani
<b>LTD</b>	Long-term-depression
<b>LTP</b>	Long-term-potential
<b>M</b>	Molar
<b>m</b>	Milli
<b>MAGUK</b>	Membrane associated guanylate kinase
<b>min</b>	minute
<b>MLC</b>	Myosin II regulatory light chain
<b>n</b>	Nano
<b>NMDA</b>	N-Methyl-D-Aspartic acid
<b>NR</b>	NMDA receptor subunit
<b>NSF</b>	N-ethylmaleimide sensitive factor
<b>N-terminus</b>	Amino terminus
<b>o/n</b>	over night
<b>P</b>	Postnatal day
<b>PAK</b>	p-21 activated kinase
<b>PBS</b>	Phosphate buffered saline
<b>PCR</b>	Polymerase chain reaction
<b>PDZ</b>	Postsynaptic density 95; drosophila Disc large; Zonula occludens-1
<b>PFA</b>	Paraformaldehyde
<b>pH</b>	<i>potentia hydrogenii</i>
<b>PI3K</b>	Phosphatidylinositol-3 kinase
<b>PICK1</b>	Protein interacting with PKC
<b>PKC</b>	Protein kinase C
<b>PSD-95</b>	Post synaptic density protein
<b>Q</b>	Glutamine
<b>R</b>	Arginine
<b>RBD/LBD</b>	Receptor/ligand binding domain
<b>RGS</b>	Regulator of heterotrimeric G protein signaling
<b>RNA</b>	Ribonucleic acid
<b>rpm</b>	Round per minute
<b>RT</b>	Room temperature
<b>RTK</b>	Receptor tyrosine kinase

<b>S</b>	Serine
<b>SAM</b>	Sterile- $\alpha$ -motif
<b>SAP97</b>	Synapse associated protein 97
<b>SDS</b>	Sodium dodecyl sulfate
<b>sec</b>	second
<b>SEM</b>	Standard error of means
<b>ser</b>	Serine
<b>SFK</b>	Src family kinases
<b>SH2/3</b>	Src homology domain 2/3
<b>SLD</b>	Synaptic localization domain
<b>TARP</b>	Transmembrane AMPA receptor regulatory protein
<b>TBS</b>	Tris buffered saline
<b>WB</b>	Western blot
<b>WT</b>	Wild type
<b>Y</b>	Tyrosine
<b><math>\beta</math>PIX</b>	p-21-activated kinase interacting exchange factor

### 3 Summary

The Eph receptors comprise the largest class of receptor tyrosine kinases (RTK) in the human genome. Their ligands, the ephrins, are membrane bound molecules, and communication via ephrins and Eph receptors occurs directly from cell to cell at short range. A second feature that distinguishes the Eph/ephrin system from other RTK families is that the ligands themselves possess a signaling capability known as 'reverse signaling'. Eph receptors and ephrins are found in many cell types, and are involved in a variety of cellular processes, both during development and in the adult organism, including cell migration, axon guidance, segmental patterning, angiogenesis and tumorigenesis. In particular, Eph/ephrins play a role in synaptic plasticity, the focus of this thesis.

Synaptic plasticity is associated with morphological changes to synaptic spines, such as new spine formation, spine remodelling and synaptogenesis at the spine heads. In the first part of this study we analyzed these processes in cultured hippocampal neurons and found that they specifically require reverse signaling by ephrinB ligands. Thus stimulation of these neurons with soluble receptors, namely EphB/Fc fusion proteins, led to increased spine maturation. Furthermore, the over-expression of a dominant negative ephrinB molecule (eB $\Delta$ C), which is able to activate Eph-receptor forward signaling but unable to transduce reverse signaling, did not stimulate, but rather impaired spine formation. Spine morphogenesis requires the local activation of cytoskeleton-remodelling pathways, which are typically under the control of rho-family GTPases such as Rac. In hippocampal neurons, we showed that receptor-activated ephrinBs interact with Grb4, a Src homology domain type 2 and 3 (SH2, SH3) containing adaptor protein, which in turn binds and recruits GIT1 together with the Rac activation complex. This mechanism downstream of ephrinB activation leads to local Rac activity at the spines. Treatments which interfere with the binding of Grb4 to ephrinB, or the binding of GIT1 to Grb4 severely impaired spine morphogenesis.

Aside from changes at the morphological level, synaptic plasticity is achieved by the modulation of the synaptic transmission property referred to as 'synaptic strength'.

Synaptic strength can be manipulated experimentally by specific stimulation patterns, producing either long-term-potential (LTP) or long-term-depression (LTD), changes which are thought to be the basis for information storage, learning and memory. Previous studies had shown that the ablation of ephrinB2 or ephrinB3 in the nervous system leads to severe defects in hippocampal LTP and LTD, and we decided, in the second part of this thesis, to investigate the molecular mechanisms underlying the plasticity defects observed in ephrinB knockouts. Since the amount of active AMPA receptors at the synapse determines its transmission properties, a process affecting synaptic strength is the regulation of AMPA-receptor trafficking. We found that ephrinB2 ligands play an important role in the stabilization of AMPA receptors at the cellular membrane. Thus treating cultured hippocampal neurons with AMPA resulted in a robust AMPA-receptor internalization, which could be inhibited by simultaneous ephrinB2 activation with soluble EphB4/Fc fusion proteins. The ablation of ephrinB2 in hippocampal neurons (conditional ephrinB2 knockout) resulted in an enhanced constitutive internalization of AMPA receptors and reduced synaptic transmission. Interaction and interference experiments revealed that ephrinB ligands and AMPA receptors are bridged by GRIP proteins. This interaction is regulated by the phosphorylation of a single serine residue in the cytoplasmic tails of ephrinB ligands, a previously undescribed feature of ephrinB-reverse signaling.

In summary, we have shown that reverse signaling by ephrinB ligands impacts and presumably coordinates diverse aspects of synaptic plasticity, ranging from the stabilization of individual AMPA receptors to the initiation of gross morphological changes. The reverse signaling pathway appears to play a fundamental role in coordinating the events of synaptogenesis.

## 4 Introduction

The human brain is a highly complex organ composed of millions of neurons and supporting cells. To understand brain function one must appreciate the diversity of cell types, their connecting networks and the physiological role of the brain's specified circuits. The brain performs many different tasks at the same time, each mediated through the interplay between individual units of the network. Cerebral functions, whether involving sensory reception, processing and storage of information and all consequent actions, is based on electrical and chemical signals transferred from cell to cell. This signal transfer between neurons is localized to specialized contact sites, namely synapses. Even after embryonic development, these contacts remain dynamic; new connections are formed while others are removed, allowing the system to change dynamically and thus providing the basis of learning and memory.

The aim of thesis is to elucidate the molecular basis of synaptic plasticity while focussing on the impact of a particular receptor-ligand system: the Eph receptors and ephrin ligands.

### 4.1 Synaptogenesis

Synaptogenesis is a complex process in which specialized sites of communication between neurons, so called functional synapses, are formed. The formation of synapses in vertebrates occurs over a prolonged developmental period. Synaptogenesis begins in the embryo and continues into early postnatal life, but also occurs in the adult organism, where it is thought to contribute significantly to memory formation and learning. During development, synapse formation is coupled to neuronal differentiation and the establishment of neuronal circuits. Correct connections have to be formed, often initially transient, between the presynaptic axon and postsynaptic dendrites. The process of synaptogenesis involves multiple molecules that influence not only the timing and location of synapse formation, but also determine the specificity and stability of the contact. Some of these molecules are soluble and act at a distance, guiding axons to their correct

receptive fields, while also promoting neuronal differentiation and maturation. Well studied secreted molecules are, for example, from the families of Wnt (combination of wingless and Int), FGF (fibroblast growth factor) and neurotrophins. Others are cell bound (cell adhesion molecules: CAMs) and act upon cell-to-cell contact. CAMs provide positioning information, verify correct targets and initiate signal cascades to induce synapse formation, including the assembly of pre- and postsynaptic specializations (Figure 4-1). Cadherins, Protocadherins, SynCAM, Neuroligin-Neurexin and Eph-ephrins are known examples. In addition, synaptic activity is one of the crucial factors deciding on the appropriateness of a synaptic contact and its consequent stabilization or removal. Even though activity is not essential for synaptogenesis in the developing organism (Verhage et al., 2000), it regulates the elimination and stability of synapses during both development and adulthood.

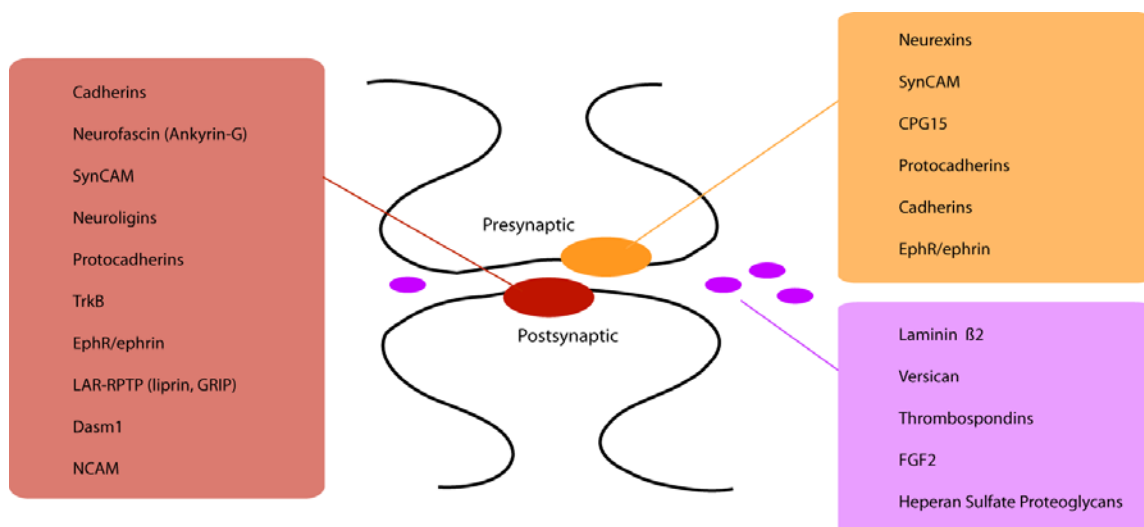


**Figure 4-1: Molecules involved in vertebrate synapse formation** (Akins and Biederer, 2006). Characterized proteins include presynaptic (orange), postsynaptic (red) and secreted or extracellular matrix proteins (purple).

In vertebrates, most of the synapses are chemical synapses transducing electrical signals from the axon into chemical signals in forms of neurotransmitters which are released from vesicles at the presynaptic terminal. Neurotransmitters diffuse through the synaptic cleft

activating neurotransmitter-gated ion-channels situated at the postsynaptic site and converting the chemical signal back into an electrical impulse. Two categories of synapses are found in the nervous system, namely inhibitory and excitatory synapses. They are so called due to their effect on the membrane potential of the postsynaptic target and differ significantly with regard to their structure and molecular organization. For example, inhibitory synapses are localized directly at dendritic shafts whereas the postsynaptic site of an excitatory synapse is more commonly situated on a short dendritic protrusion named a spine.

The focus of this thesis is put on glutamatergic synapses, the main type of excitatory synapse in the mammalian brain. Glutamatergic synapses use glutamate as a neurotransmitter which acts on AMPA- and NMDA-type ( $\text{Ca}^{2+}$ -channel) glutamate receptors expressed at the postsynaptic target site.

The functional properties of a synapse change when the organism develops due to presynaptic and postsynaptic modifications. The probability of transmitter release decreases and a larger number of transmitter-filled vesicles accumulate at the presynaptic terminal. The kinetics of the synaptic response change with the type of neurotransmitter receptor expressed at the postsynaptic site and its subunit composition, which is different in young premature synapses, compared those which are stabilized and mature. During development, most synapses are initially void of AMPA receptors but possess functional NMDA receptors. The early activity of the latter is important for the formation of the developing contact. Once the synaptic contact is established, NMDA-receptor activity can induce the insertion of AMPA receptors leading to fully functional synapses (Constantine-Paton and Cline, 1998). Moreover, even later on in the mature organism, synapses are found in different regions of the brain that still express only functional NMDA but lack AMPA receptors at the synaptic surface. These synapses are referred to as ‘silent synapses’ because, at normal resting membrane potentials, they remain functionally silent with no measurable current flow. Similarly, these synapses can be ‘unsilenced’ by NMDA-receptor activity that induces the recruitment of AMPA receptors to the postsynaptic site. The observations, that activity induces the delivery and insertion of AMPA receptors, led

to the idea that AMPA-receptor trafficking might be one of the key mechanisms of synaptic plasticity. Soon after, it was reported that additional AMPA receptors are indeed inserted to the synapse to increase synaptic transmission during some forms of plasticity, termed as long-term-potential (LTP). As mentioned before, different receptor subunits can influence synaptic properties because they differ in ligand-sensitivity, conductance and in their interaction with intracellular molecules. For example, the subunit composition of NMDA receptors changes during development. NMDA receptors consist of at least one NR1 subunit and different types of NR2 (NR2A-D) subunits. Initially, in the developing brain, the NR2B and NR2D subunits are the most prominent but are partially replaced by NR2A subunits when the organism matures (Monyer et al., 1994). Later on, the subunit composition determines the localization of NMDA receptors in mature synapses: NR2A-containing NMDA receptors are concentrated at synaptic sites whereas NR2B-containing receptors localize at both synaptic and extrasynaptic sites (Thomas et al., 2006). Furthermore, as expected, the subunit composition of synaptic AMPA receptors changes during maturation and activity, as will be described more in detail in a later section.

## 4.2 Postsynaptic density

The microanatomy of a glutamatergic synapse clearly defines pre- and postsynaptic structures that are visible in the electron microscope. The presynaptic structure includes an accumulation of synaptic vesicles and a thickened plasma membrane, the so called 'active zone', to which some of the synaptic vesicles are attached preceding exocytosis. The postsynaptic site is separated from the active zone via a gap of 20-25 nm (Lucic et al., 2005) known as the synaptic cleft, and is easily identified by an electron dense thickening of the postsynaptic membrane, a structure known as PSD (postsynaptic density). The thickening arises from an enormous accumulation of membrane associated molecules, such as glutamate receptors, receptor-tyrosine kinases, G-protein-coupled receptors, ion-channels and adhesion molecules, but also from cytoplasmic scaffolding proteins, downstream signaling units and cytoskeletal elements (Figure 4-2).

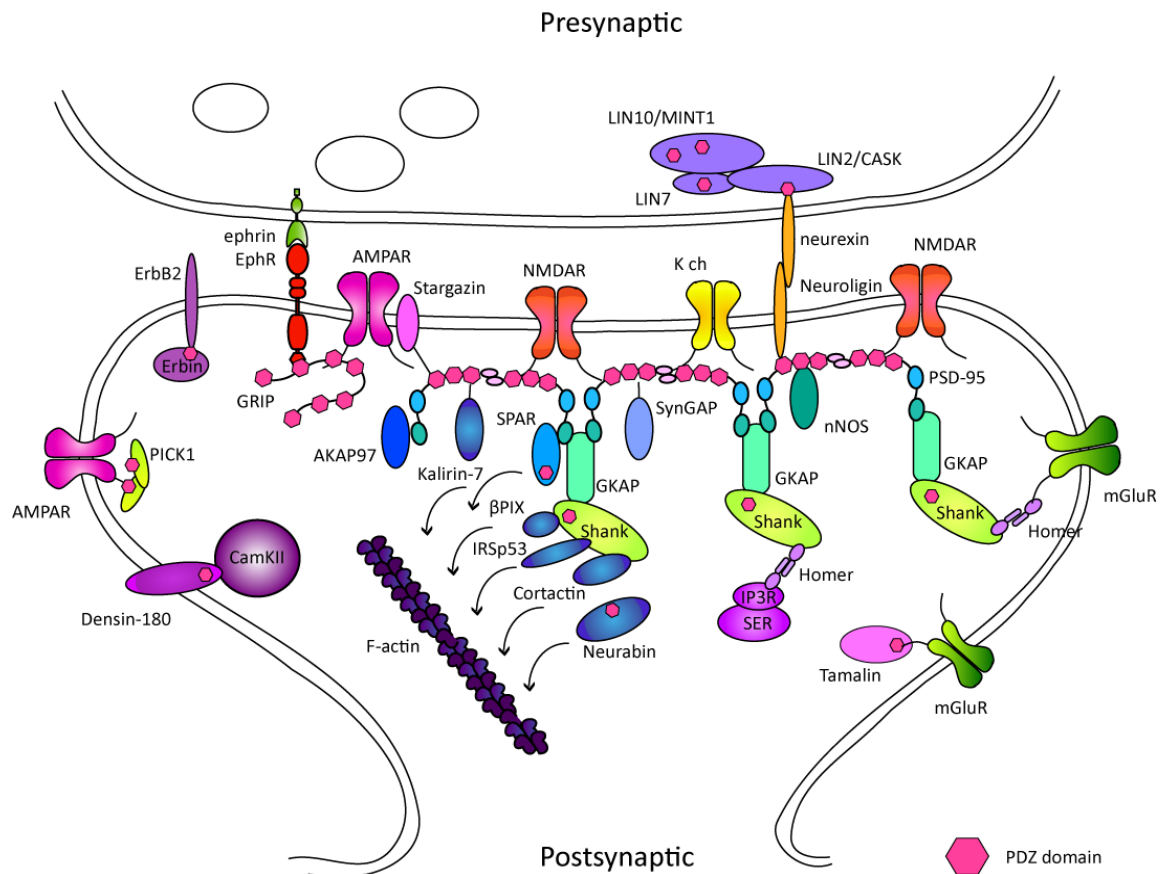


**Figure 4-2 Scheme of a glutamergic synapse** (Kim and Sheng, 2004). Only a subset of known protein interactions is illustrated with special focus on PDZ-proteins that are highly enriched in synapses. Although not shown, LIN2, LIN7 and LIN10 are also present postsynaptically, and many of the proteins of the postsynaptic domain are also present in the presynaptic terminal. Abbreviations: AKAP79 - A-kinase anchor protein 79; AMPAR - AMPA ( $\alpha$ -amino-3-hydroxy-5-methyl-4-isoxazole propionic acid) receptor;  $\beta$ PIX - PAAK-interactive exchange factor; CaMKII $\alpha$  -  $\alpha$ -subunit of Ca<sup>2+</sup>/calmodulin-dependent protein kinase II; GK, guanylate kinase-like domain; EphR, ephrin receptor; ErbB2, EGF-related peptide receptor; GKAP - guanylate kinase-associated protein; GRIP - glutamate-receptor-interacting protein; IP3R - IP3 receptor; IRSp53 - insulin-receptor substrate p53; K ch - potassium channel; LIN7 - lin7 homologue; LIN10 - lin10 homologue; mGluR - metabotropic glutamate receptor; NMDAR - NMDA (N-methyl-D-aspartate) receptor; nNOS - neuronal nitric oxide synthase; PICK1 - protein interacting with C kinase 1; PSD-95 - postsynaptic density protein 95; SER - smooth endoplasmic reticulum; SH3 - Src homology 3 domain; Shank - SH3 and ankyrin repeat-containing protein; SPAR - spine-associated RapGAP; SynGAP - synaptic Ras GTPase-activating protein.

One highly enriched scaffolding molecule is PSD-95 (Post Synaptic Density 95), which is widely used as marker for postsynaptic structures. The PSD is situated at the very tip of a dendritic spine, connected to the rest of the dendrite solely via a small thin shaft. Thus,

it occupies its own separated, and highly specialized, biochemical compartment. Sometimes even given the status of an organelle, the PSD controls the number and composition of neurotransmitter receptors and thus regulates synaptic strength and the kinetics of the synaptic response.

### 4.3 Dendritic spines

Santiago Ramón y Cajal (19<sup>th</sup> century) was the first to describe spines as small protrusions emerging from branched projections of a neuron, namely dendrites, and suggested that these are in fact contact sites between neurons (Figure 4-3)

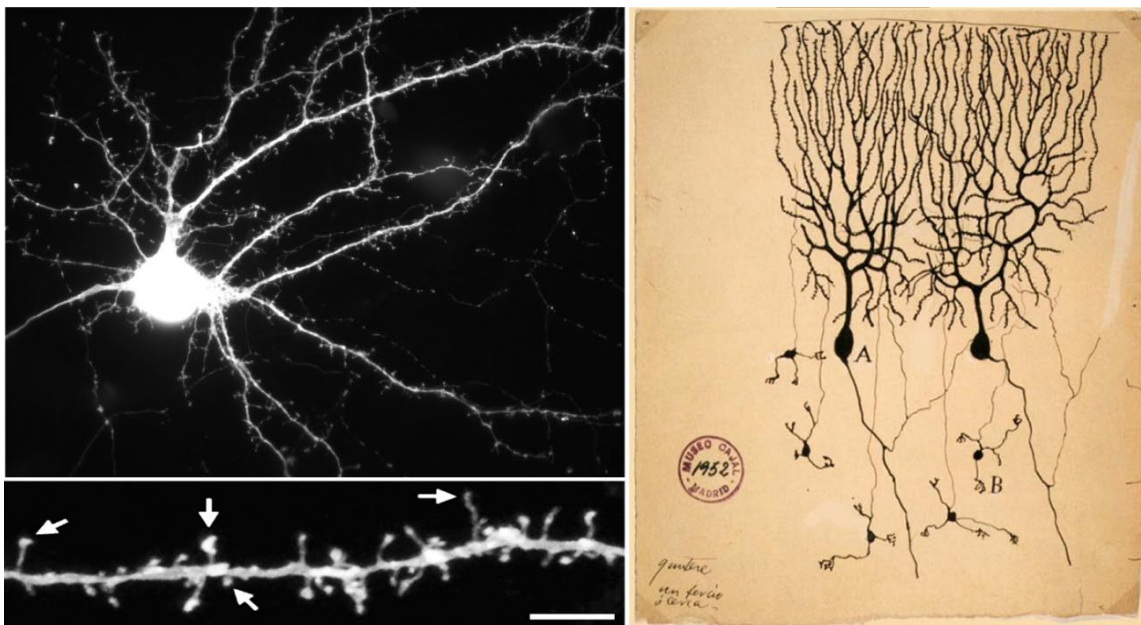


**Figure 4-3: Dendritic spines.** (a) After 14 days in culture an YFP-labeled hippocampal neuron shows a highly developed dendritic tree covered with spines of various shape and size (large picture). The enlargement of a dendrite (Harms and Dunaevsky, 2007) highlights the shape variations of spines from stubby spines, long and thin spines, to mushroom spines with defined spine heads (scale bar 5 $\mu$ m). (b) Drawing from the 20th century by Santiago Ramón y Cajal of neurons in the pigeon cerebellum. Denoted are purkinje cells (A) as an example of a bipolar neuron with small dendritic protrusions, the spines, distributed all over the dendritic tree and granule cells (B) which are multipolar.

Today dendritic spines are defined as small structures (<2  $\mu$ m) emerging from the dendrite via a thin neck, or shaft, ending in a bulbous enlargement, the spine head, which

serves as the site of synaptic contact. Spines occur in various shapes and sizes and are described being thin, stubby, cup-, or mushroom-shaped (Lippman and Dunaevsky, 2005) (Figure 4-3).

Although the shape and size of spines might be correlated to their function (Tsay and Yuste, 2004), shape descriptions are only regarded as attempts to categorize spines based on snap-shots. In actual fact, dendritic spines are dynamic structures able to change their size, form and appearance within a short time range (Parnass et al., 2000). Indeed, while looking at spine turnover rates in the cortex of adult mice, Trachtenberg et al. (2002) found that only 50 % of the spines were stable for more than 1 month (somatosensory cortex) whereas others were added, or eliminated, within hours or days. Even though peers in the field failed to agree on the proportion of stable spines, they supported the findings that some spines were stable while others were short-lived (Grutzendler et al., 2002). However, the concrete number of stable spines might be highly dependent on the cortical region and experimental procedures. Of importance is the general tendency of all the above findings, that large spines with thick ‘mushroom-shaped’ heads seem to be more stable than thinner spines, or even filopodia, and that the turnover rate of spines declines with age (Grutzendler et al., 2002; Trachtenberg et al., 2002; Zuo et al., 2005). Once the mature brain has established its neuronal circuits, the elimination rate of spines decreases and, consequently, more spines become stable over a longer time-period.

### 4.4 From filopodia to spines

By definition, filopodia are thin, long ( $>2 \mu\text{m}$ ), highly motile dendritic protrusions with short life spans. In general, young neurons possess more filopodia-like protrusions whereas older cells are more abundant in mature dendritic spines (Dailey and Smith, 1996). Put into numbers, the proportion of filopodia-like protrusions declines from 60 % in two-week-old mice to less than 2 % in 4-5 month old animals (Grutzendler et al., 2002; Zuo et al., 2005). These filopodia-like protrusions are not simply lost in older animals but have, most likely, transformed into thin or mushroom-like spines (Majewska et al., 2006). It is noteworthy, that only a small percentage of these short-lived

protrusions actually transform into spines ( $<2 \mu\text{m}$ ), while the vast majority disappear within two days of formation (Zuo et al., 2005). However, not every spine seems to arise from a filopodia-like transition stage. Other studies have confirmed the direct emergence of spines from the dendrite without a filopodia-like precursor (Engert and Bonhoeffer, 1999). *In vivo* live-imaging studies have shown that most excitatory synapses form on dendritic filopodia, transforming them into spines while the synaptic contacts are stabilized. Hence, filopodia formation and spine motility have been implied as important processes during synaptogenesis (Fiala et al., 1998; Ziv and Smith, 1996). However, – whether derived from filopodia-like precursors or directly from the dendrite – when newly developed protrusions become more stable, their volume increases and synapses form (Knott et al., 2006). The volume increase is mainly governed by an enlargement of the spine head which can then accommodate enlarged postsynaptic structures (Holtmaat et al., 2006). The PSD becomes larger and possess more AMPA receptors and signaling molecules. Thus a direct correlation can be drawn between the size of a synaptic contact and its strength.

Both the formation of spines and the subsequent morphological changes during synapse-establishment involve actin-based cytoskeleton rearrangements. A huge variety of molecules have been implicated in the regulation of these rearrangements, including different PSD-proteins and cell adhesion molecules. Among these are the Eph receptors and their ephrin ligands which have been shown to control actin-binding proteins or calcium-dependent signaling mechanisms as well as Rho and Ras family GTPases. Rho family GTPases act as molecular switches that are bound to GTP during their active state and to GDP during their inactive state. Guanosine nucleotide exchange factors (GEFs) mediate the exchange from GDP to GTP therefore activating Rho. GTPase activating proteins (GAPs) in turn promote the hydrolysis of GTP to GDP transferring Rho back into the inactive state (Luo, 2000) (Figure 4-4, b). Upstream signals, for example from Eph receptors, regulate Rho GTPases via the specific activation of GEFs or GAPs. The local activation of Rac, a member of the Rho GTPases, is known to be crucial for spine and synapse formation. Local Rac activation can occur when GIT1 (G-protein-coupled receptor kinase-interacting protein) localizes to synapses bringing along PIX (p-21-

activated kinase interacting exchange factor), which is a guanine exchange factor for Rac (Zhang et al., 2003). During spine and synapse formation, the known downstream effectors of activated Rac are PAK (p-21 activated kinase) and MLC (myosin II regulatory light chain) (Zhang et al., 2005). However, the upstream signal which actually recruits GIT1 and the PIX-Rac-PAK module to synapses remains unknown (Figure 4-4, a). The Eph/ephrin system, which is known to control cytoskeletal events, is a possible candidate for initiating local Rac signaling.

The first part of this thesis elucidates the involvement of ephrinB signaling in spine morphogenesis and the downstream signaling pathway which possibly involves Rac.

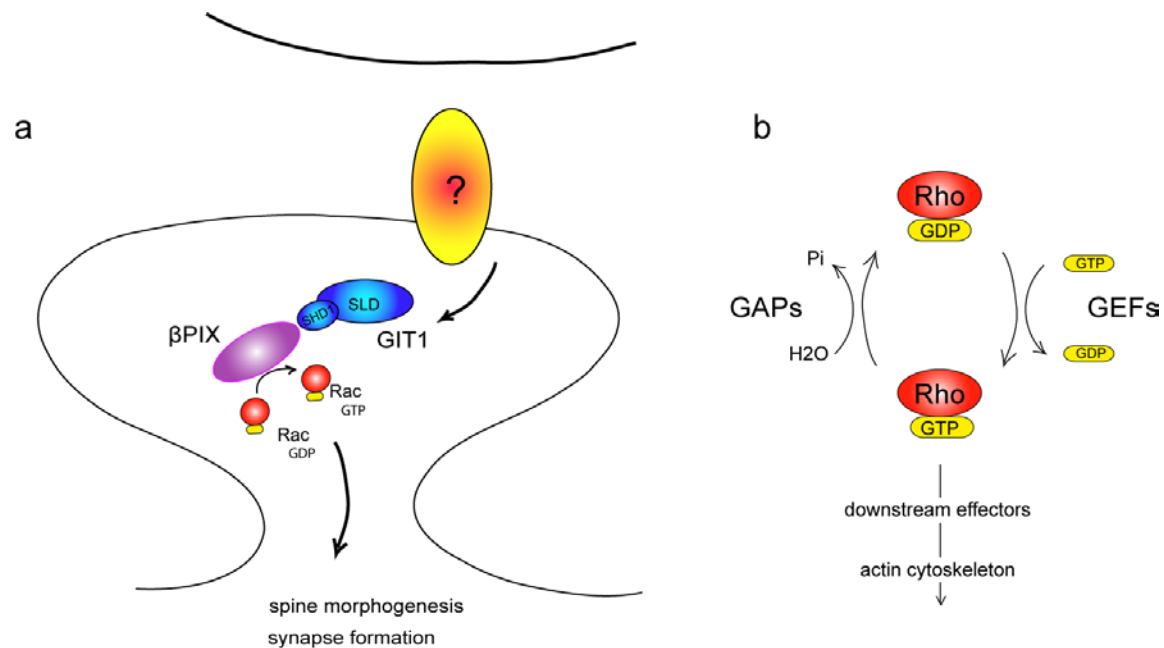


**Figure 4-4: GIT1 and  $\beta$ PIX are involved in spine formation.** (a) Local Rac activity is mediated by the assembly of a signaling complex including G-protein coupled receptor kinase-interacting protein 1 (GIT1) and the exchange factor for Rac (GEF),  $\beta$ -Pix (Zhang et al., 2003). The known downstream effectors of activated Rac during spine and synapse formation are PAK (p-21 activated kinase) and MLC (myosin II regulatory light chain). The signal upstream of GIT1 that recruits the Rac-signaling complex to the site of the forming spine is unknown. (b) Molecular switch of Rho family GTPases. Inactive Rho bound to GDP is transformed into its active GTP bound state by guanosine nucleotide exchange factors (GEFs). GTPase activity is promoted by a GTPase activating protein (GAP) that turns Rho back into its inactive GDP-bound state.

## 4.5 Synaptic plasticity

The capability of the nervous system to re-modulate its neural circuitry is generally termed as 'plasticity'. Synaptic plasticity is apparent during development when neural circuits are first formed, but it also occurs in the adult brain where it is thought to be the basis for learning and memory. On a structural level, plasticity is based on changes of the quality and number of synaptic contacts which are directed by environmental inputs. The processes involved in plasticity include spine motility, changes in the shape and size of spines, and the elimination or establishment of synaptic contacts. To study these processes during plasticity different experimental approaches have been used including learning paradigms, enrichment or avoidance of sensory inputs, and manipulations of the synaptic activity. Various studies have shown that motor- or memory-training of animals leads to an increase of synaptic contacts in the appropriate brain region. For example, Kleim et al. reported an increase in synapse density in the motor cortex and cerebellum after rats were trained to perform certain movements (Kleim et al., 1998). In another study, rats were trained for spatial learning, and a significant increase of spine density in the hippocampus was observed (Moser et al., 1994). Changes in spine morphology have been reported to be correlated to learning by West and colleagues (Geinisman et al., 2000). Furthermore, studies showed that raising animals in a rich sensory environment leads to an increase in the number, size and density of synaptic connections whereas depletion of sensory input has the opposing effect (Knott et al., 2002; Wallace and Bear, 2004).

Molecules involved in the regulation of spine formation and morphological changes play an important role in synaptic plasticity. However, morphological changes like spine formation and synaptogenesis are not the sole basis for plasticity. An additional, crucial factor is the regulation of synaptic strength in existing contact. Changes linked to synaptic strength can be addressed experimentally with stimulation patterns. Some activity patterns produce a long lasting increase in synaptic strength known as 'long-term-potential' (LTP), whereas other patterns lead to a long lasting decrease in synaptic strength, known as 'long-term-depression' (LTD). The molecular mechanisms underlying these changes

are post-translational modifications of existing proteins and, in the case of long-lasting effects, changes in gene expression.

### 4.5.1 LTP and LTD

Long-term-potential (LTP) of synaptic transmission is considered as a neuronal mechanism for information storage. This phenomenon was first described about 40 years ago by T. Bliss and colleagues when they discovered that short, high-frequency stimulation can enhance synaptic transmission in the hippocampus of rabbits for days or even weeks. Since then LTP has been thoroughly studied in the mammalian hippocampus, a region where some forms of memory formation take place. Most of the work has been performed on the synaptic connections between the presynaptic CA3 pyramidal cells and the postsynaptic CA1 cells, the so called Schaffer collateral pathway (Figure 4-5).

When the Schaffer collaterals are stimulated briefly with high-frequency electrical stimuli, the amplitude of the excitatory postsynaptic potential (EPSP) in CA1 neurons increases and remains high for a long time period: they exhibit long-term-potential. LTP has also been shown to occur at other synapses in the hippocampus, like the Mossy fibres and the Perforant path, as well as, in other brain regions including the cortex, amygdala, and the cerebellum. While synaptic transmission is increased during LTP, synapses are actively weakened during LTD, the opposing process of LTP. When Schaffer collaterals are stimulated at low-frequency for a longer time (10-15min), the EPSPs at the CA1 synapses show depression for several hours, meaning their amplitudes are decreased. Moreover, LTD can oppose LTP thus lowering the EPSP size back to unpotentiated levels. Conversely, LTP erases the decrease in EPSP size due to LTD (Bredt and Nicoll, 2003).

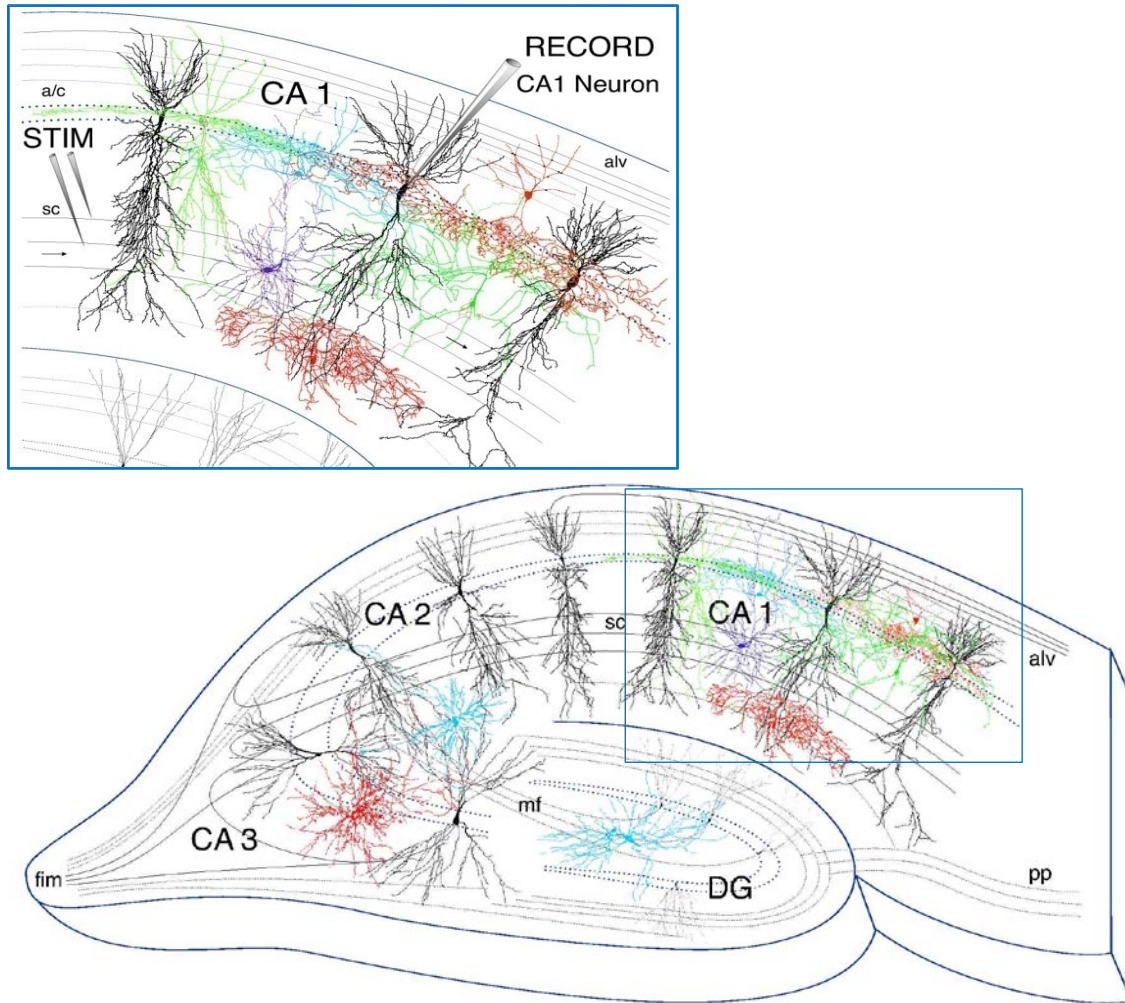


**Figure 4-5: Neuronal circuits of the hippocampus** (Maciver, 2005). In the hippocampus, most of the LTP and LTD studies have been performed at the Schaffer collateral pathway, the synaptic connection between CA3 and CA1 region neurons. Projection neurons are drawn in black, interneurons in color. Abbreviations: CA1, CA2, CA3 - cornu ammonis region 1,2 or 3 of the hippocampal formation; DG - dentate gyrus; STIM - stimulating electrode used to activate excitatory and inhibitory inputs to CA1 neurons; RECORD - recording electrode to measure pyramidal neuron response to stimulation; a/c - association/commissural pathway from septum and contralateral hippocampus; alv - alveus; sc - Schaffer collateral pathway from CA3 neurons; mf - mossy fiber pathway from dentate gyrus (DG) granule neurons; pp - perforant path axons from entorhinal cortex; fim - fimbria pathway to and from midbrain and other regions.

Both LTP and LTD at the CA1 region synapses require NMDA-receptor activation that results in the entry of  $\text{Ca}^{2+}$ -ions into the postsynaptic cell (Malenka, 1994).  $\text{Ca}^{2+}$ -influx leads to the activation of protein kinases, or phosphatases, that act on target molecules to

evoke changes in synaptic transmission. Whether  $\text{Ca}^{2+}$ -influx leads to LTP or LTD depends on the amount of  $\text{Ca}^{2+}$ -ions released into the cell. Small rises of  $\text{Ca}^{2+}$  lead to depression whereas large increases result in potentiation. The level-dependent effects of  $\text{Ca}^{2+}$  result from the selective activation of  $\text{Ca}^{2+}$ -sensitive molecules. LTP is at least partially mediated by the activation of  $\text{Ca}^{2+}$ /calmodulin-dependent kinase (CaMKII) and protein kinase C (PKC), whereas LTD results from the activation of protein phosphatases. But what actually modulates the size of EPSPs is the amount of active AMPA receptors at the postsynaptic membrane that transmit the signal after glutamate-released from the presynaptic site. The number of AMPA receptors at the synaptic surface is determined by receptor trafficking. AMPA receptors not only traffic continuously between the cell surface and intracellular pools, but also between synaptic and extra-synaptic sites (Borgdorff and Choquet, 2002; Triller and Choquet, 2005). Several lines of evidence indicate that controlling the number of AMPA receptors is a key mechanism during LTP and LTD. During LTP induction, the level of surface AMPA receptors rapidly increases due to the insertion of new receptors (Lu et al., 2001b; Pickard et al., 2001); conversely, AMPA receptors are removed from the synaptic membrane via endocytosis during LTD (Carroll et al., 1999; Heynen et al., 2000). In support of these findings, the blockage of AMPA-receptor exocytosis was shown to prevent LTP induction whereas the blockage of AMPA-receptor endocytosis prevented LTD induction (Bredt and Nicoll, 2003). In recent years, a great effort has been made to identify molecules involved in LTP and AMPA-receptor trafficking. Knockdown experiments have identified several molecules apparently involved in LTP and/or LTD induction, but the underlying molecular mechanisms remain unknown. Among these candidate molecules are different types of Eph receptors and ephrinB ligands (Grunwald et al., 2004). Thus the ablation of ephrinB2 or ephrinB3 in the nervous system led to severe defects in LTP and LTD in the Schaffer collateral pathway. The aim of the second half of this thesis is to elucidate the pathways involved in these plasticity defects.

## 4.6 AMPA receptors

AMPA receptors are a subclass of ionotropic glutamate receptors that mediate fast excitatory neuronal transmission in the mammalian central nervous system (CNS). The two other members of this group include NMDA receptors, crucial for the induction of specific forms of plasticity including LTP and LTD (Bear and Malenka, 1994), and kainate receptors that play important roles in the modulation and plasticity of the synaptic response (Lerma, 2006). AMPA receptors are hetero-tetramers composed of different combinations of the subunits GluR1, GluR2, GluR3 or GluR4, the most prominent subunit being GluR2 (Nakanishi, 1992). Each subunit possesses a large extracellular N-terminal domain, three membrane-spanning domains (TM1, TM3 and TM4), a hairpin that contributes to the pore (M2), and a cytoplasmic C-terminal domain. The four subunits have very similar extracellular and transmembrane domains, but differ in their cytoplasmic tail which provides the subunit-specific interaction with intracellular proteins. The cytoplasmic tails of GluR1 and GluR4, but also a splice variant of subunit GluR2 (GluR2L), appear to be quite long compared to those of the GluR2 and GluR3 subunit or the short splice variant GluR4S. Additionally, posttranscriptional editing and splicing increases the variability among the different subunits, modulating their properties from phosphorylation levels to physiological functions. For example, the incorporation of GluR2 subunits in AMPA receptors makes them impermeable to calcium (Hollmann et al., 1991). This calcium impermeability of GluR2 is a consequence of RNA editing at the Q/R site in the channel forming hairpin (M2) (Figure 4-6) (Burnashev et al., 1992). The genetically encoded uncharged glutamine (Q) is changed to a positively-charged arginine (R) that increases the activation energy necessary for calcium to enter the cell. During development, unedited GluR2 (Q) subunits are abundant whereas in the adult CNS nearly one hundred percent of the GluR2 subunits are edited. Besides, the arginine residue has been shown to control channel composition and, in turn, channel conductance. The R-edited GluR2 is retained unassembled in the endoplasmic reticulum (ER) supporting the formation of GluR2 hetero-tetrameres over homo-tetrameres and restricting the functionally critical number of R-subunits in AMPA-receptor tetrameres (Greger et al., 2003). Furthermore, each of the AMPA-receptor subunits GluR1–GluR4 exists in two

different forms, flip and flop, generated by alternative splicing of a 115 base pair region immediately upstream of the fourth transmembrane region (Figure 4-6) (Sommer et al., 1990; Sommer et al., 1991). The splice variants determine the speed of desensitization with the flop form desensitizing much faster than the flip form in response to glutamate. The flip form is present in prenatal AMPA receptors, and gives a sustained current in response to glutamate activation.

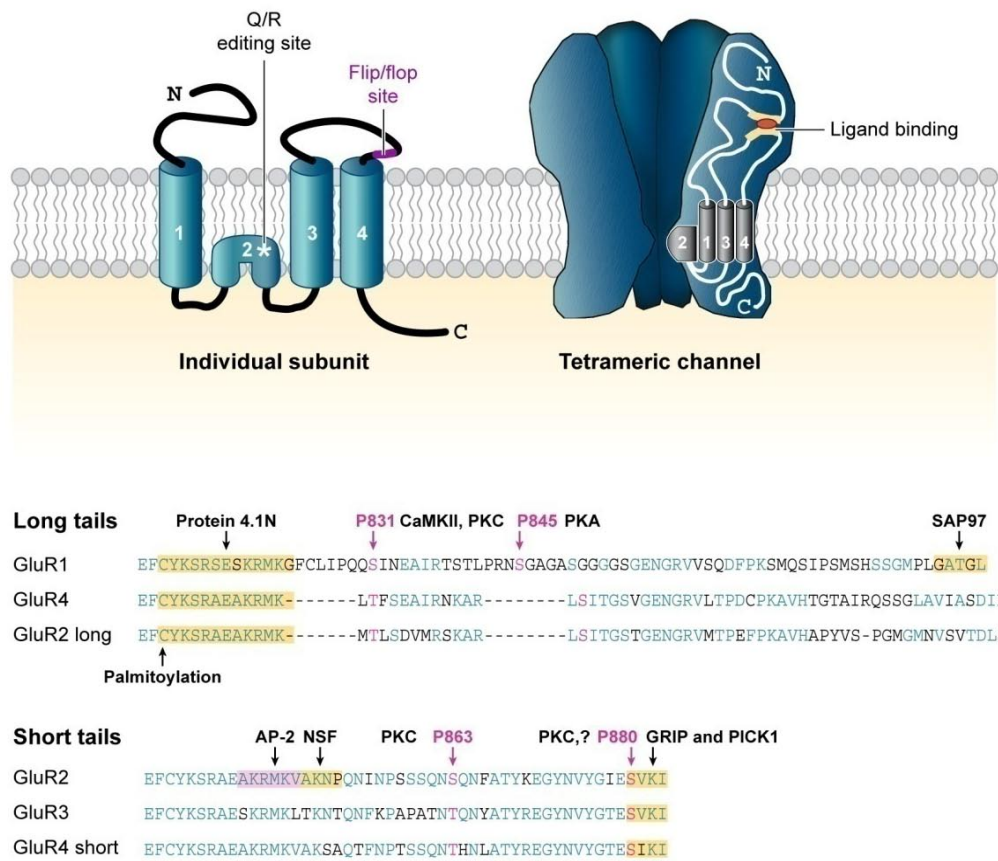


**Figure 4-6: Structure and composition of the AMPA receptor** (Shepherd and Huganir, 2007). The individual subunits are composed of four transmembrane domains, a large extracellular N-terminal domain and a subunit-specific cytoplasmic C-terminus. Post-translational modifications are indicated: The Q/R - RNA-editing controls the heteromeric assembly and conductance, the flip/flop splice variants determine the desensitization properties. The channel consists of four subunits, which are usually two dimers of a subunit such as GluR1 and -2 or GluR2 and -3. AMPA receptor C-termini differ in their amino acid sequence determining their interaction partners. Various phosphorylation sites and binding partners are highlighted. Protein abbreviations: AP-2 - adaptor protein-2; CaMKII - calcium/calmodulin-dependent protein kinase II; GRIP - glutamate receptor-interacting protein; NSF - N-ethylmaleimide-sensitive fusion protein; PICK1 - protein interacting with C kinase 1; PKA - protein kinase A; PKC - protein kinase C; SAP97 - synapse-associated protein 97.

The subunit composition of AMPA receptors changes during development and upon neuronal activity. In the mature hippocampus most AMPA receptors are composed of either GluR1-GluR2 or GluR2-GluR3 subunits, whereas GluR4-containing receptors occur mainly during early postnatal stages (Wenthold et al., 1996; Zhu et al., 2000). Upon neuronal activity and NMDA-receptor activation, GluR1-containing receptors (GluR1-GluR2 heteromers) are added to the synaptic surface increasing synaptic transmission. In contrast, GluR2 containing receptors, including GluR2-GluR3 heteromers and GluR2 homomers, cycle continuously between synaptic and non-synaptic pools independently of neuronal activity, replacing pre-existing receptors (Figure 4-7) (Hayashi et al., 2000; Malinow et al., 2000). The permanent cycle, under basal conditions and independent of neuronal activity, allows a fast control of the synaptic receptor density. The current model suggests that GluR2-GluR3 receptors preserve the total number of AMPA receptors by continuous cycling, whereas the GluR1-GluR2 receptors are added to the synapse increasing the total number of receptors in an activity-dependent manner (Malinow et al., 2000). Understanding the regulation of AMPA-receptor trafficking is therefore of great importance with regards to synaptic plasticity.

#### 4.6.1 AMPA-receptor trafficking

A variety of molecules have been found to associate with AMPA receptors thus controlling their systematic trafficking (Figure 4-7). Besides controlling trafficking, intracellular molecules interact with AMPA receptors to regulate their stabilization and their electrophysiological properties. These processes seem to be, to a great extent, controlled through interactions between the intracellular carboxy (C)-tails of AMPA receptors and the effector proteins. Many of these effector proteins contain PDZ-domains (postsynaptic density 95, PSD-95; drosophila discs large, Dlg; zonula occludens-1, ZO-1), which interact with the PDZ-binding motif of AMPA receptors located at the C-terminus of the subunit, and form a functional scaffolding complex. The GluR1 subunit carries a group I PDZ-motif and specifically interacts with the synapse-associated protein 97 (SAP97), a member of the membrane-associated guanylate kinase family (MAGUK), or with the reversion-induced LIM gene (RIL). SAP97 is essential for the transport of the subunit

from the endoplasmic reticulum to the cis golgi and dissociates from the receptor at the plasma membrane (Leonard et al., 1998; Sans et al., 2001); RIL might control actin-dependent AMPA-receptor trafficking (Schulz et al., 2004). Furthermore, GluR1 interacts with the cytoskeletal protein 4.1N that links AMPA receptors with actin to mediate their surface expression (Shen et al., 2000). In contrast, both GluR2 and GluR3 carry a group II PDZ-motif and interact with glutamate-receptor-interacting protein (GRIP1), AMPA-receptor-binding protein (ABP; also known as GRIP2) and protein interacting with C kinase 1 (PICK1) (Dong et al., 1997; Xia et al., 1999). Although these molecules bind the same site in AMPA receptors, their binding is differently regulated. This allows them to function in distinct aspects of AMPA-receptor trafficking, membrane insertion or endocytosis, and the stabilization at the synaptic membrane. Disruption of GRIP1 and ABP binding to GluR2 leads to accelerated AMPA-receptor endocytosis at synapses (Osten et al., 2000) revealing a membrane stabilizing role of these two molecules. Phosphorylation of serine 880 (ser880) in GluR2, induced upon receptor activation, leads to the dissociation of GRIP1/ABP but allows the binding of PICK1 and subsequently its endocytosis (Chung et al., 2000; Matsuda et al., 1999). Regulating the endocytosis of AMPA receptors is only one of the multiple roles of PICK1 during receptor trafficking. Indeed, PICK1 functions in the removal of AMPA receptor from the synaptic surface during LTD, in constitutive trafficking under basal conditions as well as in the recycling of internalized receptors (Hanley, 2008; Hanley and Henley, 2005; Kim et al., 2001).

Another group of PDZ-domain-containing molecules that bind AMPA receptors are the family of transmembrane AMPA receptor regulatory proteins (TARPs) including stargazing,  $\gamma$ -3,  $\gamma$ -4 and  $\gamma$ -8. TARPs show discrete and complementary expression patterns in both, neurons and glia cells in the brain (Tomita et al., 2003). They facilitate the transport of AMPA receptors from the ER to the plasma membrane and control their expression at the synapse (Ziff, 2007). Furthermore they assist in the correct folding of the receptors, and affect their channel kinetics as well as their rectification properties. Through their interaction with PSD-95, they link AMPA receptors to the postsynaptic

density which appears to be crucial for the synaptic targeting of AMPA receptors (Coleman et al., 2006; Tomita et al., 2005).

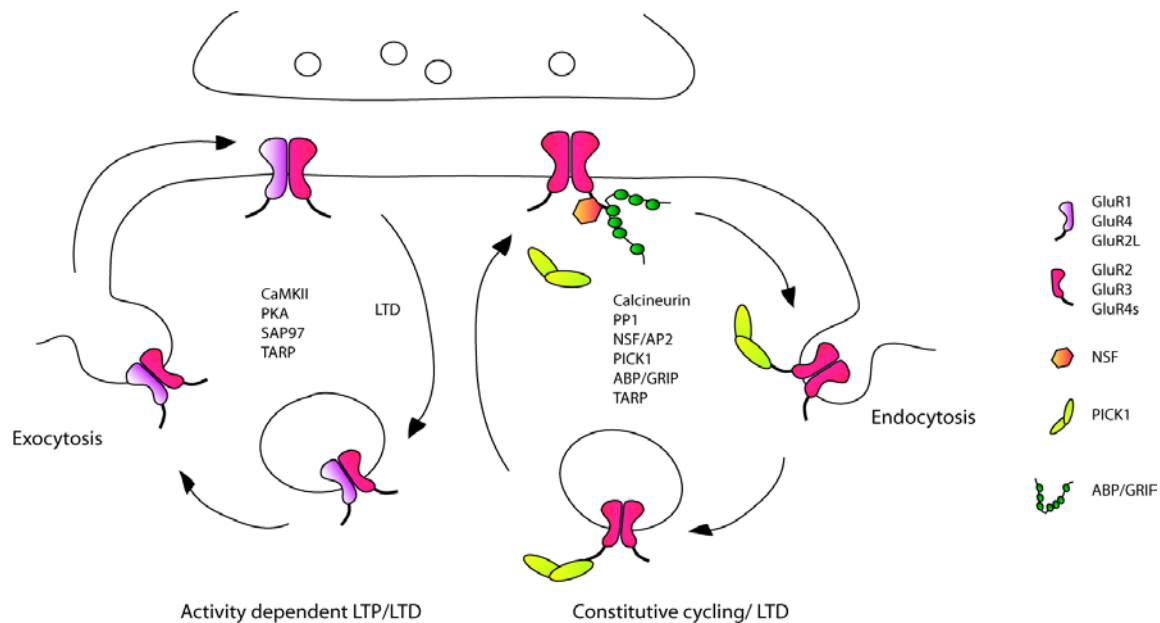


**Figure 4-7: Trafficking of synaptic AMPA receptors** (adapted from Bred and Nicoll 2003). AMPA receptors containing subunits with a long cytoplasmic tail (GluR1, GluR4 or GluR2L) are delivered to the synapse upon activity. Some evidence suggests that they are inserted in extra synaptic membrane sites and move laterally to the synapse. Proteins thought to be involved in the delivery include CaMKII, PKA, SAP97, and TARPs. In contrast, receptors containing only short tails cycle constitutively between the synapse and intracellular pools. Proteins like calcineurin, PP1, NSF/AP2, PICK1, and ABP/GRIP regulate different steps during constitutive cycling and LTD. Abbr.: CaMKII- calcium/calmodulin kinase II; PKA- protein kinase A/cAMP dependent protein kinase; TARPs- transmembrane AMPA receptor regulatory proteins; PP1- protein phosphatase 1; NSF- N-ethylmaleimide-sensitive fusion protein; AP2- clathrin adaptor protein 2; PICK1- protein interacting with C kinase 1; ABP- AMPA receptor binding protein; GRIP- glutamate receptor interacting protein.

Beside PDZ-containing proteins, the cytoplasmic tail of GluR2 interacts with N-ethylmaleimide-sensitive fusion protein (NSF), an ATPase known to play an essential role during membrane fusion (Nishimune et al., 1998). The ATPase action of NSF helps to dissociate PICK1 from GluR2 thus facilitating the delivery of AMPA receptors to the cell membrane. Furthermore, NSF allows the binding of GRIP1/ABP resulting in the membrane stabilization of AMPA receptors. Therefore, NSF is crucial in limiting the

endocytosis of AMPA receptors and to maintain constitutive cycling at a constant rate and hence to maintain a constant level of receptors at the synaptic membrane (Hanley et al., 2002).

### 4.7 PDZ-proteins

Originally termed as Disc-large homology regions (DHRs) or GLGF repeats which are based on the presence of the Gly-Leu-Gly-Phe sequence motif, these domains are now primarily referred to as PDZ-domains. The three letters are an acronym of the first three PDZ-containing proteins that were discovered: Postsynaptic density 95 (PSD-95), *Drosophila* septate junction protein Discs-large (Dlg), and tight junction protein Zonula occludens-1 (ZO-1). PDZ-domains are found in various signaling proteins throughout a diversity of organisms including bacteria, yeast, plants, and animals. Indeed, PDZ-domains represent one of the most abundant protein domains within the sequenced genome. Many PDZ-containing proteins contain multiple PDZ-domains, often arranged in tandem arrays or pairs such as the PDZ1-3 and PDZ4-6 domains of GRIP1. In addition, many of these PDZ-proteins hold other known protein interaction domains, a feature that enables them to interact with multiple binding partners simultaneously. For example, the superfamily that includes PSD97/SAP90, Dlg and ZO-1, so called membrane-associated guanylate kinases (MAGUKs), comprises one or more PDZ-domains, one SH3 (Src homology 3) domain and a catalytically inactive guanylate kinase-like domain. PDZ-proteins broadly function as scaffolding molecules which mediate specific protein-protein interactions and thereby the assembly of large molecular complexes. Furthermore, they are involved in signaling and in specific trafficking of target proteins to subcellular compartments. To a great extent PDZ-containing proteins are found at neuronal synapses where they comprise the major part of the postsynaptic density thus playing an important role in the organization of receptors and downstream signaling enzymes.

PDZ-domains comprise 80-90 amino acids and their architecture is very similar from domain to domain. They consist of six anti-parallel  $\beta$ -strands and two  $\alpha$ -helices. Their overall fold approximates a six-strand  $\beta$ -sandwich where the protein binding takes place in

the groove between  $\beta$ 2-strand and the  $\alpha$ 2-helix (Figure 4-8). They typically bind the C-terminus of the target protein. The binding specificity of PDZ-domains is determined by the interaction of the first amino acid residue of  $\alpha$ 2-helix and the side chain of the ligand's the residue at position -2, counted backwards from the C-terminus. This interaction specificity serves as basis for the classification of PDZ-domains as class I, class II and class III PDZ-domains. Besides the residue -2 of the ligand that serves as the major determinant for the PDZ-interaction, several studies demonstrated that residues at up to positions -8 (Niethammer et al., 1998; Songyang et al., 1997), or even at position -11 to -14, within the ligand might influence the interaction between ligand and PDZ-domain protein (Cai et al., 2002; van Ham and Hendriks, 2003).

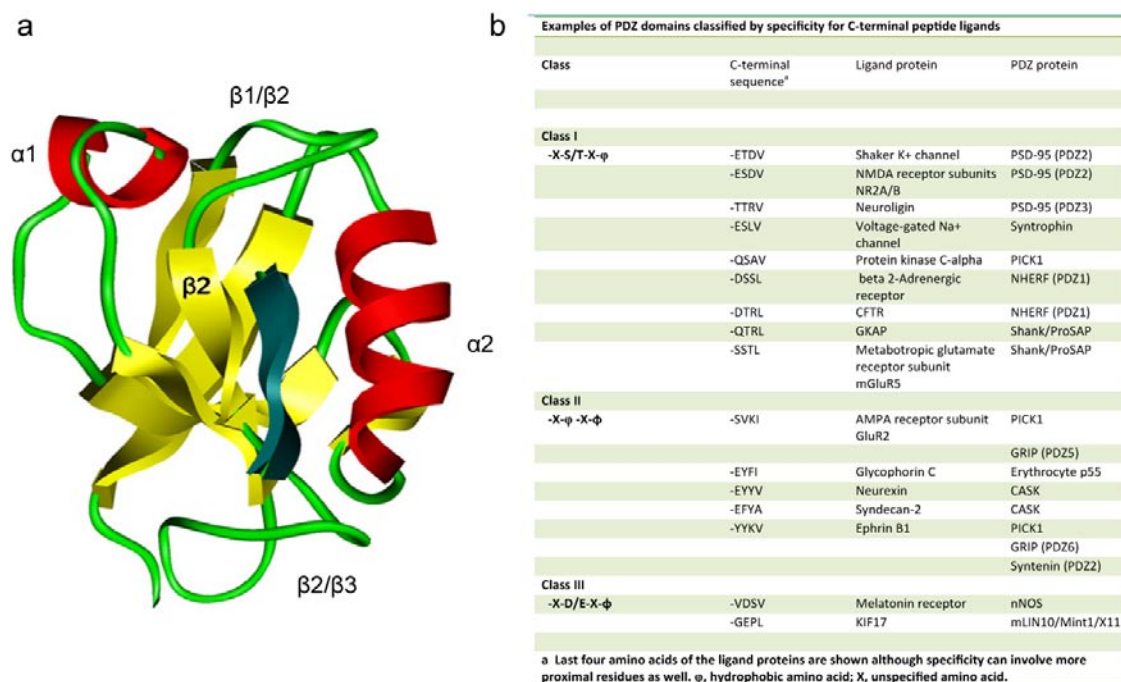


**Figure 4-8: Structure of a PDZ-domain.** (a) The common structure of a PDZ-domain that comprises six anti-parallel  $\beta$ -strands (yellow) and two  $\alpha$ -helices (red) which fold in an overall six-stranded  $\beta$ -sandwich. The peptide binding occurs in a groove between the  $\beta$ 2-strand and the  $\alpha$ 2-helix (dark blue). (b) List of different PDZ-proteins classified by their interaction qualities determined by the first residue of the  $\alpha$ 2-helix and the -2 residue of the C-terminal ligand (Hung and Sheng, 2002).

Like most protein interactions, the binding between a PDZ-domain protein and its ligand is regulated to ensure appropriate function, particularly when the C-terminus of a protein is recognized by more than one PDZ-domain protein. One way of controlling these interactions is via the phosphorylation of residues within the C-terminal sequence of the ligand. For example, the AMPA receptor subunit GluR2 binds to the PDZ-proteins GRIP1 and PICK1 both of which are involved, but function differently in AMPA-receptor trafficking (see 4.6.1). Here, phosphorylation of ser880 in the C-terminal sequence of GluR2 inhibits the binding of GRIP1 but not PICK1 (Chung et al., 2000), which results in the internalization of AMPA receptors. Ultimately, PDZ-interactions must be under the control of higher-level signals, additionally influenced by temporal or spatial separation of otherwise competing binding partners.

Most of the PDZ-domains bind to the C-terminal sequence of their ligand. In cases, where interaction occurs with internal peptide sequences, these are thought to assume conformations that mimic the C-terminus. Furthermore, PDZ-domains can bind to other PDZ-domains to form homo- and hetero-oligomers and even to other distinct protein binding motifs including ankyrin repeats, spectrin repeats and LIM domains (Cuppen et al., 1998; Maekawa et al., 1999; Xia et al., 1997).

### 4.7.1 Glutamate receptor interacting protein (GRIP)

The multi-PDZ-domain proteins GRIP1 and ABP belong to the family of GRIP proteins and comprise six or seven PDZ-domains. GRIP1 occurs in different splice variants GRIP1a, GRIP1b (1-7 PDZ domains) and GRIPc (4-7 PDZ-domain). ABP exists in two isoforms, one of 130 kDa which also exhibits seven PDZ-domains (ABP-L also termed as GRIP2 by Bruckner et al. 1999) and a shorter 98 kDa isoform which contains only six PDZ-domains. GRIP proteins were initially identified as proteins that interact with AMPA receptors, thus promoting their stabilization at synapses and intracellular compartments. Since then, numerous additional molecules that interact with GRIP proteins have been identified, supporting its role as multiple adaptor proteins (Figure 4-9).

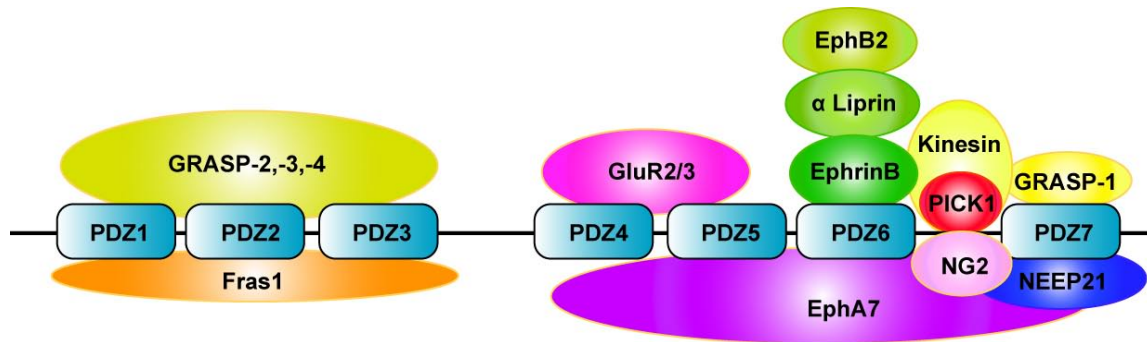


**Figure 4-9: GRIP1 interaction scheme.** The multi-PDZ-domain protein GRIP1 acts as scaffolding molecule. Depending on the subcellular compartment it interacts with various different molecules and mediates their interaction, crosstalk and transport. Abbreviations: Fras1- Fraser syndrome 1; GRASP-1, 2, 3, 4: GRIP associated protein 1-4; NEEP21: neuron-enriched endosomal protein of 21 kD; PICK1- protein interacting with C kinase 1; NG2- chondroitin sulphate proteoglycan.

GRIP proteins bind to the GluR2 and GluR3 subunit of AMPA receptors via their fifth PDZ-domain and are likely to link other molecules to AMPA receptors via their remaining free PDZ-domains. For example, GRIP1 can interact simultaneously with AMPA receptors and the motor protein kinesin; the latter binds to the linker sequence of GRIP, the region connecting PDZ6 and PDZ7, thus directing AMPA receptors to the dendrites (Hoogenraad et al., 2005). Furthermore, GRIP proteins are found to interact with  $\alpha$ -liprin, ephrinB, EphB2 via their PDZ6-domain, to EphA7 via their PDZ4-7-domain (Bruckner et al., 1999; Lin et al., 1999; Torres et al., 1998; Wyszynski et al., 2002), and to GRIP associated protein 1 (GRASP-1; neuronal RasGEF) as well as to the neuron-enriched endosomal protein of 21 kD (NEEP21). GRASP-1 regulates neuronal Ras signaling and contributes to the regulation of AMPA-receptor distribution by NMDA-receptor activity (Ye et al., 2000) whereas NEEP21-GRIP1 binding is crucial for GluR2-AMPA-receptor sorting through endosomes and their recruitment to the plasma membrane (Steiner et al., 2005). The binding of PICK1 to GRIP is thought to be the initial step in AMPA-receptor endocytosis, where PICK1 substitutes GluR2-bound GRIP. Another, neuron-independent function of GRIP1 is its interaction with the extracellular

matrix protein Fraser syndrome 1 (Fras1), an interaction which is required for the appropriate localization of Fras1 to the basal side of cells (Takamiya et al., 2004). Using a yeast-two-hybrid assay, further molecules interacting with GRIP PDZ1-3 were identified, such as GRIP associated proteins 2-4, but their functions remain unknown.

### 4.8 The Eph receptors and ephrin ligands

The first Eph receptor was identified in a search for tyrosine kinases expressed by cancer cells, and named after a **erythropoietin-producing hepatocellular carcinoma** cell line from which its cDNA was isolated (Hirai et al., 1987). The first ligands for Eph receptors (ephrins) were then identified some years later by different research groups (Bartley et al., 1994; Beckmann et al., 1994; Cheng and Flanagan, 1994).

The Eph receptors comprise the largest subfamily of receptor tyrosine kinases and are found in various cell types both in developing and mature tissue. Their ligands, the ephrins, are membrane bound molecules and signaling therefore occurs when cells come in close contact to each other. The Eph/ephrin system is involved in a variety of cellular processes including shape regulation, attachment and de-attachment, attraction and repulsion, and directed migration. The Eph/ephrins therefore play important roles during embryonic development such as in pattern formation and in the morphogenic process that govern the nervous and vascular system, whereas in the adult organism they are involved in synaptic plasticity and tumorigenesis (Palmer and Klein, 2003).

Receptor tyrosine kinases (RTKs) are cell surface receptors with an intracellular kinase domain that transmits extracellular stimuli, mostly from soluble molecules, to the inside of the cell. RTKs are activated by dimerization and directly regulate cell fate, cell growth, cell division and survival by influencing nuclear events such as gene transcription. Among the RTKs, the Eph/ephrin system has a number of unique features: Their signaling appears to directly regulate cytoskeletal changes rather than nuclear events. Additionally, their ligands are not soluble but membrane bound thus restricting cell-to-cell communication to a short-range. Moreover, the dimerization of the Eph receptors does

not suffice for functional signaling, which instead requires the formation of higher order clusters. The ephrin ligands have their own signaling potential. Upon receptor-ligand engagement signaling occurs in both the receptor- and the opposing ligand-expressing cell termed 'forward' (receptor-activated) or 'reverse' (ligand-activated) signaling respectively (Egea and Klein, 2007; Klein, 2004; Kullander and Klein, 2002).

#### **4.8.1 Classification and structure**

The Eph receptors are divided into two subclasses – A and B – based on their affinities to the class of ligands and their degree of sequence similarity. Mammals have nine A-class receptors (EphA1-8 and EphA10) and five B-class receptors (EphB1-4 and EphB6). Their overall structure is similar but they differ in their amino acid sequences and binding affinity to the ephrin ligands: A-class receptors preferentially bind to ephrinA ligands, and B-class receptors to ephrinB ligands with only a few exceptions (the receptor EphA4 binds to both ephrinA and ephrinB ligands and ephrinA5 was shown to interact with EphA receptors as well as with EphB2). The ephrin ligands show striking structural differences between the A and the B class: EphrinA ligands (ephrinA1-5) are anchored to the membrane via a glycosylphosphatidylinositol (GPI) while the ephrinB ligands (ephrinB1-3) span the plasma membrane and possess a short cytoplasmic tail with features supporting protein-protein interactions.

##### **4.8.1.1 Eph receptors**

The Eph receptors, classes A and B, contain a common structure made up of a highly conserved globular N-terminal domain (ligand binding domain; LBD) that is necessary and sufficient for ligand binding (Labrador et al., 1997), followed by a cysteine-rich region which is thought to be involved in oligomerization (Smith et al., 2004), as well as by two fibronectin type III repeats. The cytoplasmic part of the Eph receptor contains a juxtamembrane domain, a conserved kinase domain, a sterile- $\alpha$ -motif (SAM) domain and a PDZ-binding motif (see 4.7) (Figure 4-10).

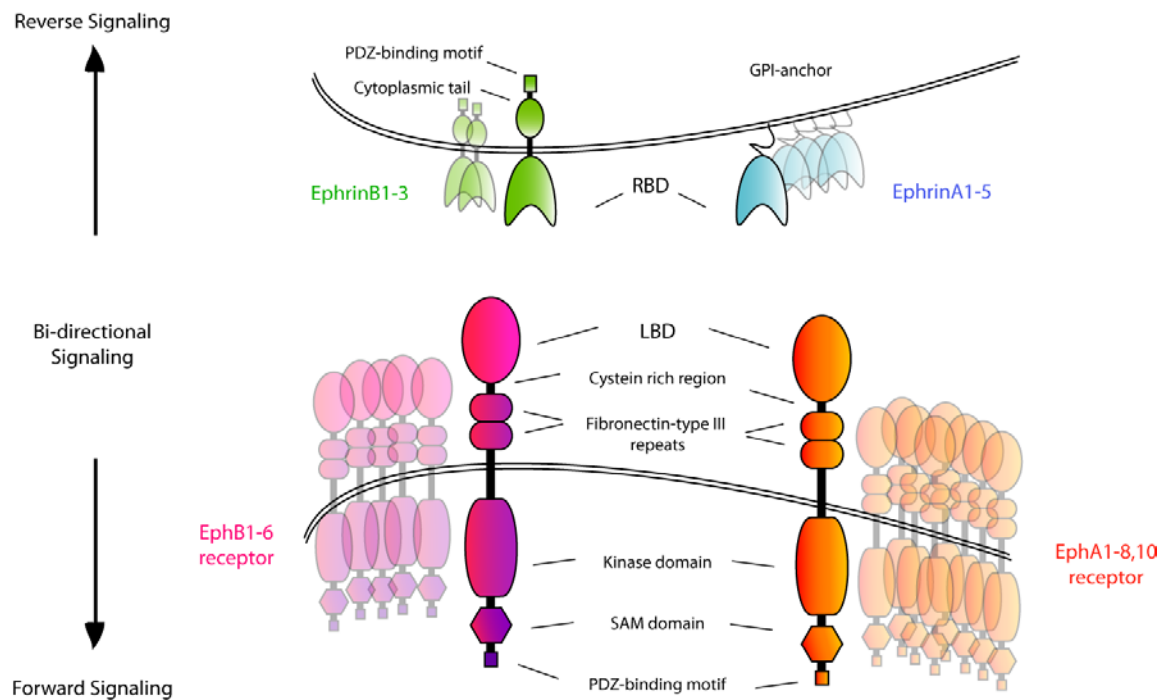


**Figure 4-10: The Eph receptors and their ephrin ligands.** The Eph receptor family of receptor tyrosine kinases and the ephrin ligands are membrane bound molecules interacting upon cell-to-cell contact. Upon engagement, bi-directional signaling occurs: so-called forward signaling in the receptor-expressing cell, and reverse signaling in the ligand-expressing cell. Eph and ephrins are classified into two groups, A and B, depending on sequence similarities and binding affinities. EphrinA ligands are membrane anchored via a GPI (glycosylphosphatidylinositol) and engage with EphA receptors, ephrinB ligands possess a short cytoplasmic domain and bind to EphB receptors. The high affinity interaction between Eph and ephrins occurs at the extracellular receptor/ligand binding domain (RBD/LBD). Abbreviations: RBL-receptor binding domain; LBD-ligand binding domain; SAM- sterile- $\alpha$ -motif; PDZ- postsynaptic density 95, PSD-95; drosophila discs large, Dlg; zonula occludens-1, ZO-1.

The juxtamembrane region regulates the kinase activity that can be activated by the auto-phosphorylation of two tyrosines within the juxtamembrane segment. It is thought that in the unphosphorylated state, the juxtamembrane adopts a conformation that associates with the kinase domain and sterically inhibits the activation segment of the kinase domain keeping it in an inactive conformation (Figure 4-11). Upon receptor activation the juxtamembrane region gets tyrosine-phosphorylated and dissociates from the kinase domain relieving its auto-inhibition and allowing it to assume its active conformation

(Wybenga-Groot et al., 2001). A more recent study suggests a dynamic model, where fluent, inter-lobal changes in conformation occur after the relief of inhibition rather than a switch to a static active conformation of the kinase domain (Wiesner et al., 2006). Once active, the kinase can phosphorylate other molecules, including the kinase domains of neighbouring Eph receptors, allowing phosphotyrosine-binding adaptor molecules to bind and thereby initiate downstream signaling cascades.

A key signaling cascade downstream of Eph receptors involves cytoskeletal rearrangements via signaling through the Rho GTPases RhoA, Cdc42, and Rac. Rho GTPases cycle between an active GTP-bound and an inactive GDP-bound conformation (Figure 4-4, b). They control cell shape and movement by promoting the formation of stress fibres (Rho), lamellipodia (Rac) and filopodia (Cdc42) (Nobes and Hall, 1995). In neurons, RhoA-activation inhibits neurite outgrowth, directs growth cone collapse and axon retraction, whereas Rac and Cdc42 promote growth cone lamellipodia formation and filopodia extensions respectively. Interestingly, Eph receptor subclasses A and B activate different Rho GTPases. EphA receptors directly activate RhoA through the constitutively bound exchange factor ephexin1 (Eph-interacting exchange protein 1), catalysing the replacement of GDP by GTP (Figure 4-11). Yet, in the absence of ephrin stimulation this exchange factor is thought to activate multiple Rho family members including RhoA, Rac1, and Cdc42 in an appropriate balance thus favouring neurite outgrowth. Only if the EphA receptor is activated will ephexin1 phosphorylation occur, causing its action to shift towards RhoA, a chain of events which leads to growth cone collapse (Wahl et al., 2000). EphB receptors have been shown to interact with intersectin, an exchange factor for Cdc42, and kalirin, an exchange factor for Rac, which both regulate growth cone dynamics and spine morphogenesis (Figure 4-11) (Irie and Yamaguchi, 2002; Murai and Pasquale, 2005; Penzes et al., 2003; Shamah et al., 2001). Furthermore, the exchange factor Tiam1 seems to bind to both A and B class Eph receptors and to ephrinB ligands and promotes neurite outgrowth (Tanaka et al., 2004).

Besides the key signaling cascade via Rho GTPases, Eph receptors have been shown to be involved in the regulation of Ras GTPases (H-ras), as well as the integrin-mediated adhesion pathways involving FAK and JNK (Murai and Pasquale, 2003).

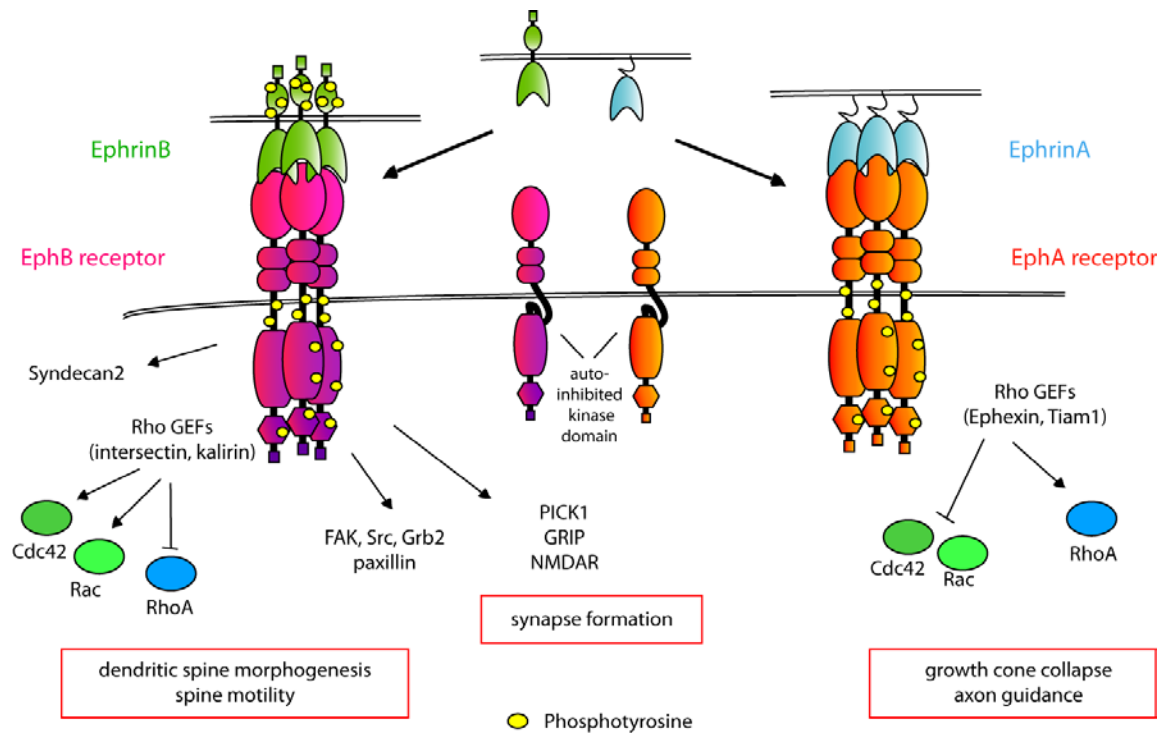


**Figure 4-11: Eph receptor interaction scheme.** In the unengaged receptor the juxtamembrane domain is folded and auto-inhibits the kinase domain. In order to promote a signal, Eph receptors and ephrin ligands need to form high order cluster assembling signaling molecules and activating the Eph receptor kinase. EphB receptors mediate cytoskeletal rearrangements via syndecan2 and the activation of small Rho family GTPases Cdc42 and Rac to promote spine morphogenesis and motility. They regulate cell adhesion via FAK signaling complexes and bind to GRIP, PICK1 and NMDA receptors modulating synapses. EphA receptors mediate repulsive cues by activating RhoA GTPases which leads to growth cone collapse, but also transduce attractive cues during axon guidance.

#### 4.8.1.2 Ephrin ligands

Among RTK ligands the ephrins are special in the way that they are membrane bound and act as receptors themselves by promoting a ‘reverse’ signal into the ligand expressing cell upon Eph receptor engagement. Ephrin ligands are divided into two groups: Both groups possess an extracellular receptor binding domain (RBD), but ephrinA ligands (ephrinA1-5) are attached to the plasma membrane via glycosylphosphatidylinositol (GPI) whereas

ephrinB ligands (ephrinB1-3) span the membrane and have a short, highly conserved cytoplasmic tail. Unlike the Eph receptors, ephrin ligands do not have an intrinsic catalytic domain and must therefore transduce their signal with the help of cytoplasmic proteins.

The cytoplasmic tail of ephrinB ligands contains five conserved tyrosines, that serve as potential phosphorylation sites, and a PDZ-binding motif (Figure 4-12, a). EphrinB-activation leads to the rapid phosphorylation of their cytoplasmic tyrosine residues (Bruckner et al., 1997), three of which are characterized as major phosphorylation sites (Kalo et al., 2001). The rapid phosphorylation is known to be mediated by Src family kinases (SFKs) that become activated and are recruited to ephrin clusters upon Eph receptor binding (Palmer et al., 2002). Cytoplasmic proteins can interact with ephrinB ligands via SH2 domains that recognize phosphorylated tyrosines. So far, the only SH2-domain protein that has been found to interact with tyrosine-phosphorylated ephrinB molecules is the growth-factor-receptor-bound protein 4 (Grb4). Grb4 is a SH2/SH3 domain-containing adaptor protein. Its association with activated ephrinBs leads to the disassembly of F-actin-containing stress fibers and increased FAK activation (Cowan and Henkemeyer, 2001). Similar to forward signaling through Eph receptors, the regulation of cytoskeletal rearrangement seems to be one of the major effects of ephrinB-reverse signaling. However, the signaling induced by rapid tyrosine phosphorylation is a short-lived event. With delayed kinetics, the cytoplasmic PDZ-domain-containing protein tyrosine phosphatase PTP-BL is recruited to activated ephrinB ligands thereby terminating the signal by ligand and SFK dephosphorylation. In contrast, PDZ-interactions were shown to persist (Palmer et al., 2002). Based on these findings, a switch-model for ephrinB-reverse signaling has been established distinguishing the fast, but short-lived phosphotyrosine-dependent signaling from the delayed, but persistent, PDZ-dependent signaling (Figure 4-12, (b)).

The PDZ-binding motif is located at the C-terminal end of ephrinB ligands, where besides phosphatases PTP-BL, it is recognized by various other PDZ-domain proteins such as GRIP1 and GRIP2, syntenin, PDZ-RGS3 and PICK1. The interaction between ephrinB ligands and these proteins has been described but the molecular pathways remain unclear

except for those of PDZ-RGS3 and ephrinB. PDZ-RGS3 contains a PDZ-domain and a regulator of heteromeric G protein signaling (RGS) domain. The catalytic RGS-domain acts as a GTPase-activating protein for G protein-coupled receptors and catalyses the hydrolysis of GTP to GDP, thus inactivating the signal. Activation of ephrinB in cerebellar granule cells was shown to inhibit G protein-coupled chemokine receptor mediated cell migration (Lu et al., 2001a).

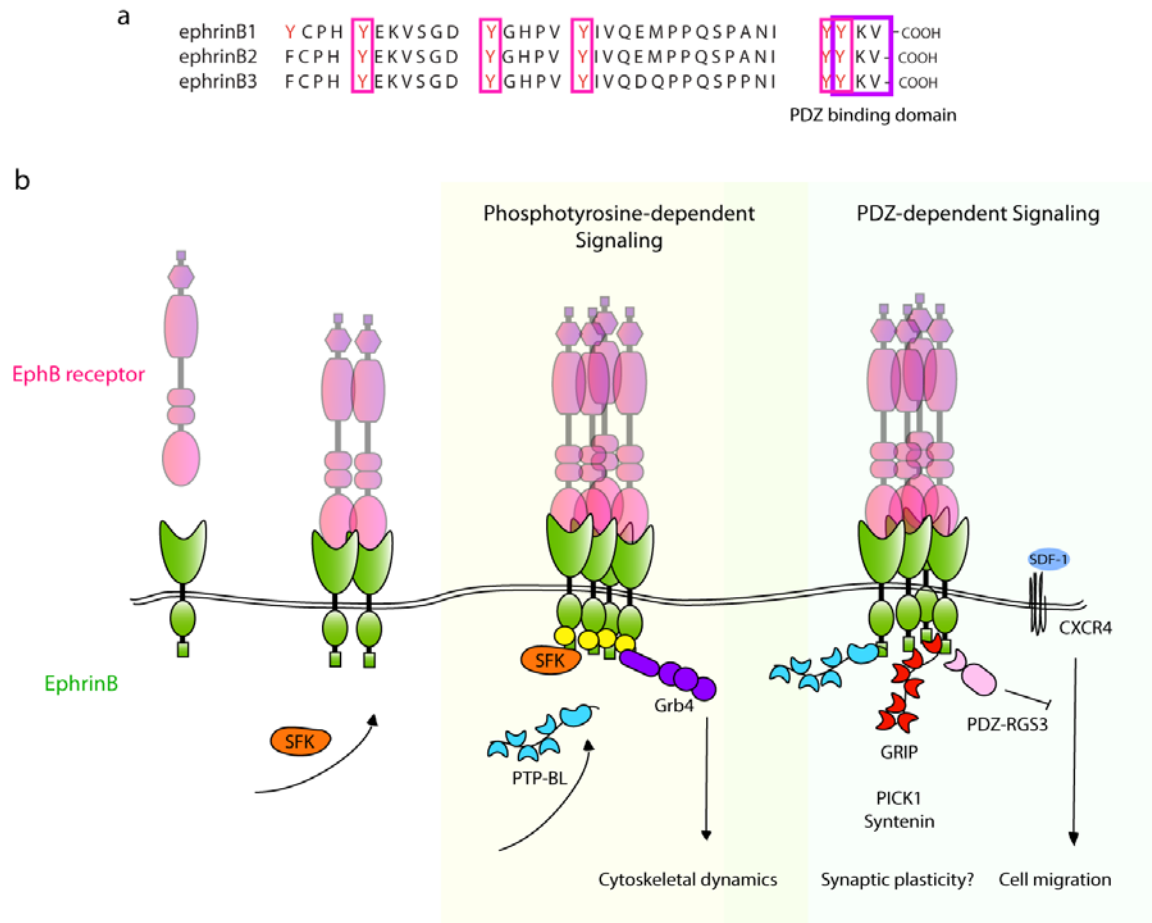


**Figure 4-12: EphrinB-reverse signaling- the switch model** (adapted from Palmer et al 2002). (a) The cytoplasmic domain of the three ephrinB ligands shows high sequence similarity. The five conserved tyrosines are highlighted in five pink boxes and serve as possible phosphorylation sites; the C-terminal PDZ-binding motif (purple box) is recognized by various PDZ-domain proteins. (b) Upon receptor engagement, ephrinB ligands are clustered, gathering signaling molecules and recruiting SFK to the membrane patches. SFK phosphorylates the ligand on tyrosines, allowing phosphotyrosine-binding molecules like Grb4 to bind and promote phosphorylation-dependent signaling. With a short delay, the phosphatase PTP-BL is recruited to activated ephrins and terminates phosphotyrosine signaling by dephosphorylating ephrin and inactivating SFK. However, still PDZ-binding takes place, including interaction with GRIP, PICK1, Syntenin and PDZ-RGS3, switching signaling from phosphotyrosine-dependent to PDZ-interaction based.

Interestingly, not only the cytoplasmic tailed ephrinB ligands but also the GPI anchored ephrinA ligands are thought to have their own signaling potential. There is evidence that ephrinA signaling participates in cellular functions but the molecular mechanism by which the signal is promoted remains unknown. For example, studies on the Eph receptor homologue VAB-1 in *C. elegans* revealed a kinase-independent function for VAB-1 in cellular organization that hints at a reverse signaling event via ephrinA ligand homologues (Wang et al., 1999). While some Eph receptors seem to inhibit integrin-mediated adhesion, ephrinA ligands have been shown to positively regulate cell adhesion and morphology via the activation of the SFK Fyn that co-localizes with ephrinA ligands in the membrane (Davy et al., 1999; Davy and Robbins, 2000; Huai and Drescher, 2001). Moreover, a recent study describes a repulsive function for ephrinA in retinal axons during guidance and mapping. Here, the p75 neurotrophin receptor (NTR) serves as a signaling partner for ephrinA and ephrin-A-p75 (NTR)-reverse signaling mediates retinal axon repulsion (Lim et al., 2008).

#### 4.8.2 Eph/ephrin interaction

The interaction of Eph receptors and ephrin ligands has been studied approached by X-ray crystallography (Himanen and Nikolov, 2002; Himanen and Nikolov, 2003; Himanen et al., 2001). The crystal structure of an EphB2-ephrin-B2-complex revealed a high affinity dimerization interface within the receptor and ligand binding domain (RBD, LBD) through which Eph receptors bind their ephrin ligands (Figure 4-13). Structurally, this binding is mediated by an extended loop of the ephrin ligand that is inserted into a channel at the surface of the receptor. The relevance of this interaction interface has been proved by studies using peptides that mimic the ephrin loop and successfully inhibit Eph-ephrin interactions. To form a cluster, two Eph-ephrin dimers join via a second distinct lower affinity interface to form a tetramer, in which each ligand interacts with two receptors and each receptor interacts with two ligands (Figure 4-13, a). The Eph and ephrin molecules are thought to be precisely positioned in these complexes which allow an aggregation, a so-called formation of higher-order clusters, and thus the initiation of bidirectional signaling. Indeed, functional Eph-ephrin signaling requires the generation of high-order

membrane clusters that assemble downstream signaling molecules. Experimentally, these cluster-formations can be induced by the application of soluble Eph- or ephrin-Fc fusion proteins (EphX/Fc or ephrinX/Fc; X- any A or B type) that have been pre-clustered with anti-Fc antibodies, an extensively used tool in this thesis. In the cell membrane these high order complexes, comprised of Eph/ephrins and associated molecules, appear as clusters of different shapes and sizes (Figure 4-13, b). The application of single, non-clustered, EphX/Fc or ephrinX/Fc molecules in contrast resembles the effect of an antagonist thus resulting in a signal blockage.

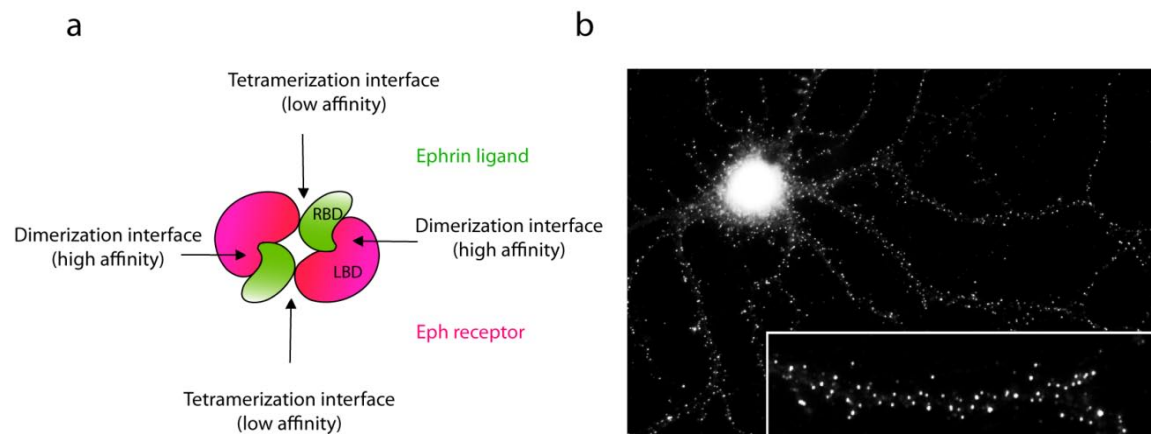


**Figure 4-13: Eph/ephrin cluster formation.** (a) Receptor-ligand interaction interfaces. The X-ray crystal structure of complexed EphB2-ephrinB2 interaction domains revealed a 2:2 heterotetramer containing two high affinity (Dimerization) and two lower affinity (Tetramerization) receptor-ligand interaction sites (Himanen and Nikolov, 2003). (b) A hippocampal neuron in culture shows punctuated ephrinB2 clusters all over the dendrites and the cell body. The neuron was stimulated with pre-clustered EphB4/Fc fusion protein to induce cluster formation.

Additional interfaces, distinct from the receptor/ligand binding domains, were found to promote high oligomerization of the receptors. These include the adjacent cysteine-rich domain and the sterile- $\alpha$ -motif (SAM) oligomerization domain located in the Eph cytoplasmic region. Furthermore, scaffolding proteins seem to be involved that bind the C-terminal PDZ-domain target site present in both Eph receptors and ephrinB ligands.

Questions concerning the composition and quality of these clusters, as well as, the number of molecules involved remain unanswered. Not much is known about the minimal size of a receptor or ligand cluster required for signalling, nor is it known whether the cluster size controls alternative signaling pathways. Considering the broad variety of Eph/ephrin-functions it seems reasonable to assume, that the molecular composition of the clusters might favor a specific signaling pathway. Another important aspect that remains uncertain is to what extent the clusters might contain different receptor or ligand types or if heterogenic mixtures occur at all.

#### 4.8.2.1 *Trans* and *Cis* interactions

In many regions of the developing organism Eph receptors and ephrins show complementary expression patterns. Receptor-ligand interaction occurs between opposing cells, namely in *trans*, allowing a crosstalk between migrating cells and the surrounding tissues. Given the ability of the Eph/ephrin system to mediate cell adhesion and repulsion, attachment and de-attachment, *trans*-interaction may be a key element in cellular compartmentalization, boundary formation and correct cell positioning in the tissue. In other cases, Eph receptors and ephrins are found to be co-expressed by the same cell, which led to the idea of a possible interaction in *cis*. The first evidence of *cis*-interaction was found in retinal axons, where the responsiveness of EphA-expressing axons was affected by ephrinA co-expression. *Cis*-interaction with co-expressed ephrinA reduced the tyrosine phosphorylation levels of EphA and the reaction to in-*trans*-applied ephrinA molecules (Carvalho et al., 2006; Hornberger et al., 1999; Yin et al., 2004). *Cis*-interaction might provide the cells with a tool for fine signal-tuning from a decrease in responsiveness up to complete inhibition. However, it is currently unknown how *cis*-interaction with ephrins reduces Eph receptor signaling. One hypothesis is that *cis*-interaction causes steric inhibition or spatial retraction separating Eph receptors from downstream signaling molecules. The occurrence of *cis*-interactions seems to depend on the cellular context rather than solely on the co-expression of receptor and ligand. Spinal motor axons, for example, co-express EphA4 receptors and ephrinA but they appear to accumulate in separate membrane domains and function independently (Marquardt et al.,

2005). However, proof for a *cis*-interaction in the B type of Eph receptors and ligands is so far missing.

### 4.8.2.2 Attraction/repulsion

Eph receptors and ephrins are known to be involved in opposing events such as repulsion/de-attachment and adhesion/attachment. Many factors are thought to regulate favor one or the other response cellular context, expression levels of receptor and ligand, splice variants and the composition of associated molecules favoring one event or the other. Cluster formation and the high-affinity interaction between Eph receptors and ephrin ligands on opposing cells can mediate cell adhesion. One mechanism that has been described to turn EphA-ephrinA-interaction into repulsion is the proteolytic cleavage of ephrinA by an ADAM proteinase. ADAM (a disintegrin and metalloprotease) proteins are membrane-anchored metalloproteases that mediate a wide variety of specific proteolytic events at the cell surface. The metalloproteinase Kuzbanian (KUZ), the *Drosophila* homolog of ADAM-10, was found to associate with ephrinA2 and to cleave the juxtamembrane domain of the ephrin molecule following receptor engagement and cluster formation. The cleavage goes hand in hand with a cytoskeletal collapse leading to de-attachment of the cells (Hattori et al., 2000). A more recent study showed that ADAM10 constitutively associates with EphA3 and that the formation of a functional EphA3/ephrinA5 complex leads to the effective cleavage of ephrin-A5 in *trans*. This mechanism ensures that only Eph bound ephrins are recognized and cleaved (Janes et al., 2005). A second mechanism to turn interaction into repulsion involves the rapid endocytosis of whole Eph/ephrin complexes leading to the retraction of interacting cells or neuronal growth cones. For example, the binding of EphB2 to ephrinB1, at the surface of opposing cells, has been reported to induce separation of the interacting cells. This separation was accompanied by the endocytosis of full-length proteins as complete EphB2/ephrinB1 complexes (transendocytosis). Transendocytosis occurred into either ligand- or receptor-expressing cells depending on the intracellular domains of the molecules. Furthermore, transendocytosis of Eph/ephrin complexes and the subsequent cell retraction has been shown to depend on actin polymerization and therefore on Rac

signaling (Marston et al., 2003; Zimmer et al., 2003). However the balance between reverse, forward and bidirectional endocytosis strongly depends on the cellular context, as does the balance between attachment and repulsion during path-finding of cells.

### **4.8.3 Eph/ephrin signaling outside the nervous system**

Aside from their function in the various cells of the nervous system, the Eph receptors and ephrins are found in cells types of other tissues such as immune cells, bone cells, stem cells, epithelial cells and in many types of tumor cells. Here, they play highly diverse roles at the level of cell-to-cell communication both during development and in the adult organism. These roles include the regulation of cell shape, attachment and de-attachment as well as cell attraction and repulsion, and directed cell migration. Hence, the interplay of the Eph receptors and ephrins at a cellular level directs the establishment of the structure and morphology of these tissues. (Arvanitis and Davy, 2008; Himanen et al., 2007; Palmer and Klein, 2003; Poliakov et al., 2004)

### **4.8.4 Eph/ephrin signaling in the nervous system**

Eph receptors and ephrin ligands were first described as axon guidance molecules mediating growth cone repulsion during the development of the central nervous system. Their functions include topographic mapping, axon guidance, cell migration and the establishment of regional patterns in the developing nervous system. Here they function, for example, in hind- and forebrain segmentation, neural crest cell and cerebellar granule cell migration, retinal and olfactory sensory axon guidance, thalamocortical projections and motor neuron-muscle innervations thus controlling the rhythmic walking. Many Eph and ephrin molecules remain abundant in the nervous system beyond the developmental stage and function in spine morphogenesis and synaptogenesis, neural-glia communication and synaptic plasticity.

#### **4.8.4.1 Eph/ephrin signaling in spine formation**

The roles of Eph receptors in spine morphogenesis have been studied extensively. In the mouse hippocampus, Eph receptors are expressed in distinct regions and here triple

EphB1/B2/B3 deficiency leads to neurons with impaired spine formation (Henkemeyer et al., 2003). As described in section 4.8.1.1, Eph receptors are involved in the regulation of actin dynamics via activation of Rho GTPases including Rho, Cdc42 and Rac1, which are required for spine formation. In addition, the molecule syndecan-2, a transmembrane heparin sulphate proteoglycan, was found to mediate EphB receptor-induced spine formation. EphB receptor activation induces syndecan-2 clustering which in turn promotes downstream signaling pathways resulting in cytoskeletal rearrangements (Ethell et al., 2001). Not much is known about how ephrin ligands participate in spine formation. In the hippocampus, Eph receptors and ephrinB ligands follow different synaptic expression patterns and their signaling occurs in a bi-directional fashion. In the synaptic connection between the CA3-CA1 region of the hippocampus the ephrinBs are exclusively expressed postsynaptically (Figure 4-14).

One goal of this thesis is to find out whether, similar to Eph receptors, ephrinB ligands are involved in spine morphogenesis.

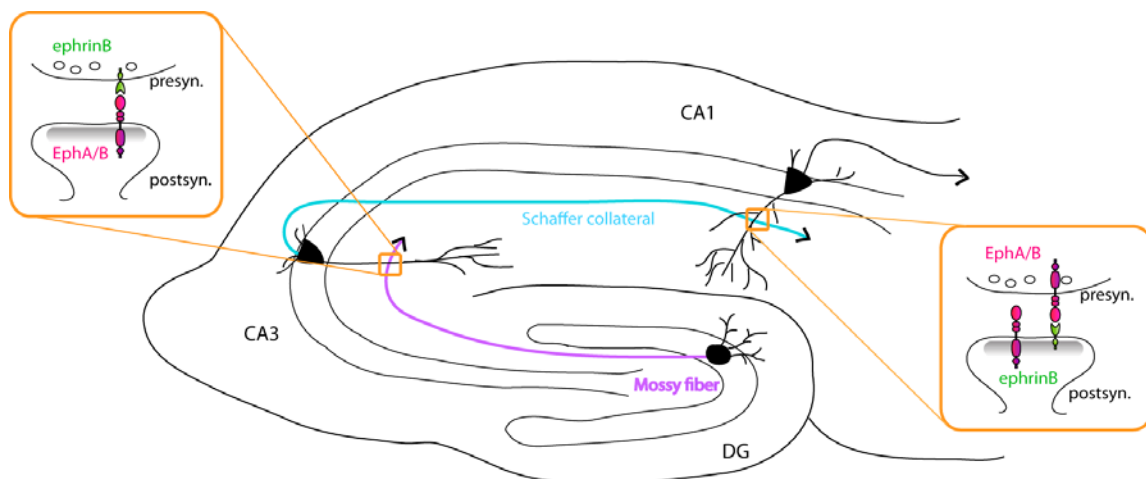


**Figure 4-14: Eph/ephrin expression in the murine hippocampus.** Schematic overview of the hippocampal pathways: The mossy fiber pathway connects presynaptic dentate gyrus (DG) and postsynaptic CA3 region neurons where Eph receptors are found postsynaptically, and ephrinBs are found presynaptically. The Schaffer collateral pathway connects presynaptic CA3 neurons and postsynaptic CA1 neurons. Here ephrinBs are found at the postsynaptic site whereas Eph receptors are expressed both pre and postsynaptically. The loss of postsynaptic ephrinB leads to defects in LTD and LTP, the molecular mechanism are unknown.

#### 4.8.4.2 Eph/ephrin signaling in synapse formation

A number of studies have investigated of EphB/ephrin *trans*-interaction in presynaptic differentiation the focus however solely addressing Eph receptor mediated forward signaling. The first evidence was provided by a study with cultured neurons where ephrinB-activated EphB receptors interact with NMDA receptors inducing their cluster formation. Subsequently, NMDA-clustering lead to the formation of presynaptic active sites (Dalva et al., 2000). Indeed, the activation of EphB2 in cultured cortical neurons potentiates the  $Ca^{2+}$ -influx through NMDA receptors and enhances  $Ca^{2+}$ -dependent gene expression that may affect synapse formation, maturation, and plasticity. Eph/ephrin interaction might therefore serve as an early initiating step promoting synapse formation and maturation (Takasu et al., 2002). The hippocampal neurons of triple EphB1-3 deficient mice showed not only impaired spine morphogenesis, but also a drastic reduction in the number of excitatory glutamatergic synapses and a decreased amount of NMDA and AMPA receptor clusters (Henkemeyer et al., 2003). Besides binding to NMDA receptors, EphB receptors interact with AMPA receptors via an independent binding domain controlling their localization and therefore presynaptic differentiation. Consequently, the knockdown of EphB2 in dissociated neurons results in a decrease of functional synaptic inputs and presynaptic specializations (Kayser et al., 2006). Recently, Kayser et al. provided a link between Eph receptor-induced spine motility and subsequent synapse formation. They showed that EphB forward signaling controls dendritic filopodia motility and allows pre- and postsynaptic partners to find each other. EphB/ephrin *trans*-synaptic interactions then stabilized nascent synaptic contacts, consequently specifically directing the formation of dendritic synapses (Kayser et al., 2008). Even though Eph receptor and ephrin ligands are differently expressed in hippocampal synapses, studies only suggest a link between reverse signaling and synapse formation without elucidating the underlying molecular mechanisms. Studies on the effect of ephrinB3 ligands in synapse number determination have been inconsistent. Grunwald et al. did not detect any differences in the synaptic structures of the hippocampus of mice lacking ephrinB3 (Grunwald et al., 2004). In contrast, Rodenas-Ruano et al. studied mice deficient in ephrinB3 and showed increased numbers of excitatory synapses in the hippocampal CA1 region, but reverse

signaling-independent changes in both pre- and postsynaptic molecules (Rodenas-Ruano et al., 2006). Furthermore, Aoto et al. who looked specifically at two different synapse types found differences in only one of them: ephrinB3 knock-out mice had reduced numbers of shaft synapses in the hippocampus while spine synapses were normal (Aoto and Chen, 2007).

### 4.8.4.3 Eph/ephrin signaling during synaptic plasticity

By activating cytoskeleton remodelling pathways, the Eph/ephrin system modulates synapse formation and spine morphogenesis and thus controls plasticity at a morphological level. Ephs and ephrins further regulate synaptic plasticity at the molecular level by influencing molecules responsible for synaptic transmission like NMDA or AMPA receptors, adaptor proteins or downstream molecules. As mentioned in the previous chapter, mice deficient in EphB2 display abnormal NMDA-receptor dependent synaptic plasticity, as well as reduced numbers of NMDA and AMPA receptors. In the CA3-CA1 region of the mouse hippocampus, ephrinB2 and ephrinB3 are solely postsynaptically expressed whereas the receptors EphB2 or EphA4 are found both, pre- and postsynaptically (Figure 4-14). The ablation of ephrinB2 or ephrinB3 in these neurons leads to strong defects in certain forms of plasticity such as LTP and LTD. To a comparable extent, the ablation of EphB2 or EphA4, both interaction partners of ephrinB2 and ephrinB3, resulted in impaired synaptic plasticity (Grunwald et al., 2004; Grunwald et al., 2001). However, the receptor-related defects were shown to be independent of the receptor's cytoplasmic domain and are thus said to be forward-signaling independent. The reintroduction of a receptor-GFP-fusion protein, where the cytoplasmic tail of the receptor was substituted by GFP, fully restored the deficiency-phenotype of the receptors. These results suggest the contribution of a signaling pathway downstream of ephrinB ligands in the regulation of long-term plasticity, but the molecular mechanism remains unclear. Since the amount of active AMPA receptors at the synapse determines its synaptic strength, a key feature of synaptic plasticity is the regulation of AMPA-receptor trafficking.

The second part of this thesis addresses the question of whether ephrinB ligands might be involved in the regulation of AMPA-receptor trafficking, explaining their impact on synaptic plasticity.

## **5 Results**

### **5.1 Grb4 and GIT1 transduce ephrinB reverse signals modulating spine morphogenesis and synapse formation**

Spine morphogenesis and synapse formation are known to be important processes both in the developing brain, when neuronal circuits are established, and in the mature brain during synaptic plasticity. These processes involve rearrangements of the cytoskeleton governed by various signaling pathways (Geinisman, 2000; Yuste and Bonhoeffer, 2001). Eph-receptor forward signaling has been shown to be required for spine morphogenesis and to act upstream of cytoskeleton remodeling events (Ethell et al., 2001; Henkemeyer et al., 2003; Penzes et al., 2003). In the hippocampus, Eph receptors and ephrinB ligands follow different synaptic expression patterns and their signaling occurs in a bi-directional fashion. For example, in the CA3-CA1 region, ephrinBs are exclusively expressed postsynaptically and their signaling is required for long-term plasticity (Grunwald et al., 2004). Therefore, similar to Eph receptors, ephrinB ligands might be involved in changes in spine morphology. The aim of this study was to investigate the impact of ephrinB-reverse signaling in spine formation and to uncover the signaling pathway acting downstream of ephrinB.

The first part of the result section will deal with my contribution to the study entitled: “Grb4 and GIT1 transduce ephrinB reverse signals modulating spine morphogenesis and synapse formation” (Nature Neuroscience 2007, Vol. 10 pages 301-10). This involved mainly measurements of spine morphology and synaptogenesis in cell cultures treated with agonists and interference molecules of ephrin signaling. The accompanying molecular biological and biochemical experiments were mainly performed by I. Segura and S. Weinges. Interaction and interference experiments (Weinges, 2006).

#### **5.1.1 EphrinB-reverse signaling promotes spine morphogenesis**

Synaptic contacts are stabilized by the formation of mature spines. During the process of spine maturation, filopodia-like dendritic protrusions acquire a typical mushroom-like

shape with bulbous heads and short dendritic shafts. Eph receptor signaling has been shown to be involved in spine morphogenesis since hippocampal neurons from EphB-receptor deficient mice fail to form dendritic spines (Henkemeyer et al., 2003). EphrinB ligands are found in postsynaptic compartments and are known to interact with postsynaptic proteins. In fact, they are the active signaling partners in the postsynaptic CA1 region. Therefore, we wanted to determine whether ephrinB ligands could modulate spine morphology. To test this, we stimulated cultured hippocampal neurons (14DIV) for 8 hours with pre-clustered EphB2-Fc or Fc (control). To visualize the protrusions, the neurons were transfected with yellow fluorescent protein (YFP) two days prior to the experiment. Spine maturation was assayed by measuring spine length, the number of spines with heads and the spine-head area (**Figure 5-1**). Combining all assigned criteria, neurons showed an increased number of mature spines with short shafts and spine heads following EphB2-Fc stimulation (**Figure 5-1, a**). The mean protrusion length was decreased from  $1.74 \mu\text{m} \pm 0.03$  (control) to  $1.10 \mu\text{m} \pm 0.02$  (EphB2-Fc) in ephrinB activated neurons (**Figure 5-1, a**). Moreover,  $60.1 \% \pm 4.1$  of the protrusions were shorter than  $1 \mu\text{m}$  in EphB2-Fc treated neurons compared to  $28.3 \% \pm 3.5$  in control neurons (Fc). Additionally, the formation of spine heads was considered to be an indication of maturity (**Figure 5-1, b** lower panel). Here, EphB2-Fc-stimulated neurons were found to have more mature spines ( $85 \% \pm 1.5$  spines with heads) compared to control cells (Fc) ( $45.3 \% \pm 2.7$ ). Moreover, the average size of the heads was significantly larger in ephrinB-activated neurons with  $0.66 \mu\text{m}^2 \pm 0.01$  spine-head area compared to  $0.37 \mu\text{m}^2 \pm 0.01$  in control cells (**Figure 5-1, c**). Taken together, these results clearly demonstrate a positive impact of ephrinB reverse signaling in spine maturation. Indeed, EphB2-Fc-application resulted in a reduction of long filopodia-like protrusions leading to an increased number of mature spines with characteristically short dendritic shafts and bulbous-shaped heads.

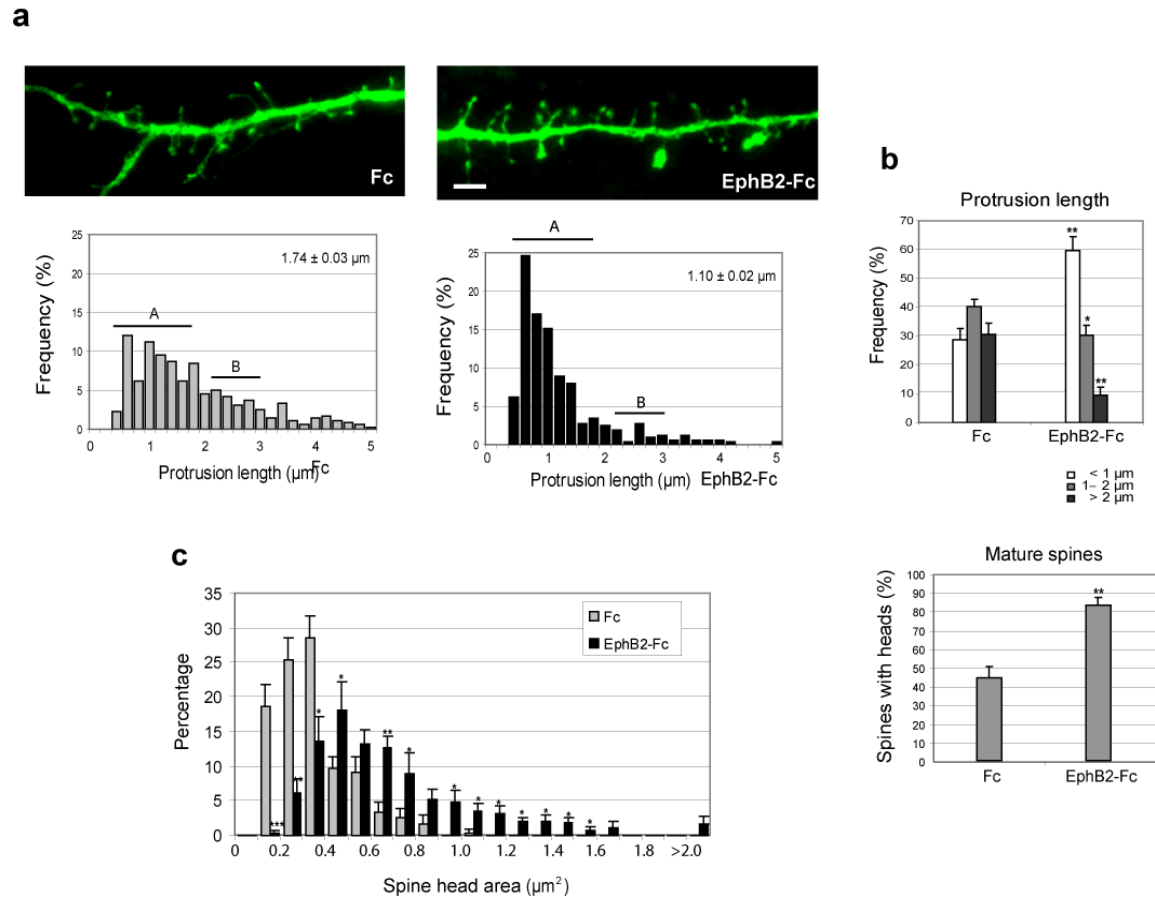


**Figure 5-1: EphrinB signaling promotes spine morphogenesis.** (a) Rat hippocampal neurons transfected with YFP (12DIV) and stimulated after two days with pre-clustered EphB2-Fc or Fc (control) for 8 hours. The length of dendritic protrusions ( $n > 500$ ) was quantified (right panels). Group A represents spines and group B represents dendritic filopodia based on the length. Scale bar, 2  $\mu\text{m}$ . (b) Statistical analysis of spine morphogenesis in hippocampal neurons stimulated with pre-clustered Fc or EphB2-Fc. The spine morphogenesis was assayed by analysis of protrusion length (upper panel) and by percentage of mature mushroom-like spines relative to total number of protrusions (lower panel). (c) Quantification of spine-head area in hippocampal neurons stimulated with pre-clustered Fc or EphB2-Fc. (SEM, \*  $P < 0.05$ ; \*\*  $P < 0.005$ ; \*\*\*  $P < 0.0005$ ).

### 5.1.2 Interference with ephrinB-reverse signaling impairs spine formation

In the previous experiment we showed that activation of ephrinB-reverse signaling promoted spine maturation in cultured hippocampal neurons. To confirm this, we inhibited ephrinB signaling by over-expressing a truncated form of ephrinB and measured the resulting effects on spine maturation. Hippocampal neurons were transfected with an ephrinB1 mutant (ephrinB1 $\Delta$ C) that lacks the intracellular domain and is therefore

incapable of signaling. This mutant is predicted to compete with endogenous ephrinB molecules for Eph-receptor binding, thus diminishing the signal.

Young hippocampal neurons (7DIV) were transfected with YFP alone to visualize the outlines of the neurons, or together with ephrinB1 $\Delta$ C-CFP. We then analyzed these neurons for the morphology of dendritic protrusions four days after transfection. The ephrinB1 $\Delta$ C expressing neurons showed remarkably more filopodia-like protrusions (>2  $\mu$ m) than the YFP expressing control cells (**Figure 5-2, a**). Consequently, the amount of mature spines (protrusions < 2  $\mu$ m) in these neurons was less frequent compared to those present in the control neurons (YFP) (**Figure 5-2, a+b**). Taken together, the mean protrusion length of 1.91  $\mu$ m  $\pm$  0.29 seen in control cells was increased to 2.55  $\mu$ m  $\pm$  0.03 in cells with impaired ephrinB signaling.

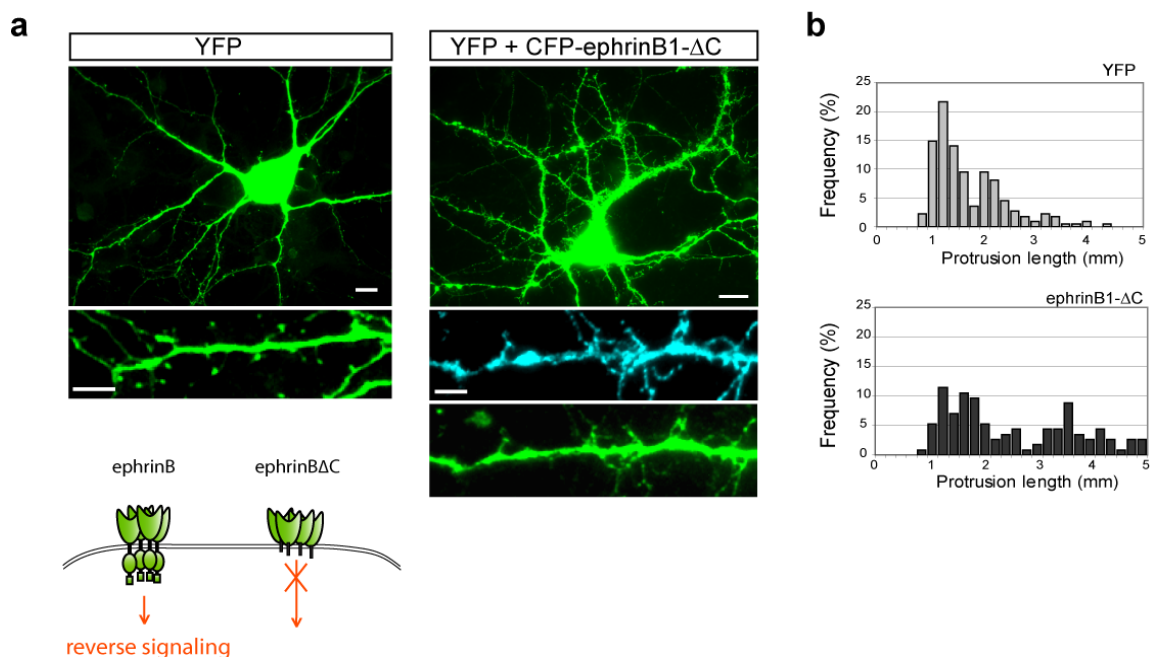


**Figure 5-2: Interference with ephrinB-reverse signaling impairs spine maturation.** (a) Hippocampal neurons (7DIV) were transfected with YFP or YFP plus ephrinB1 $\Delta$ C-CFP and analyzed for the morphology of dendritic protrusions four days later. Scale bars: 10  $\mu$ m whole neurons, 1  $\mu$ m enlargements. (b) Quantifications of the protrusion length from neurons represented in (a) ( $n > 500$ ). YFP transfected cells (upper panel), double transfected with YFP and ephrinB1 $\Delta$ C-CFP (lower panel).

Spine formation in cultured hippocampal neurons occurs after 11-14 DIV depending on cell density. We repeated the interference experiment with older neurons to confirm the relevance of ephrinB-reverse signaling on spine maturation. Neurons were transfected with YFP alone or together with ephrinB1 $\Delta$ C-CFP at day 11 in culture and analyzed the morphology of dendritic protrusions three days later. The same effect that was seen in young neurons was also observed in older neurons (14DIV) expressing the truncated version of ephrinB1. Quantifications revealed a clear shift of the distribution of spines from mature spines towards more filopodia-like protrusions (**Figure 5-3**).

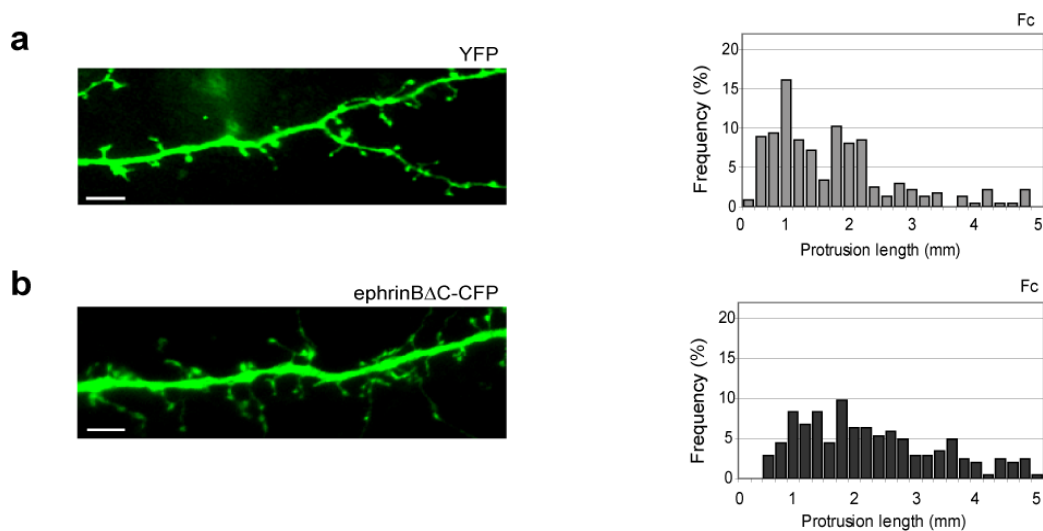


**Figure 5-3: Truncated ephrinB1 impaired spine formation in older neurons (14DIV).** (a) Hippocampal neurons transfected (11DIV) with YFP (control) to visualize the outline of the cell. Protrusions were analyzed three days after transfection. Protrusion length of control neurons was quantified and pictured as frequency per length unit. (b) Hippocampal neuron double transfected with YFP and ephrinB1 $\Delta$ C-CFP analyzed and quantified as in (a).

#### 5.1.2.1 EphrinB reverse signaling acts independent of EphB receptor forward signaling in spine maturation

Previous studies have shown that EphB receptor signaling promotes spine maturation and that interference with forward signaling alters the spine morphology of cultured neurons

(Henkemeyer et al., 2003). Therefore, we next wanted to prove that the effect seen following the transfection of ephrinB1 $\Delta$ C was specific for reverse signaling and not due to the interference with forward signaling in those neurons. In order to promote a signal, ephrinB ligands and Eph receptors need to form high-order clusters which assemble signal transducing molecules. Here, we made use of this fact and applied unclustered, single, soluble ephrinB2-Fc molecules to the cells to occupy and, therefore, block EphB receptors from signaling.

Hippocampal neurons transfected with YFP at 7DIV were treated seven days after transfection (14DIV) for 8 hours with Fc (control), or unclustered ephrinB2-Fc to block Eph receptor forward signaling, or with unclustered ephrinB2-Fc and clustered EphB2-Fc to activate ephrinB reverse signaling. As expected, Eph receptor blockage (un-eB2) resulted in an increase of filopodia-like protrusions and a reduction of mature spines compared to control cells (**Figure 5-4, a+b, g-f**). Instead, while Eph receptor signaling was blocked by unclustered ephrinB-Fc molecules, the simultaneous activation of ephrinB reverse signaling with pre-clustered EphB2-Fc evoked a significant increase in spine maturation, pictured and quantified in **Figure 5-4, c+g-f**. Additionally, to show the independence of forward signaling from impaired reverse signaling, hippocampal neurons were transfected with the mutant ephrinB1 $\Delta$ C-CFP + YFP and stimulated with pre-clustered Fc (control), EphB2-Fc or ephrinB2-Fc. Consistent with the previous observations, expression of truncated ephrinB1 impaired spine maturation thus leading to an increase of filopodia-like protrusions compared to control cells (**Figure 5-4, d, g-f**). As expected, activating reverse signaling with EphB2-Fc did not rescue the phenotype (**Figure 5-4, e, g-f**). However, despite impaired reverse signaling, the activation of EphB receptor forward signaling via pre-clustered ephrinB2-Fc molecules led to enhanced spine maturation in these neurons. Taken together, these results suggest that ephrinB reverse signaling leads to spine maturation independently of EphB forward signaling. Therefore, the impaired spine maturation seen in neurons, which over-express the signaling mutant ephrinB1 $\Delta$ C, is not likely to be caused by EphB receptor dysfunction.

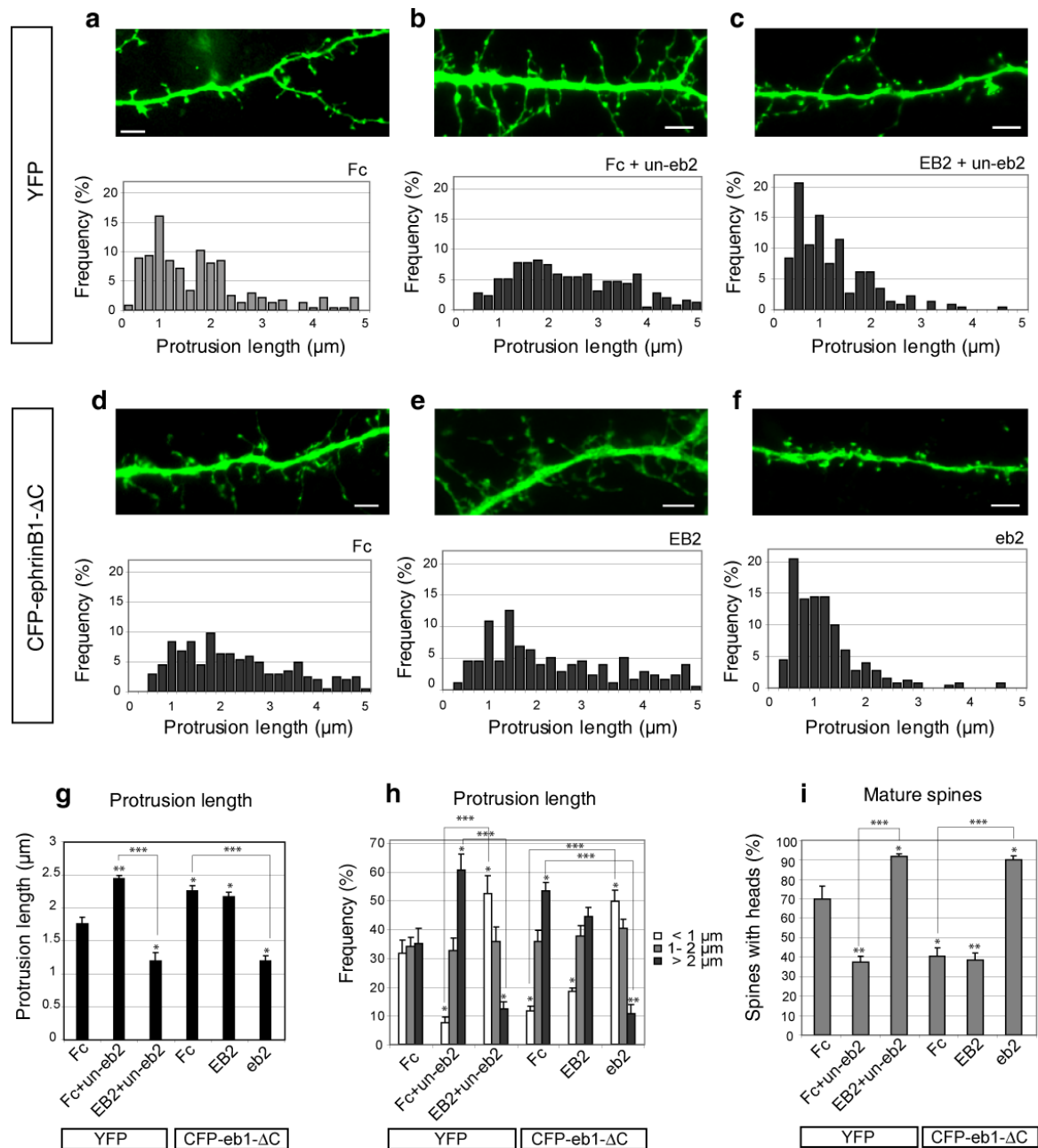


**Figure 5-4: EphrinB-reverse signaling acts independent of forward signaling in spine maturation.** (a-f) Hippocampal neurons were transfected with YFP alone or together with ephrinB1 $\Delta$ C-CFP at 7DIV. The neurons were stimulated 7 days after transfection with pre-clustered Fc (a, d), unclustered ephrinB2-Fc (b+c), or pre-clustered ephrinB2-Fc (f) or EphB2-Fc (c+e) and analyzed for the morphology of dendritic spines. Scale bars 1  $\mu$ m. (a-i) Quantification and statistical analysis of protrusion length and number of spine heads under the given conditions (n>500). (SEM, \* P<0.05; \*\* P<0.005, \*\*\* P<0.0005).

In these experiments, the proportion of filopodia-like structures in neurons (14DIV) expressing ephrinB1 $\Delta$ C was increased to  $52.9\% \pm 1.4$  compared to  $34.8\% \pm 5.3$  in YFP transfected control cells (**Figure 5-4, g**). The average protrusion length grew from  $1.76\ \mu\text{m} \pm 0.10$  to  $2.26\ \mu\text{m} \pm 0.03$  and the percentage of mature spines with heads decreased from  $70.2\% \pm 6.6$  to  $40.5\% \pm 3.1$  (**Figure 5-4, h+i**). These results suggested that ephrinB-reverse signaling promotes spine maturation and is necessary for proper spine development.

### 5.1.3 Spine morphogenesis downstream of ephrinB mediated via Grb4 and GIT1

Spine morphogenesis and spine formation are known to require local Rac activity, resulting from the assembly of a Rac-activating complex, consisting of the G-protein coupled receptor kinase-interacting protein 1 (GIT1) and the exchange factor for Rac,  $\beta$ -Pix (Zhang et al., 2003). Downstream of Rac, the p21-activated kinase and myosinII regulatory light chain promote spine formation (Zhang et al., 2005). Using various biochemical and molecular biological approaches, we have shown ephrinB ligands to be upstream of the Rac pathway, thus regulating the recruitment of involved signaling molecules to the synaptic membrane.

In particular, we found that Grb4, an adaptor protein containing SH2 and SH3 domains, and a known transducer of ephrinB reverse signals (Cowan and Henkemeyer, 2001), binds and recruits GIT1 to synapses upon ephrinB ligand activation Eph receptors. Furthermore, we identified a phosphorylation site (tyrosine392) in the synaptic localization domain (SLD) of GIT1 which is involved in the regulated binding of GIT1 to the SH2 domain of Grb4, and showed that the phosphorylation occurs upon ephrinB activation (Weinges, 2006).

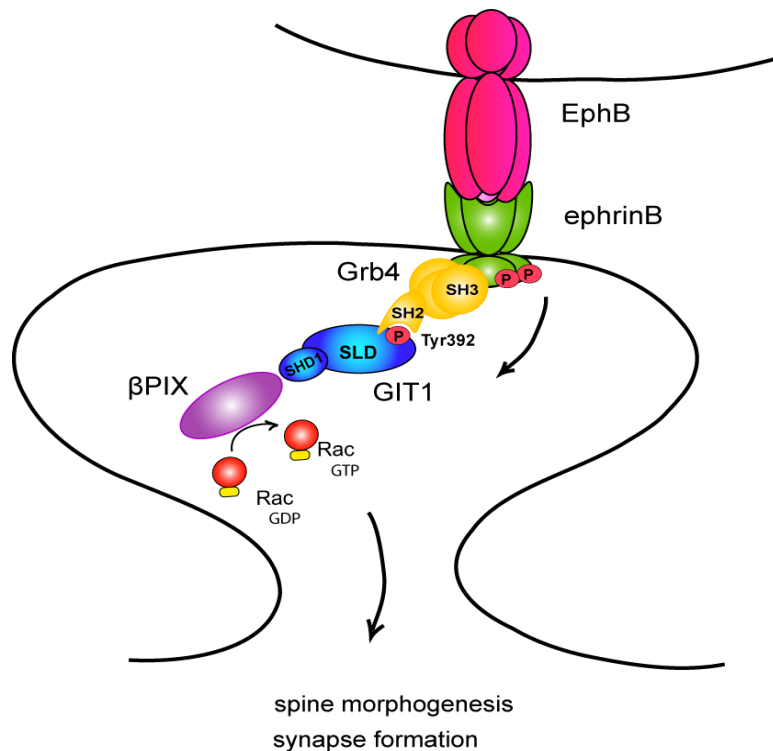


**Figure 5-5: Our model of ephrinB-reverse signaling pathway during spine formation.** EphrinB ligands are located at the synaptic membrane and are activated by opposed Eph receptors during synaptic contacting. Upon receptor binding ephrinB ligands form clusters assembling activated Src family kinases (SFK). Src phosphorylates GIT1 on tyrosine 392 located in the SLD (synaptic localization domain) and now allows Grb4 to bind. Grb4 in turn interacts with membrane anchored ephrinB via its SH3 domain and localizes the Rac signaling complex, composed of GIT1 and βPix (exchange factor for Rac) to the synaptic compartment.

### 5.1.3.1 Disruption of ephrinB signaling through Grb4-SH2 domain and an ephrinB peptide (p313-335)

To determine whether the ephrinB-Grb4-GIT1 pathway plays a physiological role in spine morphogenesis, we interfered with this pathway in two separate experiments. First, we over-expressed the SH2 domain of Grb4 (Grb4-SH2) in hippocampal neurons to interfere with the endogenous binding of GIT1 to Grb4. As a second approach, we transfected neurons with a short ephrinB peptide (p313-335), which is known to contain the amino acid sequence essential for interaction with Grb4 (Cowan and Henkemeyer, 2001). The relevance of GIT1 in spine maturation had already been shown via over-expression of GIT1-SLD, the recognition site for Grb4, which resulted in a severe increase of long, thin, filopodia-like protrusions on dendrites (Zhang et al., 2003).

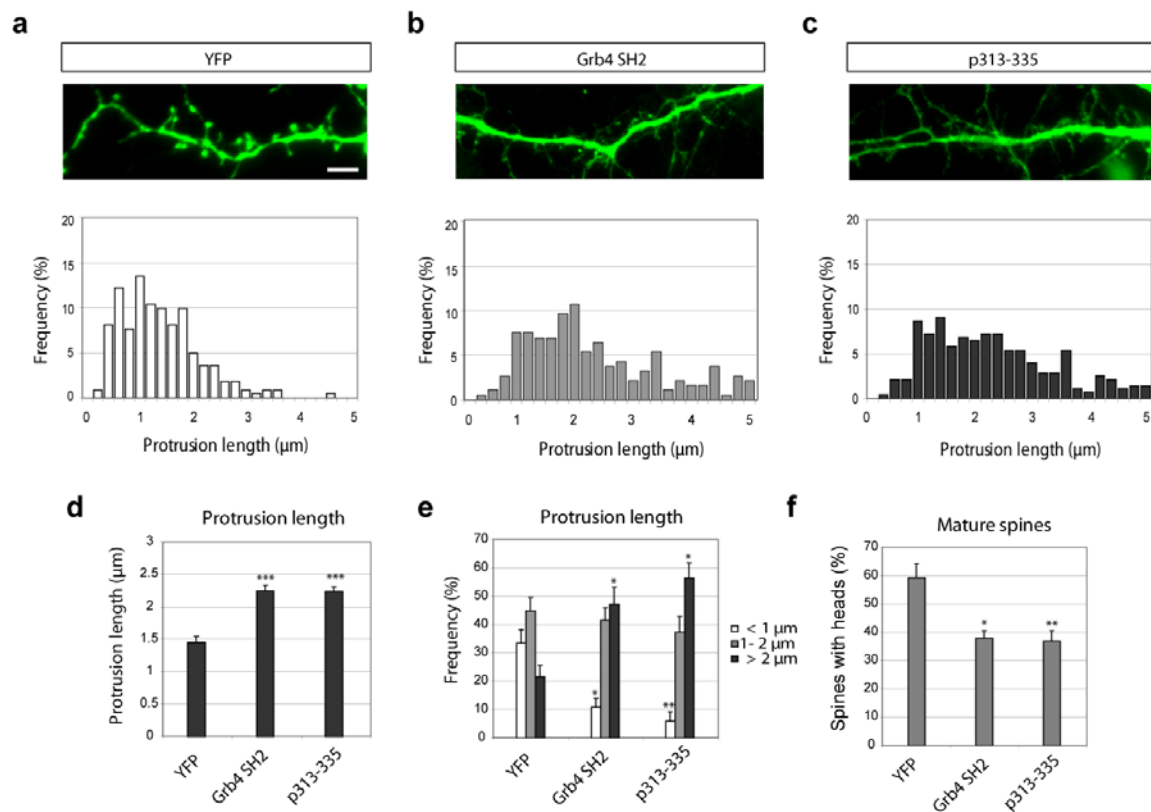


**Figure 5-6: Disruption of ephrinB signaling through Grb4-SH2 and ephrinB peptide (p313-335).** (a-c) Hippocampal neurons were transfected with YFP, Grb4-SH2 YFP or p313-335 YFP at 11DIV and analyzed for protrusion morphology three days later. Quantification of protrusion lengths of neurons expressing each of the constructs ( $n > 500$ ) are pictured in the lower panels. Scale bar 1  $\mu\text{m}$ . (d-f) Statistical analysis of protrusion length and frequency of mature spines (spines with heads) comparing YFP, Grb4-SH2 YFP and p313-335 YFP expressing neurons. (SEM, \*  $P < 0.05$ ; \*\*  $P < 0.005$ ; \*\*\*  $P < 0.0005$ ).

We transfected hippocampal neurons (11DIV) with either YFP (control), Grb4-SH2 YFP, or p313-335 YFP and analyzed the morphology of dendritic protrusion after three days. The expression of both molecules led to an increase of long, thin protrusions resembling the described GIT1-SLD phenotype (**Figure 5-6, a-c**). The average protrusion length was increased from  $1.47 \mu\text{m} \pm 0.09$  in control cells (YFP) to  $2.27 \mu\text{m} \pm 0.09$  in Grb4-SH2 YFP and to  $2.26 \mu\text{m} \pm 0.01$  in p313-335 YFP transfected neurons (**Figure 5-6, d**). The percentage of filopodia-like protrusions was significantly increased from  $21.6 \% \pm 4.0$  in control cells (YFP) to  $47.3 \% \pm 6.0$  in Grb4-SH2 YFP and to  $56.7 \% \pm 5.3$  in p313-335 YFP expressing cells (**Figure 5-6, e**). Conversely, the proportion of mature spines with heads was reduced from  $59.8 \% \pm 5.2$  in control neurons (YFP) to  $38.3 \% \pm 2.6$  in Grb4-

SH2 YFP and to  $37.3 \% \pm 3.6$  in p313-335 YFP transfected neurons (**Figure 5-6, f**). These results clearly demonstrate the relevance of the ephrinB-Grb4-GIT1 signaling pathway in spine maturation of cultured hippocampal neurons.

### 5.1.3.2 Disruption of ephrinB signaling through specific ephrinB mutants

Given that Grb4 and GIT1 are essential for proper spine formation, we next confirmed the requirement for ephrinB reverse signaling acting upstream of Grb4 and GIT1. We expressed two different ephrinB mutants, one lacking the Grb4-binding sequence (ephrinB1 $\Delta$ 313-335 CFP) and the other deficient in phosphotyrosine signaling (ephrinB1-6F CFP), in which all cytoplasmic tyrosines were replaced by phenylalanine.

Hippocampal neurons 11DIV were transfected with CFP or ephrinB1 $\Delta$ 313-335 CFP or ephrinB1 6F CFP and analyzed for spine morphogenesis three days later. Both mutants led to a severe increase of filopodia-like dendritic protrusions (**Figure 5-7, a-c**). The average protrusion length increased from  $1.78 \mu\text{m} \pm 0.08$  in control cells (CFP) to  $2.67 \mu\text{m} \pm 0.09$  in ephrinB1 $\Delta$ 313-335 CFP, and to  $2.92 \mu\text{m} \pm 0.10$  in ephrinB1 6F CFP expressing neurons (**Figure 5-7, d**). The percentage of long filopodia was increased from  $35.13 \% \pm 4.03$  in control neurons (CFP) to  $76.25 \% \pm 1.08$  or  $76.04 \% \pm 3.80$  respectively in ephrinB1 $\Delta$ 313-335 CFP or ephrinB1 6F CFP transfected neurons. Moreover, most of the protrusions in both ephrinB1-mutant expressing cells were devoid of spine heads, a criterion used for the identification of mature spines.

Taken together, these results demonstrate that the recruitment of GIT1 and Grb4 to synapses following ephrinB activation is essential for correct spine morphogenesis.

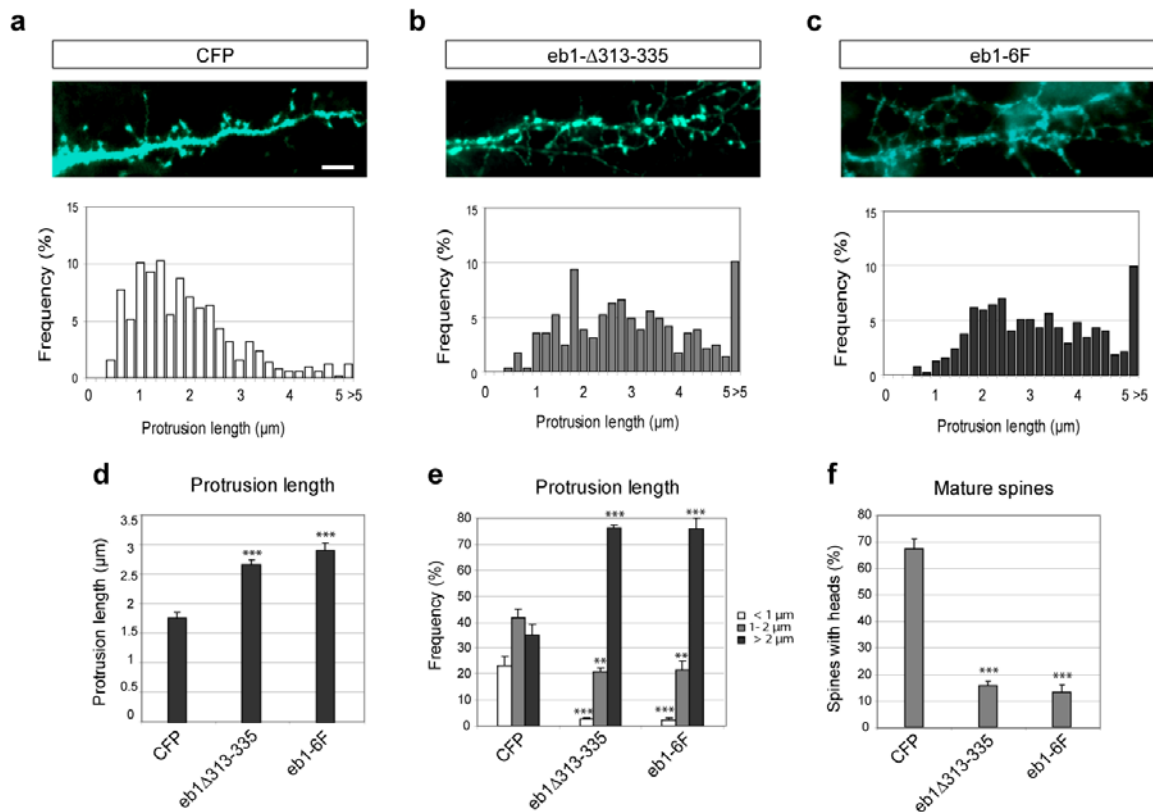


**Figure 5-7 : Disruption of ephrinB signaling through ephrinB1 $\Delta$ 313-335 and ephrinB1 6F.** (a-c) Hippocampal neurons were transfected with CFP, ephrinB1 $\Delta$ 313-335 CFP or ephrinB1 6F CFP at 11DIV and analyzed for protrusion morphology three days later. Quantification of protrusion lengths of neurons under each transfection condition (n>500) are pictured in the lower panels. Scale bar 1 $\mu$ m. (d-f) Statistical analysis of protrusion length and frequency of mature spines (spines with heads) comparing CFP, ephrinB1 $\Delta$ 313-335 CFP and ephrinB1 6F CFP expressing neurons. (SEM, \* P<0.05; \*\* P<0.005; \*\*\* P<0.0005).

### 5.1.3.3 Disruption of ephrinB signaling via Grb4 and GIT1 impairs synapse formation

Spine maturation during development and synaptic remodelling occur when synaptic contacts are stabilized. In cultured hippocampal neurons, spine morphogenesis goes hand-in-hand with the establishment of synaptic contacts and consequent synapse formation. Interruption of ephrinB-Grb4-GIT1 signaling resulted in impaired spine maturation and led to an increase in immature filopodia-like dendritic protrusions. Therefore, we wanted to investigate whether synapse formation was affected in neurons expressing the signaling

inhibitors Grb4-SH2 and p313-335. We transfected hippocampal neurons at day 11 in culture with YFP only, Grb4-SH2 YFP, or p313-335 YFP and monitored synaptic markers three days after transfection. We used two different markers (PSD-95 as a postsynaptic molecule and synapsin1 as a presynaptic molecule) to detect synapses using immunofluorescence. Synapse density was determined by counting the numbers of PSD-95 or synapsin1 positive clusters along different dendrite stretches for each condition. The numbers were normalized to a dendrite stretch of 100  $\mu\text{m}$ . The neurons expressing Grb4-SH2 or p313-335 showed a significant reduction in the number of clusters of both synaptic markers indicating a severe impairment in synapse maturation.

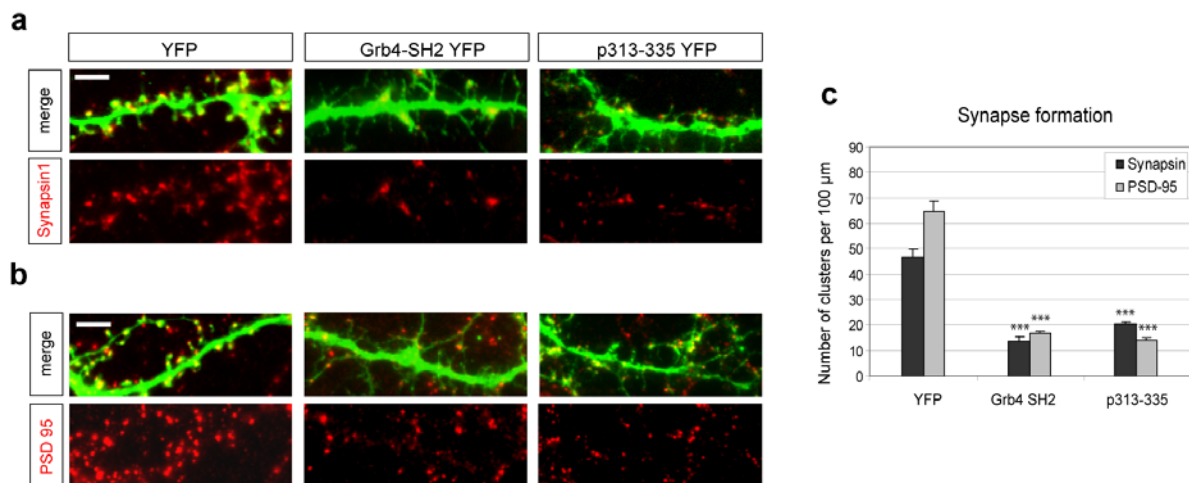


**Figure 5-8: Disruption of ephrinB-Grb4-GIT1 pathway affects synapse formation.** (a+b) Hippocampal neurons (11DIV) were transfected with YFP (control) or with Grb4-SH2 YFP or p313-335 YFP to interfere with downstream ephrinB signaling. Three days after transfection the neurons were analyzed for synapse formation via immunofluorescence using antibodies against the synaptic markers PSD-95 (red) or synapsin1 (red). Scale bars 1  $\mu\text{m}$ . (c) Quantification of synapse density per dendrite stretch for each transfection condition counting numbers of PSD-95 or Synapsin1 positive puncta. (SEM, \*\*\*  $P < 0.0005$ ).

Taken together, ephrinB-reverse signaling via the recruitment of Grb4 and GIT1 is important not only for proper spine formation but is also necessary for neurons to make and stabilize synaptic contacts.

## 5.2 Serine phosphorylation of ephrinB2 regulates trafficking of synaptic AMPA receptors

Previous studies have shown that ephrinB2 molecules play an important role in hippocampal plasticity (Grunwald et al., 2004). Indeed, mice lacking ephrinB2 have strong defects in Schaffer collateral long term potentiation (LTP) and long term depression (LTD), but the underlying molecular mechanisms are unknown. The results presented in the previous section point to a signaling complex containing Grb4 and GIT1 that is involved in the regulation of spine formation by ephrinB ligand signaling (Segura et al., 2007). In addition to synapse morphology, ephrinB ligands might regulate other processes associated with synaptic plasticity. Since the number of active AMPA receptors at the postsynaptic site determines the strength and responsiveness of the synaptic contact, AMPA-receptor trafficking is a key process involved in LTP and LTD. LTP is known to be controlled by the incorporation of additional AMPA receptors into the active synapse, whereas, during LTD, AMPA receptors are removed from the postsynaptic sites by endocytosis (Beattie et al., 2000; Brecht and Nicoll, 2003; Hayashi et al., 2000; Lee et al., 2002; Plant et al., 2006; Shi et al., 2001). In the following study we investigated whether the plasticity defects seen in ephrinB2 conditional knockouts are due to mis-regulation of AMPA-receptor trafficking.

### 5.2.1 EphrinB2 reverse signaling regulates AMPA-receptor trafficking

Two different approaches were used to study AMPA-receptor trafficking and to show the influence of ephrinB2 reverse signaling on this process. We used the biochemical technique of surface biotinylation to detect changes in the number of receptors present at the cell surface. A complementary immunofluorescence method we call “antibody feeding assay” was used to track receptor molecules moving in and out of the plasma membrane.

### 5.2.1.1 EphrinB2 reverse signaling prevents endocytosis of GluR2 in 293 GluR2 cells

In our biochemical experiments, 293 HEK cells stably expressing the GluR2 subunit of the AMPA receptor were transfected with ephrinB2 YFP and AMPA-receptor trafficking under various stimulation conditions was analyzed using surface biotinylation (7 Material and Methods). Cells plated in 10 cm culture dishes were starved for 24 hours after transfection and treated with a thiol-cleavable amine-reactive biotin to mark all proteins currently at the cell surface. Afterwards, the biotin-labelled cells were stimulated with pre-clustered EphB4-Fc or Fc (control) for 30 minutes and/or with 100  $\mu$ M AMPA for 5 minutes and their lysates analyzed for GluR2 internalization in Western blots (**Figure 5-9**).

Stimulation with AMPA resulted in a robust internalization of GluR2 indicated by a strong signal on the Western blot (**Figure 5-9**). In contrast, simultaneous activation of ephrinB2 by EphB4-Fc, the ephrinB2 specific receptor, completely inhibited AMPA-induced GluR2 internalization. EphB4-Fc stimulation alone slightly reduced the level of AMPA-receptor endocytosis compared to the control condition (Fc).

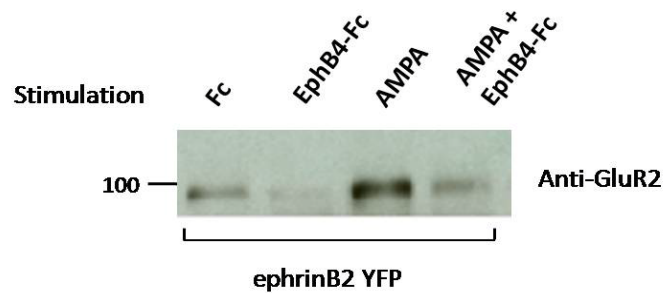


**Figure 5-9: EphrinB2 activation inhibits AMPA-receptor internalization in 293 GluR2 cells.** Surface biotinylation assay using 293 HEK GluR2 cells transfected with ephrinB2 YFP and stimulated as indicated. The cells were incubated with biotin to label cell surface proteins. After stimulation, the remaining surface biotin was removed and the internalized biotin-marked molecules precipitated from the cell lysates with straptavidin beads. AMPA-receptor internalization was analyzed by Western blot using anti-GluR2 antibodies. The strength of the signal correlates to the amount of internalized AMPA receptors.

### 5.2.1.2 EphrinB2 reverse signaling blocks AMPA-receptor endocytosis in cultured hippocampal neurons

We next investigated the influence of ephrinB2 on AMPA receptors in a more physiological system using primary hippocampal neurons. First, in analogy to the 293 cell-experiment, we analyzed AMPA-receptor internalization as before by surface biotinylation (**Figure 5-10, a**). Hippocampal neurons isolated from E19 rats and cultivated for 14-18 DIV were stimulated with pre-clustered EphB4-Fc or Fc for 1 hour and 100  $\mu$ M AMPA was added for the last 10 minutes. As expected, AMPA stimulation resulted in an increased level of AMPA-receptor internalization (GluR2) when compared to the control condition (Fc). Again, in a manner similar to that observed in 293 GluR2 cells, simultaneous activation of ephrinB2 reverse signaling resulted in a strong inhibition of the AMPA-induced AMPA-receptor endocytosis. Quantifications of four independent experiments revealed this inhibition to be highly significant.

The inhibitory effect of ephrinB2 was additionally analyzed using an ‘antibody feeding assay’ (Lin et al., 2000; Man et al., 2000). Here, a specific primary antibody (anti-GluR2 or GluR1) was applied to the cells to mark the surface pool of AMPA receptors. Thereafter, the cells were stimulated to allow receptor internalization followed by fixation with PFA. AMPA-receptors retained on the cell surface were labelled with a green-tagged secondary antibody. Following permeabilization, a red-tagged secondary antibody was used to mark receptors internalized during the experiment. Representative images of each condition are shown in **Figure 5-10, b**.

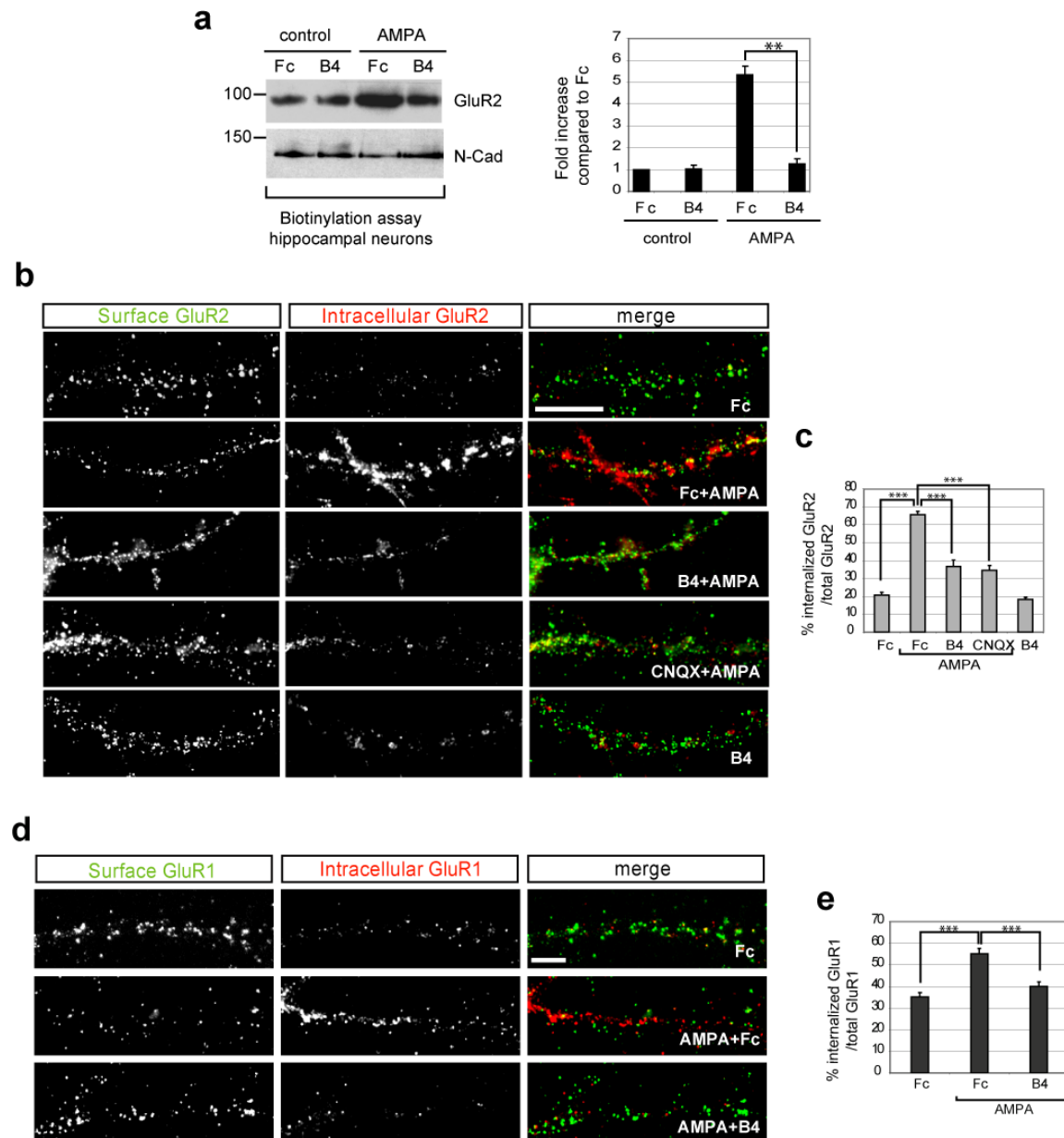


**Figure 5-10: EphrinB2 inhibits AMPA-receptor internalization in hippocampal neurons.** (a) AMPA-receptor internalization (GluR2) in hippocampal neurons 21DIV under the indicated stimulation conditions analyzed using surface biotinylation assay (left panel) as in Figure 5-9. N-cadherin levels (N-Cad) were unaffected. Quantification of four independent experiments (right panel) indicated as fold increase compared to Fc (control) (SEM,  $** P < 0.005$ ). (b) AMPA-receptor internalization under various stimulation conditions (B4: pre-clustered EphB4-Fc; CNQX: specific AMPA-receptor antagonist) visualized using the ‘antibody feeding assay’. Neurons 15-21 DIV were labeled with primary antibodies (anti-GluR2), stimulated, fixed and incubated with a first secondary antibody (green), recognizing surface retained receptors. A second secondary antibody (red) was applied after permeabilization to mark internalized receptors. Scale bar, 5  $\mu\text{m}$ . (c) Quantification of AMPA-receptor internalization based on fluorescence intensities, shown as the percentage of internalized GluR2 (red) versus total GluR2 (red + green). The conditions analyzed are those illustrated in b. (SEM,  $*** P < 0.0005$ ). (d) AMPA-receptor internalization monitored as trafficking of GluR1 and visualized using the ‘antibody feeding assay’ as in b. Scale bar, 5  $\mu\text{m}$ . (e) Quantification of GluR1 internalization as in c. Conditions analyzed are represented in d (SEM,  $*** P < 0.0001$ ).

The internalization levels were quantified as percentage of internalized GluR2 versus total GluR2 (**Figure 5-10, c**). In control conditions, the basal level of AMPA-receptor internalization was  $20.7 \% \pm 1.6$  (green fluorescence signal **Figure 5-10, b**). Stimulation with  $100 \mu\text{M}$  AMPA led to a strong AMPA-receptor internalization of  $65.7 \% \pm 1.9$  seen as an intense red signal (internalized GluR2) and a weak green signal (remnant surface receptors). Simultaneous ephrinB2 activation by pre-clustered EphB4-Fc significantly blocked AMPA-evoked internalization ( $36.8 \% \pm 3.3$ ), to an extent comparable to that of a competitive antagonist of AMPA receptors ( $34.6 \% \pm 2.7$ ), namely 6-cyano-7-nitquinoxaline-2, 3-dione (CNQX).

AMPA receptors at active synapses are heteromers mainly composed of GluR1 and GluR2 subunits. We therefore confirmed our observations using antibodies against GluR1 (**Figure 5-10, d+e**). EphrinB2 activation resulted in a significant inhibition of AMPA-induced GluR1 endocytosis ( $40.0 \% \pm 2.2$  compared to solely AMPA stimulation  $55.1 \% \pm 2.4$ ).

### 5.2.1.3 EphrinB2 inhibits also the AMPA-receptor endocytosis following NMDA stimulation

AMPA-receptor internalization is known to be induced in two different manners, first, by its direct activation through the specific agonist AMPA, and second indirectly via NMDA-receptor activation. The latter has been shown to be important for the expression of long-term depression (LTD) triggered by NMDA-receptor activation (Beattie et al., 2000). Therefore, we next tested whether ephrinB2 ligands would also inhibit AMPA-receptor endocytosis in neurons stimulated with NMDA. In these experiments, cultured hippocampal neurons were treated with pre-clustered EphB4-Fc or Fc for 1 hour while  $50 \mu\text{M}$  NMDA was added shortly for 2 minutes (10 minutes before the reaction was stopped). AMPA receptor endocytosis was visualized by the antibody feeding assay method, as illustrated in **Figure 5-11, a**, and quantified as percentage of internalized GluR2 versus total GluR2 (**Figure 5-11, b**). The basal level of AMPA-receptor endocytosis of  $29.8 \% \pm 2.2$  was increased after NMDA application ( $51.8 \% \pm 1.6$ ) and was efficiently blocked by ephrinB2 activation ( $33.1 \% \pm 1.8$ ).

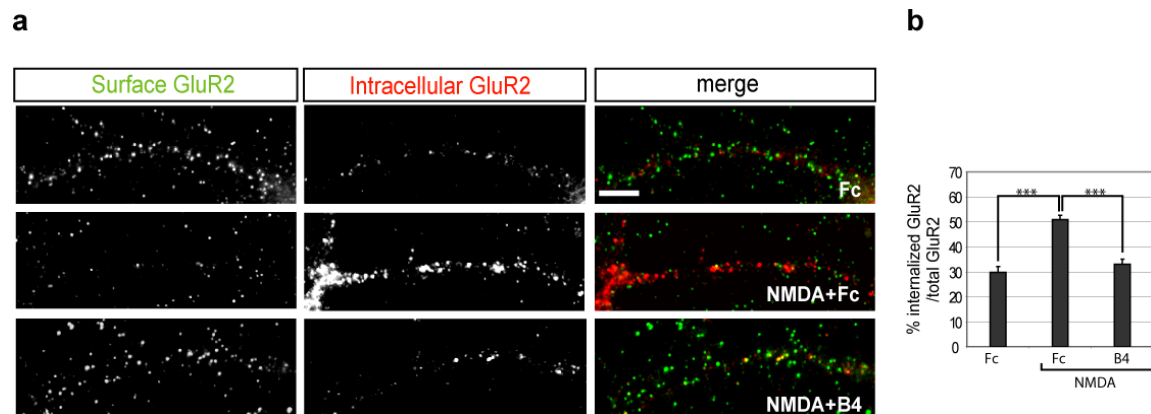


**Figure 5-11: EphrinB2 blocks NMDA-induced AMPA-receptor endocytosis.** Hippocampal neurons (15-18DIV) stimulated as indicated and analyzed for AMPA-receptor (GluR2) internalization using the ‘antibody feeding assay’ as in Figure 5-9. (a) Neurons were incubated with Fc alone or with 50  $\mu$ M NMDA for 2 minutes together with pre-clustered EphB4-Fc or Fc (control). Surface retained receptors appear in green, internalized in red puncta. Scale bar, 5  $\mu$ m. (b) Quantification of AMPA-receptor internalization based on fluorescence intensities as in Figure 5-10 b. The conditions analyzed are those illustrated in b (SEM, \*\*\*  $P < 0.0001$ ).

Taken together, these results suggest that ephrinB2 reverse signaling regulates AMPA-receptor trafficking by stabilizing the receptors at the cell membrane. Moreover, ephrinB2 reverse signaling was also seen to inhibit NMDA-induced AMPA-receptor internalization suggesting a broader role for ephrinBs in the regulation of glutamate-receptor trafficking.

### 5.2.2 Lack of ephrinB2 leads to enhanced AMPA-receptor internalization and reduced synaptic transmission

We next addressed how AMPA-receptor trafficking is regulated in neurons that lack ephrinB2. The genomic ablation of ephrinB2 results in embryonic lethality (E11) due to a severe developmental defect in the vasculature (Adams et al., 2001; Wang et al., 1998). Therefore, to analyze AMPA-receptor endocytosis, we made use of a previously generated conditional ephrinB2 knockout mouse (ephrinB2<sup>lox/lox</sup>) crossed to a Nestin-Cre line that specifically deletes ephrinB2 from the nervous system (Grunwald et al., 2004).

### 5.2.2.1 EphrinB2 protein is absent in Nestin-Cre<sup>+</sup> ephrinB2<sup>lox/lox</sup> mice

First, we confirmed the successful ablation of the ephrinB2 protein in the nervous system of conditional ephrinB2 knockout Nestin-Cre<sup>+</sup> animals (eB2KO) by various methods (Figure 5-12). Cortices from E17 eB2KO or control litter mates were homogenised and analyzed by Western blot as total lysates, or after a specific EphB4-Fc-pulldown that enriches the ephrinB2 protein (Figure 5-12, a+b). Neither the total lysates nor the specific pulldown showed a detectable level of ephrinB2 protein in these animals.

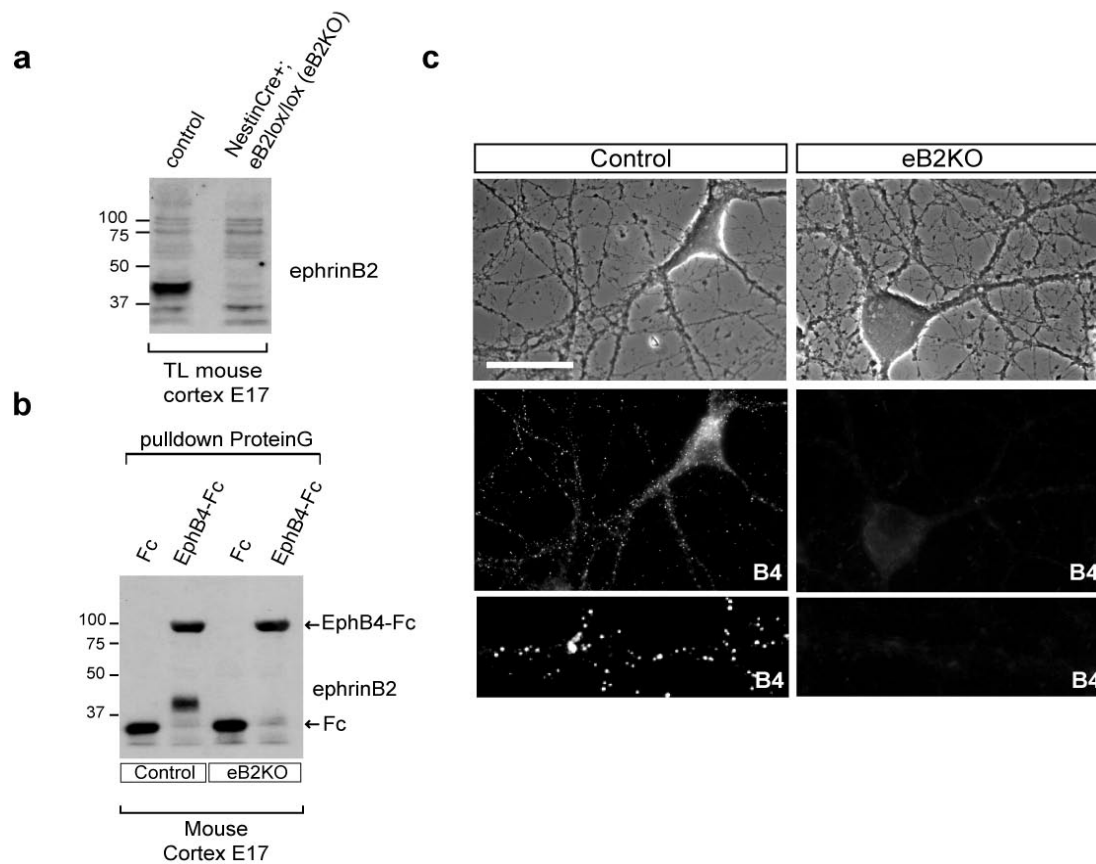


**Figure 5-12: EphrinB2 protein is absent in eB2KO neurons.** (a) Total cortex lysates (TL) of E17 embryos analyzed by Western blot using anti-ephrinB2 (R&D) antibodies. (b) EphrinB2 specific pulldown (EphB4-Fc) showed complete absence of ephrinB2 protein E17 cortex lysates of eB2KO mice in Western blot. (c) Primary hippocampal neurons 17DIV isolated from eB2KO or control litter mates stimulated with pre-clustered EphB4-Fc to induce ephrinB2 clusters. Cluster formation was visualized using anti-hFc cy2 antibodies. Scale bar, 5  $\mu$ m.

Additionally, we analyzed primary hippocampal neurons of eB2KO and control littermates for ephrinB2-expression. Neurons (17DIV) were stimulated with pre-clustered EphB4-Fc or Fc (control) for 20 minutes and ephrinB2 clusters were visualized

by indirect detection of EphB4-Fc using anti-hFc-cy2 antibodies. While control cells showed punctuated, positive signals, typical for ephrinB2 surface clusters, the eB2KO neurons were completely devoid of any signal (**Figure 5-12, c**).

### 5.2.2.2 eB2KO mouse neurons show enhanced constitutive AMPA-receptor internalization

After verifying the absence of the ephrinB2 protein we analyzed the levels of AMPA-receptor internalization in hippocampal neurons from eB2KO and control litter mates. Hippocampal neurons isolated from E17 eB2KO mice and control littermates were cultured for 15-17 days and the levels of AMPA-receptor endocytosis were determined by the antibody feeding assay method as in **Figure 5-10, a+b**.

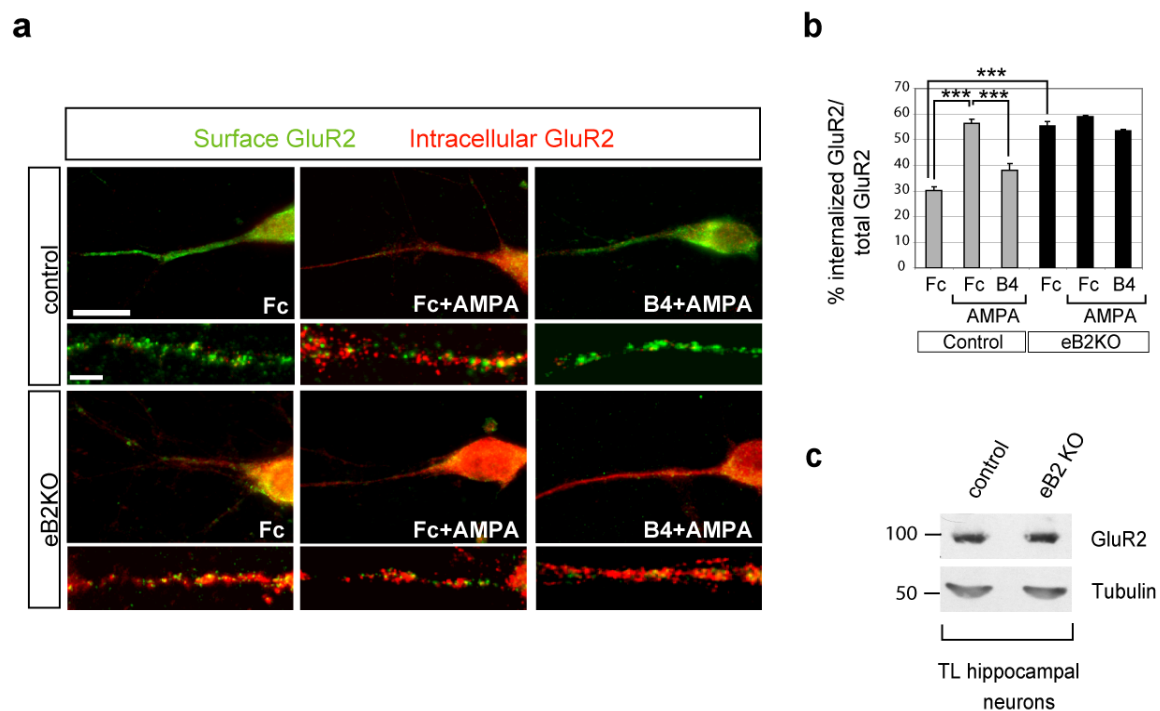


**Figure 5-13: EphrinB2 KO neurons show increased AMPA-receptor internalization.** (a) Hippocampal neurons from eB2KO and control litter mates cultured for 16DIV and analyzed for AMPA-receptor endocytosis by the antibody feeding assay under the indicated conditions as in Figure 5-10, b. Scale bars, 20  $\mu\text{m}$  whole neurons, 5  $\mu\text{m}$  enlargements. (b) Quantification of AMPA-receptor internalization pictured as percentage of internalized GluR2 versus total GluR2 under the conditions presented in a (SEM, \*\*\*  $P < 0.0001$ ). (c) Total level of GluR2 was not affected in eB2KO neurons analyzed in Western blot using anti-GluR2 and anti-tubulin (control) antibodies.

Under control condition (Fc), eB2KO neurons already showed an increased level of AMPA-receptor internalization ( $55.4 \% \pm 1.7$ ) compared to control cells ( $30.3 \% \pm 1.4$ ). As expected, simultaneous stimulation with pre-clustered EphB4-Fc and  $100 \mu\text{M}$  AMPA did not inhibit AMPA-induced receptor internalization since ephrinB2 is not present in these neurons. The lack of ephrinB2 protein resulted in a destabilization of AMPA receptors at the cell surface but had no effect on the total levels of GluR2 (

**Figure 5-13, c**). When total lysates of cultured hippocampal neurons (17DIV) from eB2KO mice and control litter mates were analyzed by Western blot, the levels of GluR2, in relation to tubulin, were unchanged. Thus, ephrinB2 regulates AMPA-receptor trafficking by influencing the levels of receptors at the surface.

### 5.2.2.3 eB2KO neurons show reduced synaptic transmission

The endocytosis rate and, consequently the actual surface presence of AMPA receptors, turned out to be affected in eB2KO neurons. Since the amount of AMPA receptors at synaptic sites influences synaptic transmission, we next investigated the electrophysiological properties of these eB2KO neurons. We recorded miniature excitatory postsynaptic currents (mEPSCs) that are caused by the spontaneous release of single presynaptic vesicles. The amplitude of the mEPSCs correlates with the number of synaptic AMPA receptors and can be used as a read-out for synaptic transmission properties. The electrophysiological analysis of mEPSCs in cultured eB2KO, and control litter mate neurons, was performed by Matthias Traut (MPI of Neurobiology, AG Stein). The eB2KO cells showed smaller mEPSCs and their mean amplitude was significantly reduced from  $19.3 \text{ pA} \pm 1.1$  in control neurons to  $16.6 \text{ pA} \pm 0.6$  in eB2KO neurons (**Figure 5-14, a+b**). Even though the synaptic transmission was reduced in KO neurons, the number of synapses, determined by the number of PSD-95 (post-synaptic marker) and synapsin1 (pre-synaptic marker) positive puncta per  $100 \mu\text{m}$ -dendrite stretch, remained equal (**Figure 5-14, c**). Thus the lack of ephrinB2 in these neurons leads to increased AMPA-receptor endocytosis resulting in a decreased number of AMPA receptors at the synapse at a given time point.

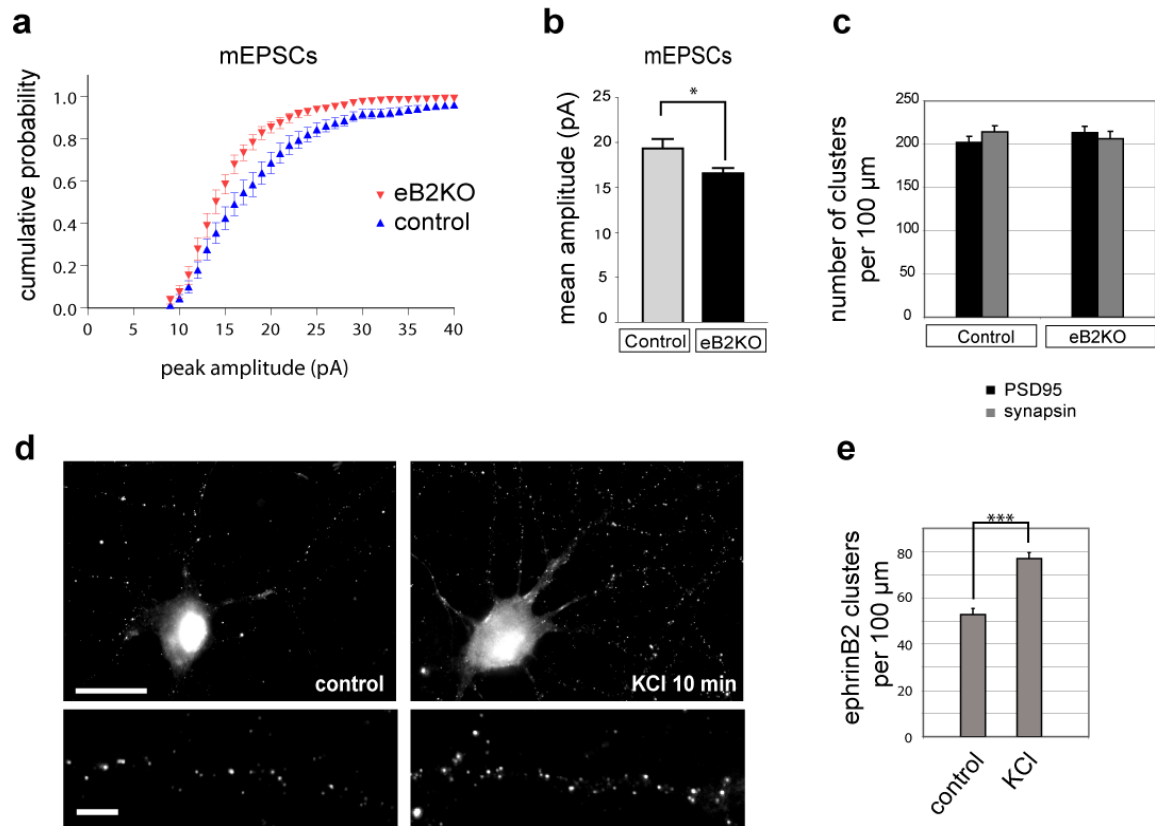


**Figure 5-14: eB2KO neurons show reduced synaptic transmission.** (a) Cumulative probability histogram of mEPSC amplitudes of control (blue) and eB2KO (red) hippocampal neurons (Kolmogorov-Smirnov test,  $P < 0.05$ , 80 events per cell, control  $n=10$  cells, eB2KO  $n=13$  cells). (b) Mean of mEPSC amplitudes in control and eB2KO hippocampal neurons (SEM, \*  $P < 0.05$ ). (c) Number of synapses in cultured hippocampal neurons of eB2KO and control litter mates. Quantified were numbers of PSD-95 positive or synapsin1 positive clusters per 100  $\mu\text{m}$ -dendrite stretches. (d) Stimulation with 10 mM KCl induces ephrinB2-cluster formation in hippocampal neurons. Surface clusters visualized via indirect detection with EphB4-Fc and anti-hFc antibodies. Scale bars, 20  $\mu\text{m}$  whole neurons, 5  $\mu\text{m}$  enlargements. (e) Quantification of ephrinB2 clusters after KCl stimulation pictured as number of clusters per 100  $\mu\text{m}$ -dendrite stretch (SEM, \*\*\*  $P < 0.00001$ ).

#### 5.2.2.4 Hyperpolarization leads to ephrinB2 cluster formation

The synaptic strength depends on the number of AMPA receptors at the synaptic surface. Insertion of additional AMPA receptors or endocytosis, respectively, is regulated by activity and assures the plasticity of synaptic contacts. Since ephrinB2 activation seemed to

stabilize AMPA receptors at the cell surface, we wanted to determine whether ephrinB2 clustering and reverse signaling could be influenced by neuronal activity. Therefore, we induced a change of the membrane potential in cultured hippocampal neurons by applying a hyperpolarizing 10 mM KCl solution for 10 minutes and examined the induction of ephrinB2 clusters. EphrinB2-cluster formation was visualized via indirect detection through EphB4-Fc and anti-hFc cy2 antibodies and was quantified as number of clusters per 100  $\mu\text{m}$ -dendrite stretch (**Figure 5-14, c**). The hyperpolarization resulted in a significant increased number of ephrinB2 clusters from  $52.8 \pm 2.6$  at control neurons to  $77.6 \pm 2.6$  after KCl-stimulation.

### 5.2.3 GRIP molecules link ephrinB ligands to AMPA receptors

In the previous section we showed that ephrinB2 ligands regulate AMPA-receptor trafficking by stabilizing the receptors at the cell surface. We next investigated the molecular mechanism of this effect. A candidate for the linker between ephrinB2 ligands and AMPA receptors is the group of glutamate-receptor-interacting proteins (GRIP1/ABP), known to bind to both AMPA receptors (Dong et al., 1997) and ephrinB ligands (Bruckner et al., 1999; Torres et al., 1998). Indeed, the association of GluR2 with ABP and/or GRIP was shown to be essential for maintaining the synaptic surface accumulation of AMPA receptors, possibly by limiting their endocytotic rate (Osten et al., 2000). First, we investigated the presence of a triple interaction between GRIP, ephrinB2 and AMPA receptors in neuronal tissue. We immunoprecipitated ephrinB from mouse brain (P20) and analyzed the samples by Western blot using different specific antibodies (**Figure 5-15, a**). Both GRIP1 and GluR2 were found to co-immunoprecipitate with ephrinB (left panel), whereas MAP2 (microtubule-associated protein 2), which is highly abundant in total lysates of neurons and thus serves as negative control, did not appear in the ephrinB-immunoprecipitates (right panel).

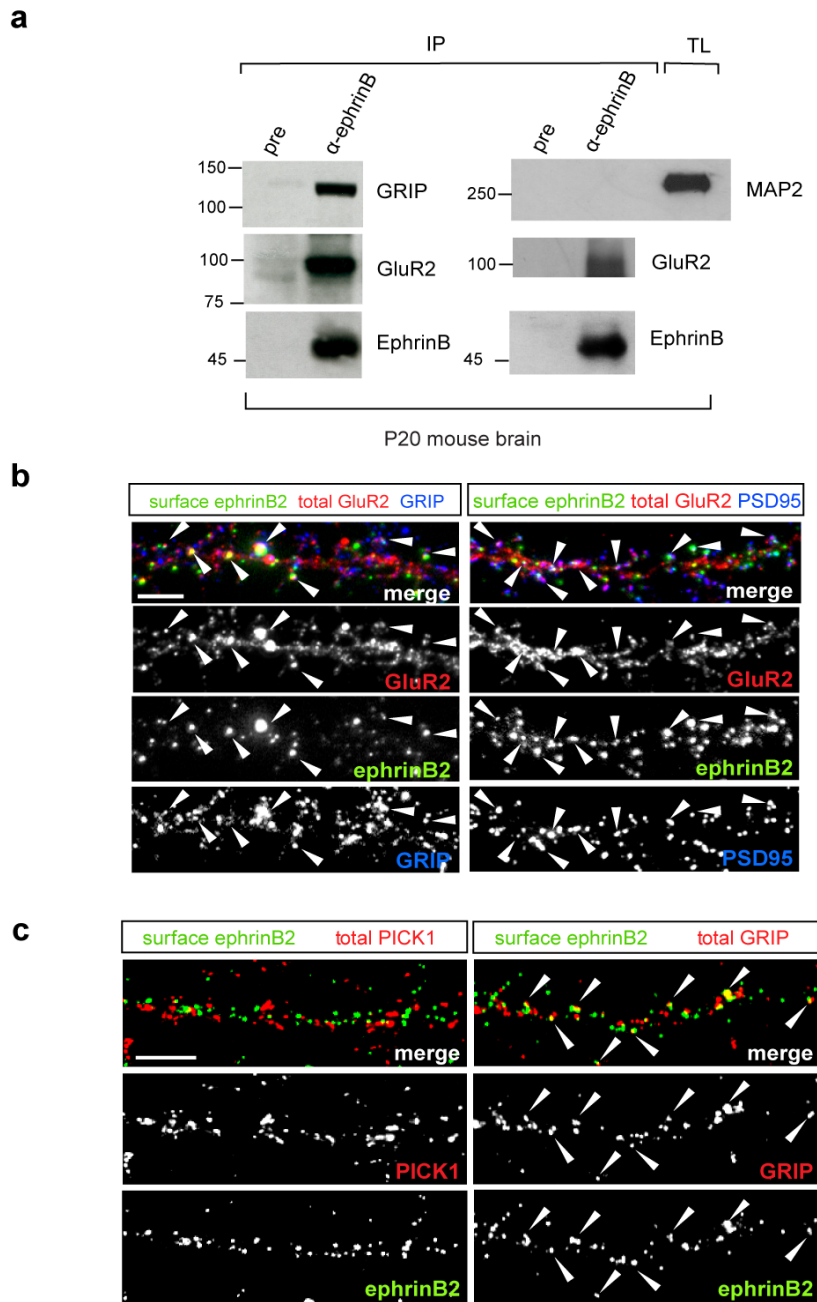


**Figure 5-15: EphrinB2, GRIP and GluR2 interact in neuronal tissue.** (a) Immunoprecipitation of ephrinB from mouse brain (P20) analyzed by Western blot showed co-precipitation of GluR2 and GRIP1 (left panel) but not microtubule-associated protein 2 (MAP2) (right panel). (b) EphrinB2, GRIP1 and GluR2 co-localize in cultured hippocampal neurons (21DIV), partially GluR2-ephrinB clusters overlap with postsynaptic markers (PSD-95). EphrinB2 cluster formation was induced by EphB4-Fc stimulation and visualized using anti-hFc cy2 antibodies. Arrowheads indicate triple co-localizations of ephrinB2, GluR2 and GRIP or PSD-95. (c) Unlike GRIP1 PICK1, a known AMPA receptor interactor, does not co-localize with surface clusters of ephrinB2 in hippocampal neurons (21DIV). Cluster formations visualized as in b. Arrowheads indicate co-localization of GRIP and ephrinB2. Scale bar, 5  $\mu$ m.

To determine the cellular compartment in which this triple interaction occurs, we analyzed cultured hippocampal neurons (21DIV) by immunofluorescence using antibodies against GRIP1, PSD-95, GluR2 and hFc (**Figure 5-15, b**). Neurons were stimulated with pre-clustered EphB4-Fc for 20 minutes and ephrinB2 clusters were visualized with anti-hFc cy2 antibodies. Surface ephrinB2 was found to co-localize nicely with GluR2 and GRIP1 (indicated with arrowheads in the left panels) (**Figure 5-15, b**). Additionally, GluR2 and ephrinB2 showed co-localization with the postsynaptic marker PSD-95 (arrowheads, right panels), suggesting that this co-localization occurs, partially, at postsynaptic sites.

Besides GRIP1, another protein that is known to be involved in AMPA-receptor trafficking was considered as a candidate for the linker between GluR2 and ephrinB2. PICK1 was shown to bind to both GluR2 (Xia et al., 1999) and, by *in vitro* interaction studies, to ephrinB (Torres et al., 1998). Consistent with this, we were able to co-immunoprecipitate PICK1 with ephrinB from the mouse brain (data not shown). However, immunofluorescence studies of cultured neurons revealed no co-localization of PICK1 with surface ephrinB2 clusters (**Figure 5-15, c**) but only with intracellular pools of ephrinB2. Thus, if the ephrinB2-PICK1 interaction plays a role in AMPA-receptor internalization, it is likely to be at a later stage and might be only related to the internalized pools of AMPA receptors.

#### **5.2.4 GRIP molecules are required for ephrinB ligand-mediated AMPA-receptor stabilization**

GRIP1 co-localizes together with GluR2 and ephrinB2 in hippocampal neurons. A further question that needed to be addressed was whether this interaction was important for ephrinB2 mediated AMPA-receptor stabilization at the cell surface

##### **5.2.4.1 Interference of GRIP binding to ephrinB2 by a GRIP-peptide (PDZ6)**

GRIP proteins are PDZ-domain-containing proteins which bind via their PDZ6-domain to ephrinBs (Bruckner et al., 1999; Torres et al., 1998) and via their PDZ4 and PDZ5-domains to AMPA receptors (Dong et al., 1997). Here, we performed an interference

approach by over-expressing the PDZ6-domain of GRIP in hippocampal neurons. This PDZ-domain acts as a dominant negative molecule binding to ephrinBs and thereby preventing endogenous GRIP1 to bind (Figure 5-16, a+b).

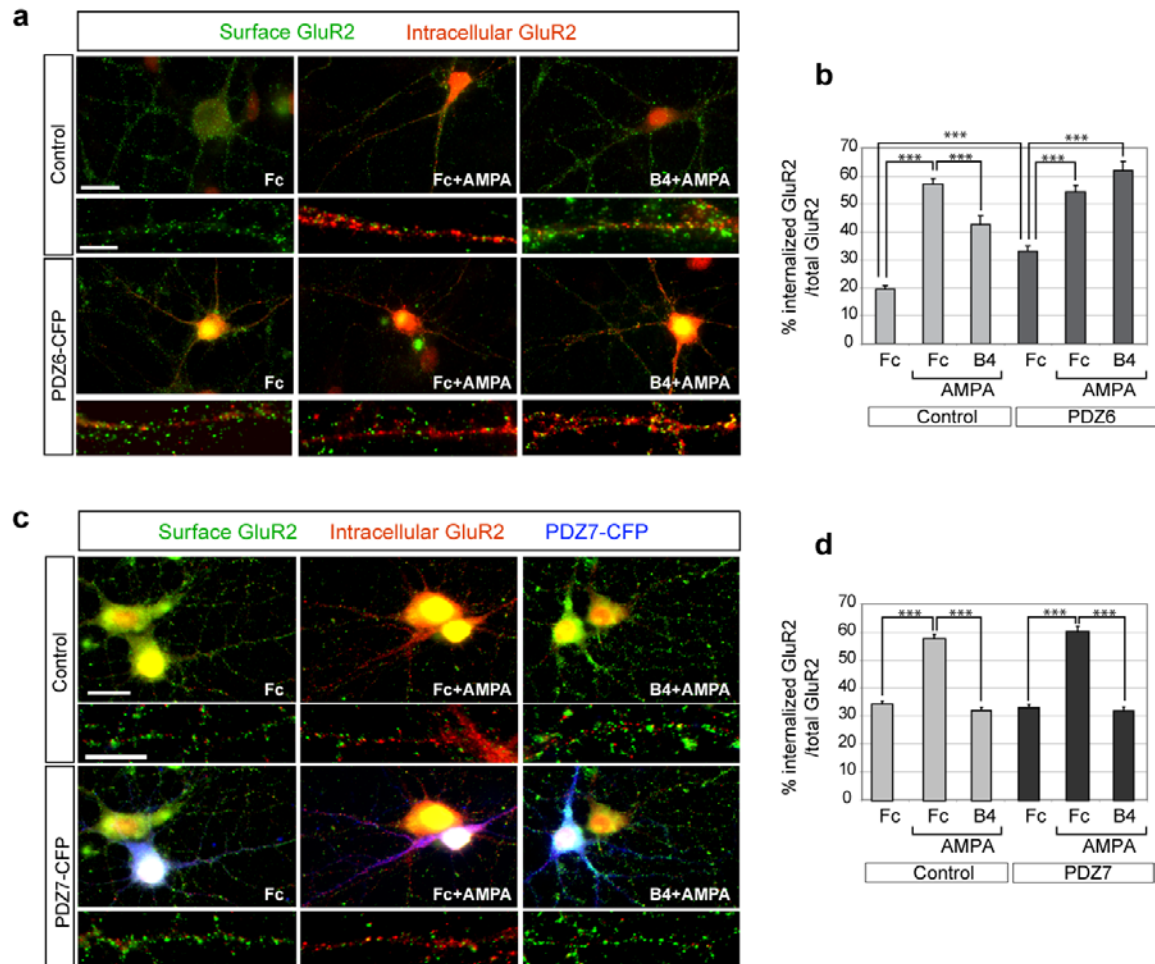


**Figure 5-16: Interference with GRIP-ephrinB2 interaction impairs AMPA-receptor stabilization.** (a) Hippocampal neurons transfected with the dominant negative molecule GRIP1-PDZ6-CFP were assayed for AMPA-receptor internalization by the antibody feeding assay. Neurons were stimulated as indicated with pre-clustered Fc (control) or EphB4-Fc alone or together with 100  $\mu$ M AMPA. Internalized receptors appear in red, surface remaining receptors in green. Scale bars, 20  $\mu$ m whole neurons, 5  $\mu$ m enlargements. (b) Quantification of AMPA-receptor internalization pictured as percentage of internalized GluR2 versus total GluR2 in transfected neurons and control cells under the conditions presented in a. (SEM, \*\*\*  $P < 0.0001$ ). (c) Over-expression of GRIP1-PDZ7-CFP in hippocampal neurons did not affect AMPA-receptor internalization when assayed under the conditions as in (a). (d) Quantification of GluR2 internalization of PDZ7 transfected neurons and control cells as in b. Scale bars, 20  $\mu$ m whole neurons, 5  $\mu$ m enlargements. (SEM, \*\*\*  $P < 0.0001$ ).

Hippocampal neurons were transfected with PDZ6-CFP at 11 days in culture and analyzed 2-4 days later by the aforementioned antibody feeding assay. Under control conditions (Fc) transfected neurons already showed a slight increase in AMPA-receptor internalization compared to untransfected control cells ( $33.1 \% \pm 1.8$  internalization in GRIP1 PDZ6 transfected neurons compared to  $19.5 \% \pm 1.3$  in control transfected neurons). AMPA-receptor endocytosis was successfully induced by  $100 \mu\text{M}$  AMPA in both the PDZ6 over-expressing and control cells. Importantly, AMPA-induced receptor endocytosis was no longer inhibited by ephrinB2 activation with pre-clustered EphB4-Fc in the PDZ6-expressing cells. Therefore, interfering with the binding of GRIP1 to ephrinB2 seemed to disrupt AMPA-receptor stabilization via ephrinB2.

To verify, whether the effect seen in PDZ6-over-expressing neurons was specific, we transfected neurons with a different PDZ-domain of GRIP (PDZ7), unable to bind to ephrinB2, and determined AMPA-receptor endocytosis in these neurons (**Figure 5-16, c+d**). The analysis of PDZ7-CFP expressing cells revealed no differences in AMPA-receptor internalization compared to control cells. The same levels of AMPA-receptor endocytosis were observed under control conditions (Fc) ( $33.8 \% \pm 1$  transfected compared to  $34.3 \% \pm 1.2$  untransfected neurons) and ephrinB2 activation successfully inhibited AMPA-induced receptor internalization in control and PDZ7-expressing cells ( $32.5 \% \pm 1.2$  to  $32.6 \% \pm 1.4$  respectively).

#### 5.2.4.2 Interference of GRIP binding to ephrinB2 by ephrinB2-peptide

A second way to interfere with GRIP binding to ephrinB2 is to over-express an ephrinB2 peptide that contains the GRIP-binding sequence. The sequence of the last 22 amino acids of ephrinB2 was cloned into a CFP-N-terminal-fusion plasmid to generate B2-pepWT CFP. Hippocampal neurons (11DIV) were transfected with B2-pepWT CFP and analyzed for AMPA-receptor internalization by the antibody feeding assay method 2-4 days later. This treatment increased AMPA-receptor internalization even without AMPA stimulation ( $45.7 \% \pm 1.9$  compared to  $23.2 \% \pm 1.3$  in the untransfected controls) (**Figure 5-17**). AMPA treatment resulted in an increase of AMPA-receptor endocytosis in both transfected ( $56.2 \% \pm 2.0$ ) and untransfected neurons ( $56.3 \% \pm 2.0$ ). Simultaneous

activation of ephrinB2 effectively blocked AMPA-induced receptor endocytosis in control cells ( $29.5 \% \pm 1.6$ ). In B2-pepWT CFP-expressing neurons a smaller reduction ( $45.7 \% \pm 2.1$ ) was observed. Most probably the peptide was not able to completely inhibit endogenous ephrinB2-GRIP interaction.

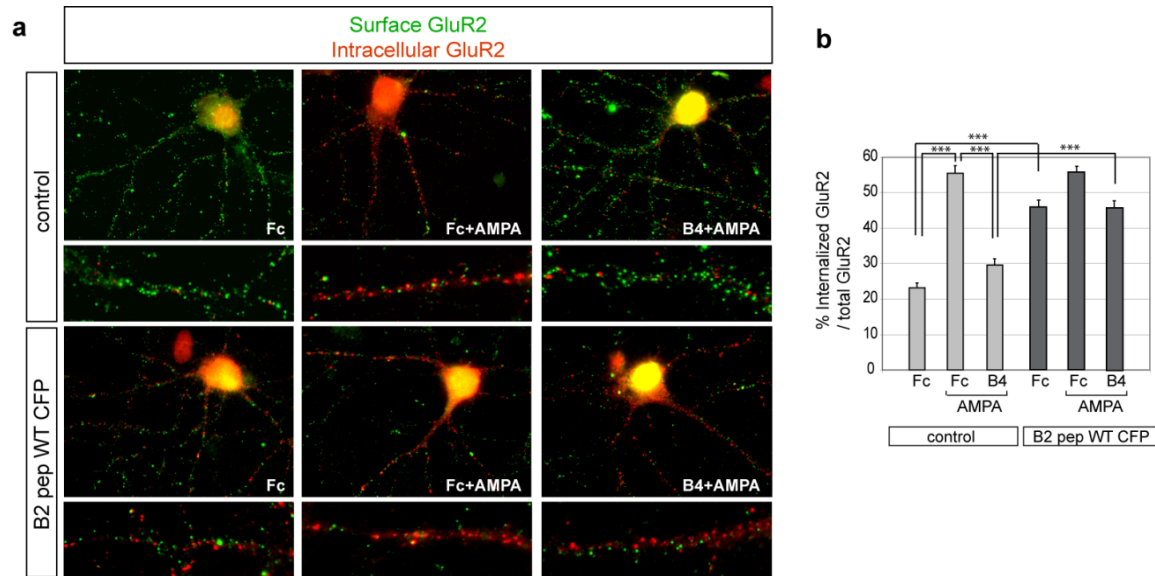


**Figure 5-17: Interference with GRIP-ephrinB2 interaction with an ephrinB2 peptide.** (a) Hippocampal neurons transfected with the ephrinB2 peptide B2-pepWT CFP were assayed for AMPA-receptor internalization by the antibody feeding assay. Neurons were stimulated as indicated with pre-clustered Fc (control) or EphB4-Fc alone or together with  $100 \mu\text{M}$  AMPA. Internalized receptors appear in red, surface remaining receptors in green. (b) Quantification of AMPA receptor internalization as in Figure 5-16 (SEM,  $*** P < 0.0001$ ).

#### 5.2.4.3 EphrinB2 activation decreased GluR2 phosphorylation levels

The binding of GRIP to AMPA receptors is known to be regulated by the phosphorylation of Serine880 (ser880) in GluR2. GRIP1 stabilizes AMPA receptors at membranes while binding to the unphosphorylated GluR2 subunit (Matsuda et al., 1999). Upon receptor activation, the GluR2 subunit is phosphorylated at ser880. This event leads to the dissociation of GRIP1 and enables PICK1 to bind to GluR2 thus initiating AMPA-receptor internalization (Chung et al., 2000). Furthermore, binding of GRIP to GluR2 has been

shown to inhibit ser880 phosphorylation (Fu et al., 2003). Since ephrinB2 seemed to stabilize AMPA receptors at the surface via GRIP1, we wondered whether ephrinB2 activation might have a direct effect on the serine-phosphorylation status of GluR2. Therefore, we stimulated cultured hippocampal neurons (18DIV) with pre-clustered Fc (control), EphB4-Fc alone, or EphB4-Fc together with AMPA and assayed levels of ser880 phosphorylation by Western blot with a phosphorylation-specific antibody. As expected, AMPA-receptor activation with 100  $\mu$ M AMPA led to high levels of ser880 phosphorylation of the GluR2 subunit. Importantly, co-stimulation together with EphB4-Fc inhibited AMPA-induced serine-phosphorylation, supporting our model that ephrinB2 stabilizes AMPA receptors at the membrane via GRIP1.

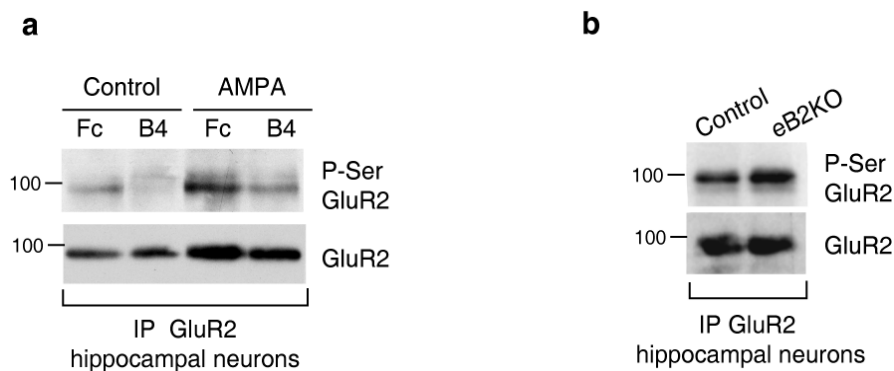


**Figure 5-18: EphrinB2 inhibits activation induced ser880 phosphorylation in GluR2.** (a) Hippocampal neurons (20DIV) were stimulated as indicated with pre-clustered Fc, EphB4-Fc alone or together with 100  $\mu$ M AMPA, immunoprecipitated (IP) for GluR2 and analyzed by Western blot for phospho-ser880 GluR2 and total GluR2. (b) Lack of ephrinB2 increased phospho-ser880 GluR2 levels in cultured hippocampal neurons. eB2KO and control littermate neurons were cultured for 16 days and analyzed for levels of ser880-phosphorylation by immunoprecipitation of GluR2 and analysis by Western blot.

### 5.2.5 GRIP binding to ephrinB ligands is regulated by activation through EphB receptors

Like GRIP binding to GluR2, the association of GRIP with ephrinB also appears to be regulated. The following experiments were performed by Manuel Zimmer (MPI of Neurobiology, AG Klein) and are described in his thesis. Since they are part of our collaborative publication I will briefly describe them in the following section

NIH3T3 cells stably expressing myc-tagged GRIP and HA-tagged ephrinB were stimulated with pre-clustered Fc (control) or EphB2-Fc and the lysates were immunoprecipitated for ephrinB using anti-HA antibodies. Only upon activation with the receptor (EphB2-Fc) was GRIP seen to bind and co-immunoprecipitate with ephrinB-HA (**Figure 5-19, a**). The intracellular tail of the ephrinB ligand is responsible for the receptor-induced interaction with GRIP. No interaction was seen in stable clones (NIH3T3) expressing a truncated form of ephrinB lacking the intracellular part (eB $\Delta$ C).

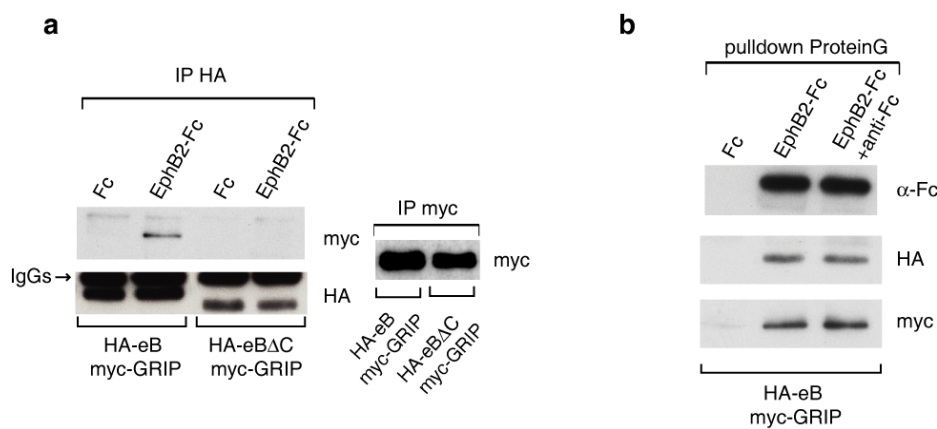


**Figure 5-19: GRIP binding to ephrinB regulated by receptor binding.** (a) GRIP binding to ephrinB ligands is induced by stimulation with EphB receptors. Stable cell lines co-expressing a myc-tagged version of GRIP (myc-GRIP) and an HA-tagged version of wild-type or C-terminally truncated ephrinB were generated from NIH3T3 cells. Lysates from these cells were immunoprecipitated with anti-HA antibodies and analyzed by Western Blot using anti-HA and anti-myc antibodies. Immunoprecipitation with anti-myc antibodies showed same levels of GRIP expression in both cell lines (right panel). (b) EphB2-Fc, GRIP and ephrinB interact in a ternary complex. NIH3T3 cells stably expressing HA-ephrinB and myc-GRIP were stimulated with Fc, EphB2-Fc or clustered EphB2-Fc (EphB2-Fc+anti-Fc). Lysates were used for ProteinG affinity purification.

Additionally, GRIP, ephrinB and EphB2 interact in a ternary complex. When NIH3T3 cells, stably expressing ephrinB-HA and GRIP-myc, were stimulated with pre-clustered EphB2-Fc, ephrinB and GRIP were found in precipitates from ephrinB-specific pull-down experiments (**Figure 5-19, b**)

### 5.2.6 Serine phosphorylation in ephrinB ligands regulates PDZ-interactions

The following experiments were performed by Amparo Acker-Palmer (**Figure 5-20, Figure 5-21, d**), and in collaboration with Manuel Zimmer and Elsa Martinez (**Figure 5-21, a+b**).

In the course of a different study concerning the tyrosine phosphorylation of ephrinB ligands (Palmer et al., 2002), Acker-Palmer observed that ephrinB ligands were also phosphorylated on serine residues. Further analysis using an *in vitro* kinase assay (**Figure 5-20, b**) revealed serine-9 as the major phosphorylation site. Tyrosine dependent signaling was shown to be independent of serine phosphorylation. A line of NIH3T3 cells was derived which stably express a mutant ephrinB1 (HA-eB S-9>A) where serine-9 was changed to alanine and, therefore, silenced for phosphorylation. Upon receptor activation (pre-clustered EphB2-Fc) the recruitment of tyrosine kinase Src, as well as the membrane cluster formation in these cells was unaffected (A. Acker-Palmer, data not shown). Furthermore, when the stable clones were stimulated with EphB2-Fc no differences in tyrosine-phosphorylation levels were observed compared to clones expressing the wild type version of ephrinB (HA-eB) (**Figure 5-20, c**).

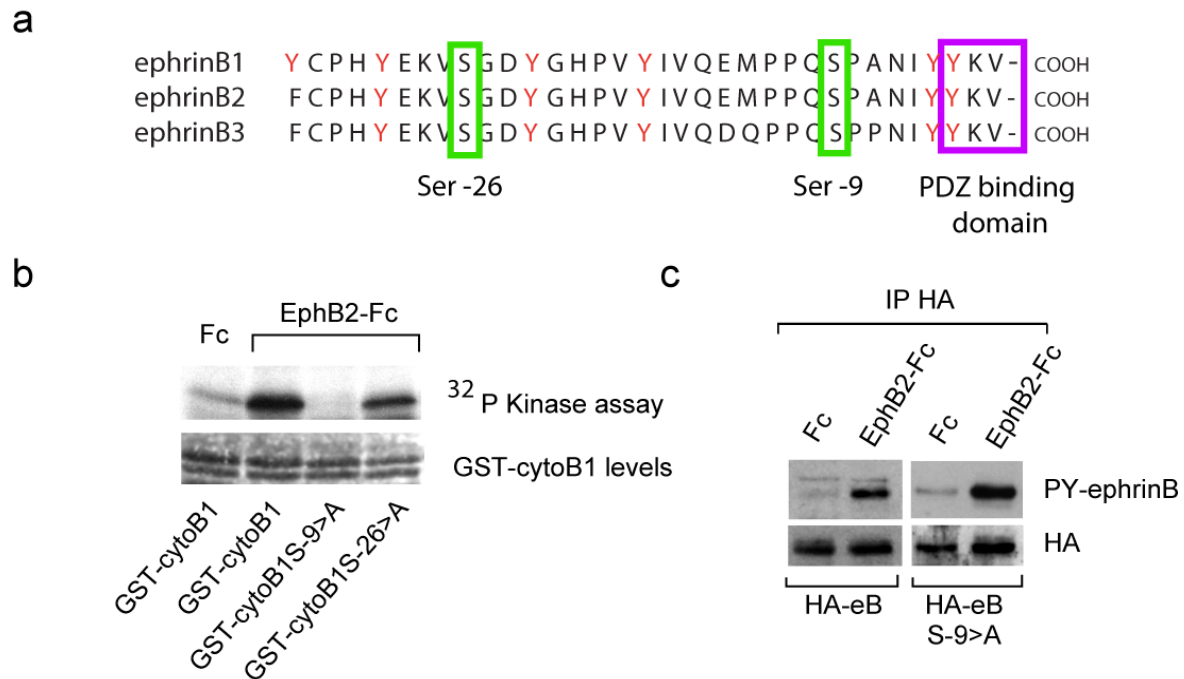


**Figure 5-20: EphrinB is phosphorylated in serine residues.** (a) The scheme of the intracellular part of ephrinB ligands shows five conserved tyrosine residues (red), two conserved serine residues (green boxes) and one c-terminal PDZ-binding motif (purple box). (b) In vitro kinase assay using total lysates of EphB2 activated NIH3T3 cells and the cytoplasmic domain of ephrinB1 fused to GST (GST-cytoB1) or the mutants GST-cytoB1 S-9>A and GST-cytoB1 S-26>A as a substrate showed Serine-9 as the major phosphorylation site. (c) Serine phosphorylation does not affect tyrosine signaling. NIH3T3 cells stably expressing ephrinB-HA wildtype or ephrinB S-9>A-HA mutant were stimulated with pre-clustered Fc or EphB2-Fc and assayed for tyrosine phosphorylation levels by immunoprecipitation with anti- HA antibodies and by Western blot using anti-tyrosine antibodies (4G10).

### 5.2.6.1 Serine-9 regulates the binding to GRIP

The major phosphorylation site in ephrinB ligands, namely serine-9, is found in close proximity to the C-terminal PDZ-binding motif. It has been postulated that residues up to 11-14 amino acids upstream of this motif may influence the binding capabilities of PDZ-target sites (Cai et al., 2002; van Ham and Hendriks, 2003). GRIP1 binding to GluR2 has been shown to be regulated by serine phosphorylation. Therefore, we wanted to determine whether serine-phosphorylation in ephrinB ligands might regulate its PDZ-binding properties.

NIH3T3 cells stably expressing myc-GRIP together with either HA-eB, HA-eB S-9>A, or HA-eB S-9>E (the latter mimics serine phosphorylation) were stimulated with pre-clustered Fc (control) or EphB2-Fc for 10 minutes and the lysates immunoprecipitated for ephrinB (**Figure 5-21, a**). Western blot analysis revealed the ephrinB S-9>A mutant to be incapable of interacting with GRIP, whereas the ephrinB S-9>E mutant was found to bind GRIP constitutively. The levels of GRIP protein were equal in all cell lines (small panels).

### 5.2.6.2 Tyrosine phosphorylation is not required for GRIP binding

GRIP binding to ephrinB seemed to be solely dependent on the phosphorylation of serine-9. A possible phosphotyrosine dependence of this interaction was excluded after performing *in vitro* and *in vivo* interaction studies. Here, NIH3T3 cells, stably expressing myc-GRIP and either HA-eB or HA-eB 6F>Y, in which tyrosine residues are mutated to phenylalanine and silenced for phosphorylation, were treated as described in 5.2.6.1. Western blot analysis revealed that the binding of GRIP to HA-eB 6Y>F was not affected (**Figure 5-21, b**). We next confirmed that the regulation of GRIP binding to ephrinB does not depend on tyrosine-phosphorylation *in vivo*. To do so, we analyzed brain lysates from knock-in mice in which the cDNA encoding ephrinB2, either wild type (ephrinB2-WT) or mutated on its tyrosine residues (ephrinB2-5Y), was inserted into the ephrinB2 gene locus (Makinen et al., 2005). Immunoprecipitation from brain lysates of these mice showed that both the ephrinB2-5Y and the ephrinB2-WT proteins equally associate with GRIP *in vivo* (**Figure 5-21, c**). Moreover, EphB-induced ephrinB tyrosine phosphorylation in cells has been shown to be transient and decreases progressively after removal of the stimulating factor EphB2-Fc (Amparo Acker-Palmer, 2002). However, this de-phosphorylation of ephrinB ligands did not affect the binding of GRIP (**Figure 5-21, d**). Taken together, these results indicate that PDZ-interaction is not affected by tyrosine phosphorylation but, interestingly, is exclusively regulated by the newly characterized serine phosphorylation of ephrinB ligands.

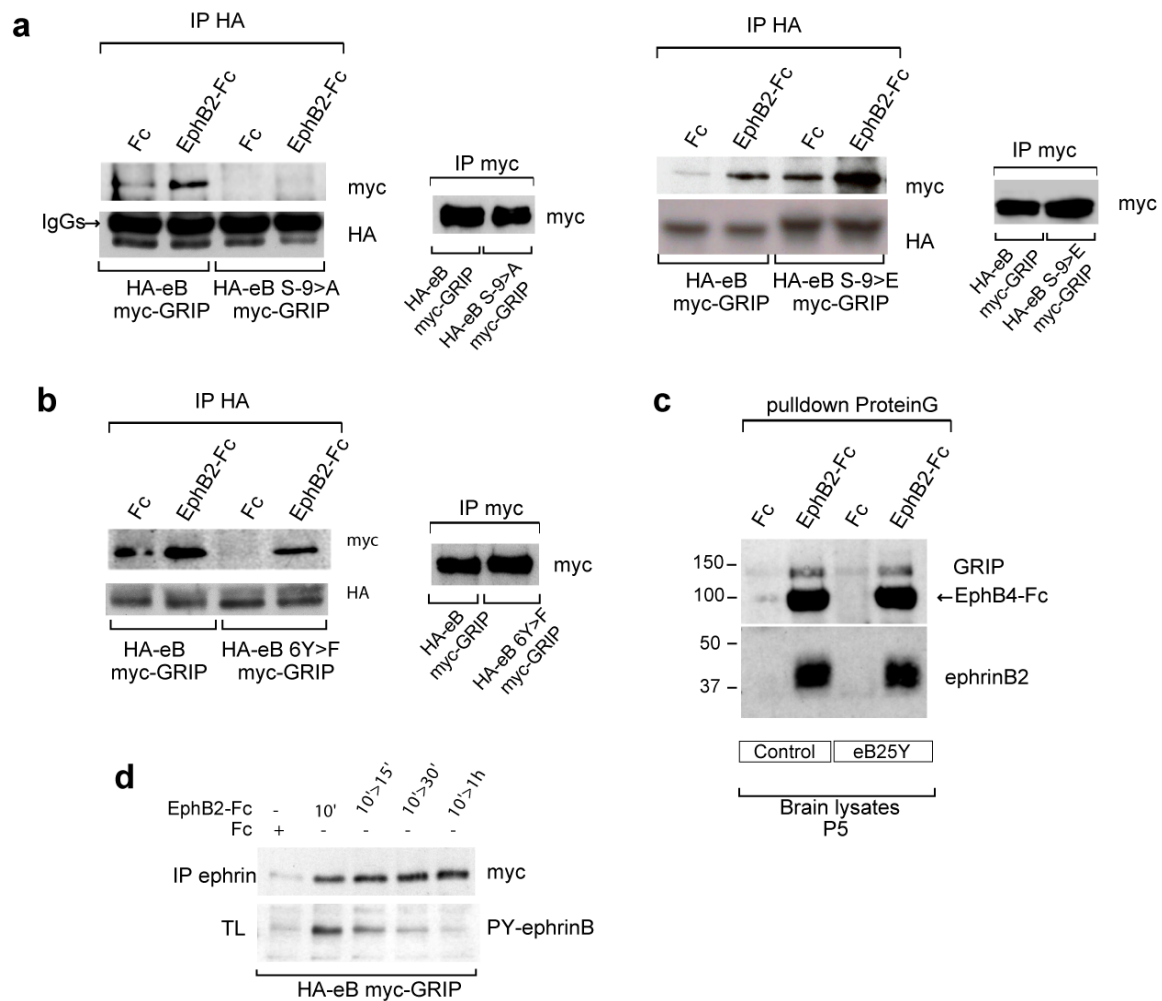


**Figure 5-21: Serine-9 phosphorylation regulated GRIP binding.** (a) Lysates from NIH3T3 cells stably expressing myc-GRIP and HA-ephrinB (HA-eB) or the mutants HA-ephrinB S-9>A (HA-eB S-9>A) and HA-ephrinB S-9>E (HA-eB S-9>E) were stimulated with Fc or EphB2-Fc and analyzed by immunoprecipitation (IP) with anti-HA antibodies and by Western Blot with anti-myc and anti-HA antibodies. IP with anti-myc antibodies showed same levels of GRIP expression in all cell lines. (b-d) Tyrosine phosphorylation of ephrinB ligands does not regulate GRIP binding in vitro and in vivo. Lysates from NIH3T3 cells stably expressing HA-ephrinB (HA-eB) or the mutant HA-ephrinB 6Y>F (HA-eB 6Y>F) together with myc-GRIP were immunoprecipitated with anti-HA antibodies and analyzed by Western Blot with anti-myc and anti-HA antibodies (b). Brain lysates from ephrinB2-5Y knock-in mice and their control littermates were used for EphB4-Fc pulldowns and analyzed by Western Blot using anti-ephrinB2 and anti-GRIP1 antibodies (c). NIH3T3 cells stably expressing HA-ephrinB (HA-eB) and myc-GRIP were stimulated with pre-clustered EphB2-Fc for 10 minutes and lysed after the indicated time points analyzed by anti-HA immunoprecipitation and by Western blot using anti-myc and anti-tyrosine antibodies (d).

### 5.2.7 Serine phosphorylation of ephrinB ligands regulates AMPA-receptor internalization

In the previous sections we showed that GRIP1, GluR2 and ephrinB2 interact in neurons. In fact, the binding of GRIP1 to ephrinB2 is required for ephrinB2 mediated AMPA-receptor stabilization since over-expression of GRIP1-PDZ6 domain interfered with this function. In addition, we demonstrated that the binding of GRIP to ephrinB is regulated upon receptor binding and we mapped the site of regulation to a serine residue located in proximity to the PDZ-binding motif of ephrinB. To confirm the importance of ephrinB2 and particularly the role of its serine phosphorylation in AMPA-receptor endocytosis, we performed a rescue experiment. EphrinB2 KO neurons, which show constitutive internalization of AMPA receptors, were transfected with ephrinB2, ephrinB2 S-9>A or ephrinB2 S-9>E and assayed for the rescue of this phenotype.

#### 5.2.7.1 EphrinB2 constructs are functional

For the rescue experiment two mutant constructs (ephrinB2 S-9>A and ephrinB S-9>E) were generated from wild type ephrinB2-CFP by site directed mutagenesis PCR (Material and Methods 7). Prior to the actual experiment the different constructs were tested for proper surface expression and cluster formation abilities. Neurons (17DIV) were transfected with the three different ephrinB2 plasmids and stimulated with pre-clustered EphB4-Fc to induce surface clusters. All constructs were appropriately expressed in neurons and they all showed the typical ephrinB cluster formation after EphB4-Fc application (**Figure 5-22**).

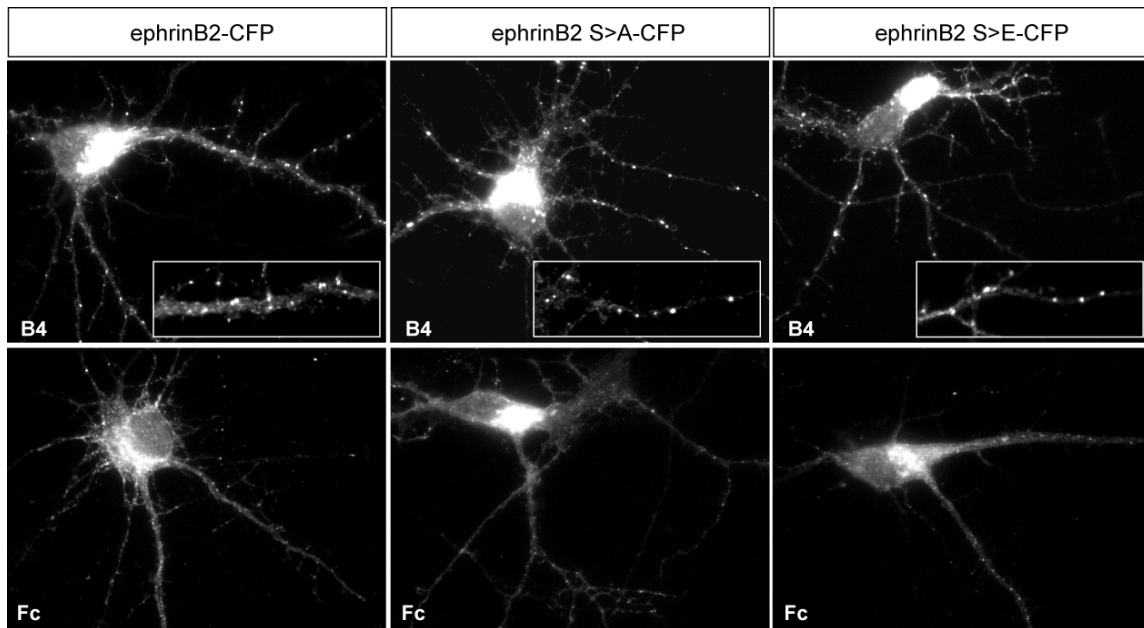


**Figure 5-22: EphrinB2 constructs are functional.** Hippocampal neurons transfected with ephrinB2-CFP, ephrinB2 S>A-CFP or ephrinB2 S>E-CFP were stimulated with pre-clustered EphB4-Fc or Fc (control) and assayed for surface cluster formation. EphrinB2 surface clusters were visualized by detection of surface bound EphB4-Fc with anti-hFc cy2 antibodies.

### 5.2.7.2 EphrinB wild type, but not the serine mutant rescues the eB2KO phenotype

Hippocampal neurons isolated from conditional eB2KO mice showed increased levels of AMPA-receptor internalization under basal conditions. These neurons were transfected with ephrinB2-CFP, ephrinB2 S>A-CFP or ephrinB2 S>E-CFP and analyzed for AMPA-receptor endocytosis after five days of expression. The cells were stimulated with pre-clustered EphB4-Fc for 1 hour to activate the reintroduced ephrinB prior to performing the antibody feeding assay. Neurons expressing the wild type version of ephrinB2 (ephrinB2-CFP) showed a significant decrease in AMPA-receptor internalization ( $34.5\% \pm 4.3$ ) compared to untransfected control cells ( $60.0\% \pm 4.7$ ) (Figure 5-23, a+b; left panel). When ephrinB2 mutated at serine-9 to alanine was introduced to the eB2KO neurons, the internalization rate of transfected and non-transfected cells ( $52.0\% \pm 3.1$  and  $49.1 \pm 3.3$  respectively) was unaffected (Figure 5-23, a+b; middle panel).

Conversely, the mutant ephrinB2 S>E that binds GRIP1 constitutively rescued the KO phenotype. (**Figure 5-23, a+b**; right panel).

Taken together, reintroduction of the ephrinB2 wild type protein to ephrinB2-KO neurons rescued their phenotype (high levels of AMPA-receptor endocytosis), highlighting the importance of ephrinB2 in the regulation of AMPA-receptor trafficking. However, the phosphorylation mutant ephrinB2 S>A, which is incapable of binding to GRIP1, did not lead to rescue underscoring the relevance of GRIP1-ephrinB2 interaction in stabilizing AMPA receptors at the cell surface.

In summary, we describe a novel regulatory mechanism involving the serine phosphorylation of ephrinB ligands. Our findings open a new research perspective which will help to broaden our understanding of how serine phosphorylation contributes to the different functions of Eph and ephrins.

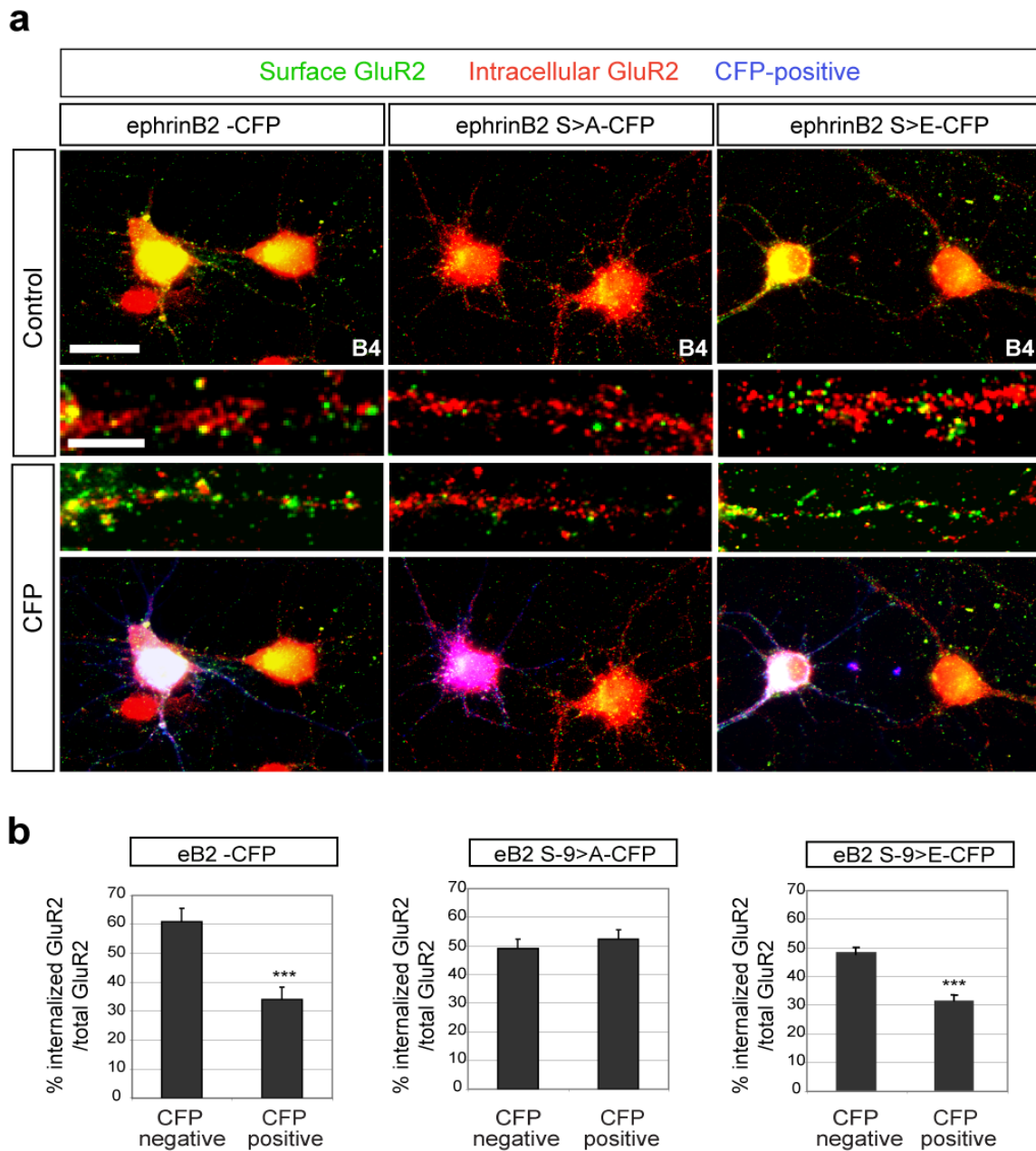


**Figure 5-23: EphrinB2 serine-9 phosphorylation required for AMPA-receptor stabilization.** (a) Rescue experiment using hippocampal neurons from eB2KO mice that showed constitutive AMPA-receptor internalization. Cells transfected with ephrinB2 -CFP (eB2 -CFP), ephrinB2 S>A-CFP (eB2 S-9>A-CFP) or ephrinB2 S>E-CFP (eB2 S-9>E-CFP) were stimulated with pre-clustered EphB4-Fc and analyzed for AMPA-receptor trafficking by the antibody feeding assay. Surface remaining receptors were labelled in green, internalized GluR2 in red. Scale bars, 20  $\mu$ m whole neurons, 5  $\mu$ m enlargements. (b) Quantification of AMPA-receptor internalization in eB2 -CFP-transfected neurons (left panel), eB2 S-9>A-CFP-transfected neurons (middle panel) and eB2 S-9>E-CFP-transfected neurons (right panel) versus untransfected neurons shown representatively in a. Quantification pictured as percentage of internalized GluR2 versus total GluR2 in transfected neurons and control cells (SEM, \*\*\* P < 0.0001).



## **6 Discussion**

### **6.1 Grb4 and GIT1 transduce ephrinB reverse signals modulating spine morphogenesis and synapse formation**

#### **6.1.1 EphrinB ligands induce spine morphogenesis**

EphB receptor forward signaling is known to be involved in spine maturation and synaptogenesis.. Hippocampal neurons of triple EphB1-3 receptor knockout mice showed reduced numbers of mature spines and synapses (Henkemeyer et al., 2003). Furthermore, the activation of EphB receptor forward signaling by application of soluble ephrinB ligand molecules induced spine maturation in cultured neurons (Henkemeyer et al., 2003; Segura et al., 2007). In vivo, Eph-receptor forward signaling, dependent on GRIP1 interactions, has been shown to be essential for the mossy fiber pathway plasticity where ephrinB ligands expressed at the presynaptic dentate gyrus neurons stimulate EphB receptors at the postsynaptic CA3 region (Contractor et al., 2002). In the Schaffer collateral pathway only ephrin B ligands are expressed at the postsynaptic CA1 region and therefore reverse signaling has been postulated to control this form of plasticity (Grunwald et al., 2004). The molecular pathways of ephrinB-reverse signaling involved in Schaffer collateral plasticity were until now unknown. We now show that ephrinB-reverse signaling can modulate spine morphogenesis and elucidate the molecular pathway that governs this function.

We cultured hippocampal neurons for 14 days, during which most of the neurons in culture develop a mature dendritic tree with a mix of spine- and filopodia-like protrusions, as well as functional synaptic contacts expressing AMPA receptors at their surface. These neurons highly express ephrinB ligands, which we showed were enriched in postsynaptic fractions of brains, and co-localized with postsynaptic markers in these cultured neurons. Stimulation of the neurons with recombinant clustered EphB2-Fc fusion-proteins resulted in a reduction of long, filopodia-like protrusions and led to an increased number of mature spines with characteristically short dendritic shafts and

bulbous shaped heads. More importantly, the increased spine maturation induced by ephrinB activation did not require Eph receptor signaling since neurons with blocked receptor signaling were still able to develop mature spines. Eph receptors and ephrinB ligands seem to have independent roles in spine maturation since the induction of Eph receptor mediated spine maturation occurred despite the inhibition of reverse signaling by over-expression of a dominant negative ephrinB molecule (ephrinB $\Delta$ C- lacking the intracellular domain). Therefore, it is evident that ephrinB ligands have their own signaling role in the complex network that governs spine maturation and synapse formation.

In cultured hippocampal neurons, the contribution of ephrinBs is decisive, and over-expression of the dominant negative ephrinB $\Delta$ C resulted in severely impaired spine maturation. These neurons appeared to have increased filopodia-like protrusions compared to control cells, giving them a 'hairy' phenotype. In adult mice, no obvious spine morphogenesis phenotype of mice lacking ephrinB3 or ephrinB2 has been reported in the literature. This could be explained by a possible redundancy and compensation among the three ephrinB molecules. Impaired ephrinB-reverse signaling shifted the distribution of dendritic protrusions from mature to more immature filopodia-like spines and, as a result, a reduced number of mature synaptic contacts was apparent. This observation is in line with the idea that synaptic contacts are stabilized and mature upon the formation of dendritic spines. Opinions differ on the importance of ephrinB3 or ephrinB2 in the adult central nervous system. Knockout mutants show contradictory results range from "no difference" to an increase in the total number or even a decrease of a certain synapse type such as shaft synapses (Aoto and Chen, 2007; Grunwald et al., 2004; Rodenas-Ruano et al., 2006). The reasons for these differences could lie in the genetic background of the mice or in the degree to which other ephrinB ligands compensate for the missing ephrinB ligand. Nevertheless, the effect of ephrinB-reverse signaling we observed in isolated neurons maturing in culture was striking. *In vivo*, spine morphology defects will most likely only appear to be striking in triple ephrinB1-B3 knockouts.

Even though our results were obtained in young developing neurons, the pathway we elucidated downstream of ephrinB ligands could possibly remain relevant throughout the life time of a neuron. EphrinB expression remains relatively constant during adulthood and could therefore quite possibly function in regulating spine morphogenesis and synapse formation in mature animals. Spine dynamics, including spine formation, stabilization and/or removal, is one of the key components during plasticity and serves as a basis for learning and memory. Similarly to their role during developmental spine morphogenesis, the ephrinB ligands could well mediate spine formation and stabilization underlying adult synaptic plasticity.

The bi-directional ephrin/Eph signaling system appears to be used differently depending on the synapses involved (Grunwald et al., 2004). In vivo, at the mossy fiber-CA3 synapse, ephrinB3 is exclusively expressed by presynaptic dentate gyrus cells while the EphB2 receptor is expressed by both presynaptic dentate gyrus and postsynaptic CA3 neurons. At this synapse, EphB2 receptors interact specifically with postsynaptic proteins (NMDA receptors) to regulate LTP and, moreover, act as receptors for presynaptic-ephrinB-ligand-induced NMDA-independent forms of plasticity. At the synapse between CA3 and CA1 neurons, ephrinBs are mainly localized postsynaptically in CA1 neurons, while the relevant Eph receptors are expressed by both pre- and postsynaptic neurons. Here, the role of Eph receptors and ephrinB ligands at the synapse is still very poorly understood. For example, given that a postsynaptic neuron simultaneously expresses Eph receptors and ephrin B ligands, it is possible that its receptors could act in *cis* to activate the ligands. So far, however, this has not been studied. The Eph/ephrin system is not the only one which is acting both pre- and postsynaptically. Other bi-directional signaling systems, such as transmembrane semaphorins, have also been shown to function both pre- and postsynaptically during synaptogenesis. It is important to emphasize that the pathway described in this thesis could well act downstream of ephrinB ligands at pre and postsynaptic sites, since the cultures we used express these ligands both pre- and postsynaptically.

### 6.1.2 Grb4 and GIT1 transduce ephrinB reverse signals

In this study we have dissected the signaling pathway downstream of ephrinB ligands that stimulates spine maturation. Spine formation and morphogenesis were previously shown to require local Rac activity, produced by the assembly of a signaling complex including G-protein coupled receptor kinase-interacting protein 1 (GIT1) and the exchange factor for Rac,  $\beta$ -Pix. Downstream of Rac a signaling pathway including p21-activated kinase and myosinII regulatory light chain (MLC) was shown to be essential for synapse formation (Zhang et al., 2003; Zhang et al., 2005). Interestingly, the molecule recruiting this signaling module to synapses remained so far unknown. We have now shown that ephrinB ligands recruit the GIT1- $\beta$ PIX-Rac complex, via the adaptor protein Grb4, to the synaptic membrane thereby initiating spine formation. In cultured hippocampal neurons this can be induced by activation of ephrinB ligands with soluble EphB2-Fc receptor fusion proteins. Under physiological conditions, this would mean that a positive signal from an opposing cell, achieved by cell-to-cell contact exposing Eph receptors to ephrinB ligands, is able to induce spine morphogenesis, contact stabilization and consequently synapse maturation. Similar processes are known to be triggered by other membrane-bound molecules such as cadherins, protocadherins, synCAM and neuroligin-neurexins.

We verified the relevance of the GIT1- $\beta$ PIX-Rac signaling pathway during ephrinB-evoked spine formation by inhibiting it with dominant negative effectors at various levels. We used the ephrinB peptide (p313-335) that binds to Grb4 and prevents its binding to endogenous ephrinB, therefore disrupting the recruitment of Grb4-GIT1- $\beta$ PIX-Rac to the synaptic membrane. We also interfered with the binding of Grb4 to GIT1 by over-expressing the SLD domain of Grb4. Both interference experiments resulted in a complete impairment of ephrinB-evoked spine morphogenesis; the neurons showed a strong 'hairy' phenotype and a reduced number of synaptic contacts. The latter result is in accordance with an observation described by Zhang et al. (2003), who found a strong increase of filopodia-like protrusions when the SLD domain of Grb4 was introduced into cultured hippocampal neurons (Zhang et al., 2003). Additionally, and to verify the requirement of ephrinB ligands immediately upstream of the Grb4-GIT1- $\beta$ PIX-Rac complex, we over-expressed

ephrinB signaling mutants (ephrinB $\Delta$ 313-335 – lacking the Grb4 binding site, and eprhinB1-6F – tyrosine phosphorylation mutant). These complementary experiments resulted in the same phenotype disturbing the proper formation and maturation of spines. Therefore, we suggest that Grb4 serves as the bridging molecule between ephrinB ligands and GIT1 thus recruiting the Rac-activation complex to synapses.

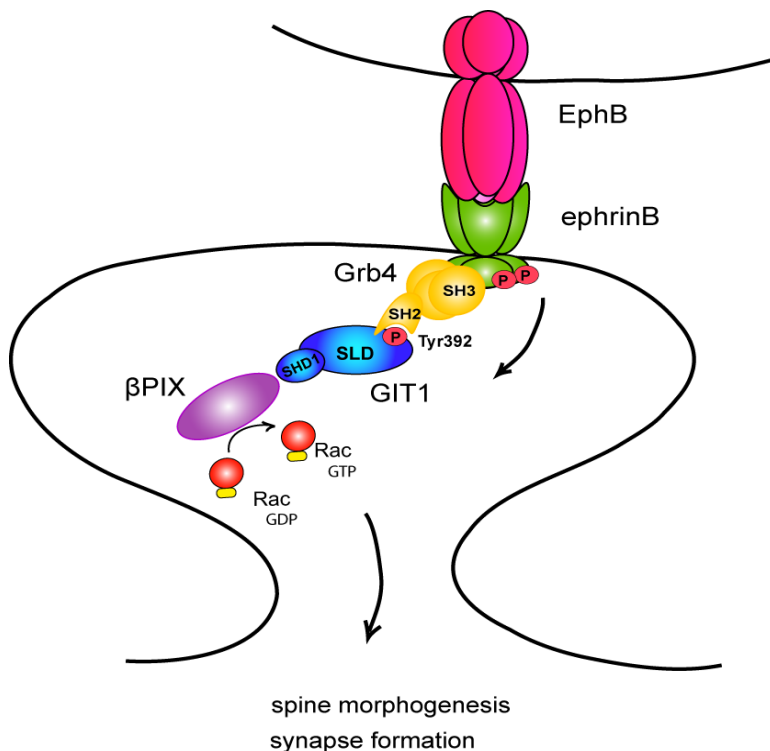


**Figure 6-1: Our model of ephrinB-reverse signaling pathway during spine formation.** EphrinB ligands are located at the synaptic membrane and are activated by opposed Eph receptors during synaptic contacting. Upon receptor binding ephrinB ligands form clusters assembling activated Src family kinases (SFK). Src phosphorylates GIT1 on tyrosine 392 located in the SLD (synaptic localization domain) and now allows Grb4 to bind. Grb4 in turn interacts with membrane anchored ephrinB via its SH3 domain and localizes the Rac signaling complex, composed of GIT1 and βPix (exchange factor for Rac) to the synaptic compartment.

In conclusion, for the first time, we have shown an important role for ephrinB-reverse signaling in spine formation and have mapped out the ephrinB-reverse signaling pathway involved in this process, thus shedding light onto the molecular mechanisms that might govern ephrinB-reverse signaling function in important processes involving spine morphogenesis such as synaptic plasticity (Segura et al., 2007).

## 6.2 Serine phosphorylation of ephrinB2 regulates trafficking of synaptic AMPA receptors

EphrinB ligands are known as multifunctional molecules highly expressed on neuronal cells such as hippocampal neurons. The results discussed in section 6.1 point to a signaling complex containing Grb4 and GIT1 that is involved in the regulation of spine formation by ephrinB ligand signaling (Segura et al., 2007). In addition to changes in synapse morphology, ephrinB ligands might be regulating other important processes associated with synaptic plasticity. One factor crucial for synaptic plasticity is the number of active AMPA receptors at the synaptic surface. Long-term synaptic changes, such as LTP and LTD, require that AMPA receptors traffic to or away from the synapse. In recent years, great efforts have been made to identify molecules involved in LTP induction and AMPA receptor trafficking. The ablation of ephrinB ligands in mice leads to pronounced defects in both hippocampal LTD and LTP, and impaired AMPA-receptor trafficking could explain the plasticity defects seen in these animals. We now provide evidence that ephrinB2 ligands are involved in the stabilization of AMPA receptors at the cell surface of neurons contributing to the regulation of AMPA-receptor trafficking. Furthermore, this role seems to be specific to ephrinB2 and, therefore, cannot be compensated for by other ephrinB ligand family members.

We used two different expression systems (293GluR2 cells and primary hippocampal neurons), and two different approaches (biotinylation and immunofluorescence assays) to verify the impact of ephrinB2 molecules on AMPA-receptor internalization. In every assay used, ephrinB2 activation led to a robust inhibition of AMPA-induced AMPA-receptor internalization to an extent comparable to that of the AMPA receptor antagonist CNQX. Basic levels of AMPA-receptor internalization under non-stimulated conditions (Fc-fragment) as well as the levels induced by AMPA stimulation were consistent with previous findings (Lin et al., 2000). Basic trafficking levels arise from AMPA receptors that exchange continuously between their surface and intracellular pools, as well as between synaptic and extra-synaptic sites. This allows rapid modulation of synaptic

receptor-density independent of neuronal activity. In our assays, EphB4 stimulation alone did not lead to a significant change in the basic levels of AMPA-receptor trafficking, a phenomenon which is most probably due to insufficient sensitivity of our assay. We observed a large increase of AMPA-receptor internalization in neurons lacking ephrinB2 ligands (eB2KO neurons) which strongly supports the role of ephrinB2 in stabilizing AMPA receptors. As expected, EphB4 stimulation of these neurons did not lead to the inhibition of AMPA-induced AMPA-receptor internalization observed in wild type neurons since they lack ephrinB2, the specific ligand for EphB4 receptors. The re-introduction of functional ephrinB2 molecules into the eB2KO neurons largely restored the inhibition of AMPA receptor internalization in neurons stimulated with EphB4.

In the hippocampus most AMPA receptors are composed of either GluR1-GluR2 or GluR2-GluR3 subunits; GluR2 homomers are rare. We observed an inhibitory effect of ephrinB2 on both GluR1 and GluR2-subunit internalization. This suggests a more general role for ephrinB2 ligands in AMPA-receptor stabilization. GluR1-containing receptors are predominantly situated at synapses, whereas GluR2 containing receptors (GluR2-GluR3 heteromers and GluR2 homomers) cycle continuously between synaptic and non-synaptic pools, thus preserving the total number of AMPA receptors. In accordance with this, our immunofluorescence assays showed that AMPA receptors (GluR2) co-localized with ephrinB2 patches both at synaptic and extrasynaptic. It is likely that ephrinB2 molecules function to stabilize AMPA receptors at both of these areas of the plasma membrane. EphrinB2 molecules are then thought to keep AMPA receptors ready to be fused to synaptic sites if required, thereby replacing other receptors and maintaining the total number of AMPA receptors at the surface.

The ablation of ephrinB2 in cultured neurons lacking ephrinB2 (eB2KO) resulted in a small, but significant, decrease in the amplitude of mEPSCs (mini excitatory postsynaptic currents) compared to wild type neurons. Nevertheless, we did not observe any differences in the number of synaptic contacts between eB2KO and wild type neurons in culture, quantified as numbers of PSD-95 and synapsin positive puncta per dendrite stretch. The mean amplitude of mEPSCs is a read-out for the transmission properties of

the analyzed synaptic contacts, namely the synaptic strength, which correlates with the amount of active AMPA receptors at the synaptic membrane. Thus, the decreased mEPSPs in the eB2KO neurons indicate that these neurons have trouble gaining or retaining AMPA receptors at the synaptic membrane. However, the decrease is smaller than one might expect from the striking differences observed in the AMPA receptor surface trafficking assays. There are many possible explanations for these results. The increased internalization rate observed in the eB2KO neurons might possibly be compensated by a more rapid recycling of the AMPA receptors. A snap-shot of the synaptic membrane would then only reveal a minor difference. The antibody feeding assay used in this study takes such a 'snap-shot', marking surface AMPA receptors at a certain time point and consequently monitoring the trafficking of these very same receptors. This assay does not allow any conclusions to be drawn about the recycling rate of AMPA receptors, or those freshly exocytosed to replace internalized receptors. Most probably, the differences would become more profound only when the system is challenged. Indeed, when Grunwald et al. investigated the defects of eB2KO mice during defects during LTP and LTD induction, they did not observe differences in the basal synaptic transmission when performing baseline recordings from hippocampal slices from these mice (Grunwald et al., 2004). Most probably, chemical LTP-induction in the isolated neurons could be an approach to reveal more manifest differences.

A second possible explanation for the relatively small decrease in mEPSP-amplitude in eB2KO mice is that the stabilizing effects of ephrinB2 ligands might apply predominantly to AMPA receptors at extrasynaptic sites, which would not affect basal synaptic transmission. Lateral fusion of AMPA receptors from extra synaptic sites may be important during LTP induction (Borgdorff and Choquet, 2002). Destabilization of extrasynaptic receptors has its strongest effects during LTP induction, when a stable supply of AMPA receptors is required. Challenging the system by evoking LTP may provide the best measure of the importance of ephrinB2-mediated AMPA receptor stabilization. However, the effect might be similar to that seen in the GluR1 knockouts (Zamanillo et al., 1999), or the transmembrane AMPA receptor regulatory protein (TARP)  $\gamma$ -8

knockouts (Rouach et al., 2005). Both knockouts show a significant decrease in extrasynaptic receptors but modest if any changes in synaptic AMPA receptors despite impaired LTP. Similarly, destabilized extrasynaptic AMPA receptors would also explain the strong defects observed in the LTP in ephrinB2 knockouts.

AMPA-receptor internalization can be induced in two different ways, either directly through receptor activation with the specific agonist AMPA, or indirectly through the activation of NMDA receptors. At synapses of the CA1 region, LTP and LTD both require NMDA-receptor activation that results in the entry of  $Ca^{2+}$ -ions into the postsynaptic cell thus inducing  $Ca^{2+}$ -dependent signaling cascades. We were able to show that ephrinB2 ligands stabilize AMPA receptors during both NMDA-induced and AMPA-induced AMPA-receptor internalization. This observation indicates a broader role for ephrinB2 in AMPA-receptor stabilization. Apart from the observation that ephrinB2 regulates the trafficking of GluR1 and GluR2 subunits, and that GluR1/2 receptors are increasingly added to the synapse in an activity-dependent manner, ephrinB2 has also been shown to stabilize AMPA receptors upon NMDA activation. These observations strongly favour a role for ephrinB2 in the regulation of AMPA-receptor trafficking during LTP. Moreover, we showed that neuronal activity was able to increase the number of ephrinB2 clusters, thus activating ephrinB2 ligands. During the depolarization of cultured neurons with KCl, which mimics neuronal activity, we observed that the number of ephrinB2 clusters per dendrite stretch increased, suggesting that ephrinB2 ligands are required to modulate the synaptic strength during neuronal activity and plasticity.

### 6.2.1 GRIP as the bridging molecule

During this study we were able to identify the molecular mechanism for the stabilization of AMPA receptors by ephrinB2 ligands. This mechanism involves GRIP proteins as bridging molecules, which bind to ephrinB ligands via their PDZ6 domain and to AMPA receptors via PDZ4 and PDZ5. We propose that the binding of GRIP1 to both ephrinB2 ligands and AMPA receptors prevents PKC from phosphorylating AMPA receptors on serine 880 (ser880) thereby preventing their internalization.

Consistent with the idea that GRIP1 could link ephrinB2 and AMPA receptors, we were able to show the triple interaction of ephrinB2, GRIP and AMPA receptors in immunoprecipitation assays and immunofluorescence co-localization studies. We interfered with GRIP binding to ephrinB2 ligands by over-expressing either the ephrinB2-binding site of GRIP (GRIP-PDZ6), or the GRIP-interaction sequence of ephrinB2 as dominant negative molecules. Both inhibitors significantly decreased the stabilizing effect of ephrinB2 on AMPA-induced AMPA-receptor internalization. In both cases, inhibition with partner-specific sequences led to the same result. Additionally, the over-expression of a different PDZ-domain of GRIP, namely PDZ7, which does not bind to ephrinB2 ligands, had no effects on the AMPA receptor stabilization.

It is known that GRIP binds to GluR2 un-phosphorylated in ser880 thereby stabilizing AMPA receptors at the membrane. The phosphorylation of ser880 leads to the dissociation of GRIP and, subsequently, to the internalization of AMPA receptors. In agreement with these findings we observed a reduction in the phosphorylation of ser880 in neurons in which AMPA-induced AMPA-receptor internalization was inhibited by ephrinB2 activation when compared to solely AMPA-stimulated neurons. In addition, eB2KO neurons, with increased levels of constitutive AMPA-receptor internalization, showed higher ser880-phosphorylation levels compared to wild type neurons under the same culture conditions. In summary, these data suggest that GRIP is the bridging molecule between AMPA receptors and ephrinB2 ligands. EphrinB2 activation stabilizes the binding of GRIP to GluR2 and most probably sterically inhibits the access of PKC to GluR2 and subsequently its phosphorylation on ser880 (Figure 6-2).

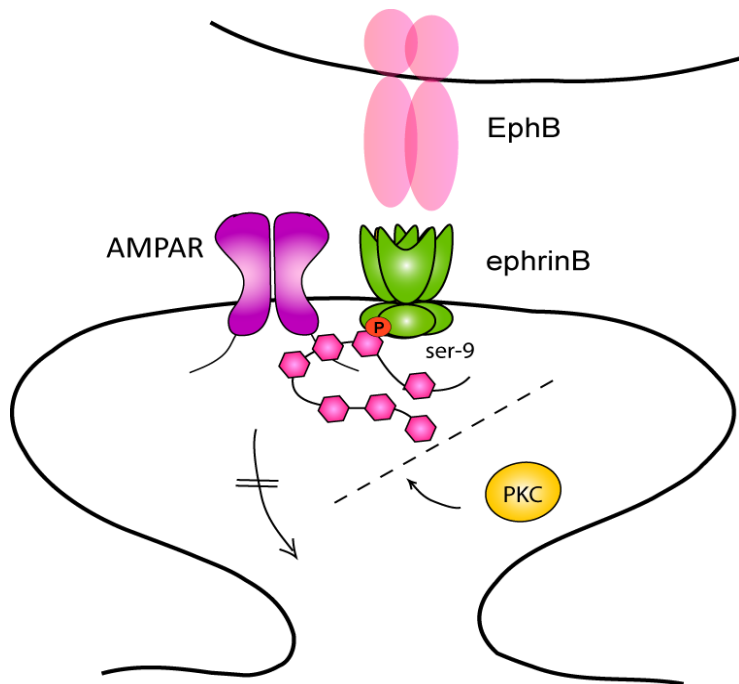


**Figure 6-2: EphrinB2-AMPA-GRIP interaction model.** Activated, serine-phosphorylated ephrinB2 ligands stabilize the binding of GRIP to AMPA-receptor subunit GluR2. The phosphorylation of GluR2 at ser880 is inhibited, probably due to steric inhibition of PKC, and subsequently its internalization. AMPAR- AMPA receptor; PKC- Protein kinase C; ser-9- serine residue at position -9; P- Phosphorylation site.

### 6.2.2 PICK1 as a ephrin-AMPA receptor linker

Although we favor GRIP as bridging molecule between AMPA receptors and ephrinB2 ligands, we also analyzed PICK1 (Protein Interacting with C-Kinase 1) as an alternative bridging molecule. PICK1 is a 55 kDa, cytosolic protein with a single PDZ- and BAR-domain (Bin/amphiphysin/Rvs). Similarly to GRIP, PICK1 is known to play a role in AMPA-receptor trafficking and was shown to bind to both AMPA receptors and ephrinB ligands (Torres et al., 1998; Xia et al., 1999). We were able to confirm the interaction of PICK1, GluR2 and ephrinB2 by co-immunoprecipitations from mouse brain lysates, using antibodies against each of these three molecules. The co-immunoprecipitations showed that all three molecules interact with each other, but these interactions could occur in a pair-wise manner and, therefore, not necessarily, imply a triple interaction. Indeed, we did not find the triple co-localization of GluR2, PICK1 and ephrinB2 at the surface of cultured neurons, where the stabilization of AMPA receptors observed in our assays

should occur. Thus, we cannot exclude the existence of such a ‘triple’ interaction which might appear at a site distinct from the plasma membrane, possibly at a different stage during AMPA-receptor trafficking. Furthermore, PICK1 is thought to be involved in the endocytosis of AMPA receptors rather than in its surface expression. The BAR-domain of PICK1 contains a cluster of positively charged residues that mediate the interaction with negatively charged phospholipids in the membrane. BAR-domains are thought to either recognize sites of possible membrane deepening, or even, actively bend the membrane for subsequent invagination therefore facilitating endocytosis (Peter et al., 2004). In summary, PICK1 might be involved in the later stages of AMPA-receptor internalization but was excluded as a candidate molecule for the stabilization induced by ephrinB2.

### **6.2.3 GRIP binding to ephrinB regulated via serine phosphorylation**

We not only provide evidence that ephrinB2 ligands regulate the internalization of AMPA receptors via GRIP, but, in addition, we reveal the regulatory mechanism of the GRIP-ephrinB interaction. The AMPA-receptor stabilization, observed in our assays, occurred following the activation of ephrinB2 ligands by its receptor. Using a cellular expression system, we found, in a similar manner, that the binding of GRIP to ephrinB is regulated via the engagement with its receptor and depends on the cytoplasmic tail of ephrinBs. Furthermore, using this system, we were able to show that serine -9 (ser-9) localized in the C-terminus of ephrinBs regulates the binding of GRIP. Once this serine is phosphorylated GRIP is able to bind. In a second round of peptide-interference experiments, we expressed both the WT ephrinB peptide and a phosphorylation-silenced mutant ephrinB peptide (B2 pep S>A CFP; data not shown), which should not sequester endogenous GRIP. As expected, B2 pep S>A CFP failed to interfere with the stabilizing effect of ephrinB2 ligands on AMPA receptors. To conclude, we performed a rescue experiment confirming that the binding of GRIP to ephrinB, via phosphorylated ser-9, is required for the stabilizing function of ephrinB2 on AMPA receptors. The reintroduction of the ephrinB2 into eB2KO neurons as well as the gain of function mutant ephrinB2 S>E (mimicking serine phosphorylation), successfully rescued the knockout phenotype whereas the loss of function mutant ephrinB2 S>A failed to do so.

The finding that serine phosphorylation regulates PDZ-interactions is novel for ephrinB ligands but has been described for other PDZ-binding partners. A prominent example is the GRIP-GluR2 interaction that is regulated by the phosphorylation of ser880 in the GluR2 subunit of AMPA receptors. It is arguable, that the ser880 is located immediately at the PDZ-binding motif of GluR2 whereas the ser-9 of the ephrinB ligands is five positions upstream. How could the serine residue then influence the PDZ-binding of ephrinB ligands? It has been reported for other molecules that residues up to 11-14 positions upstream of the binding motif may influence the binding capabilities of PDZ-target sites (Cai et al., 2002; van Ham and Hendriks, 2003). Furthermore, serine phosphorylation seems to play a prominent role in signaling during plasticity. The serine kinase PKC is highly activated during LTP induction, phosphorylating many effector molecules involved in plasticity. It is tempting to speculate that PKC contributes to the serine phosphorylation of ephrinB ligands which in turn mediates the AMPA-receptor stabilization at the surface.

### 6.2.4 Serine phosphorylation of ephrinB ligands

Our finding that serine phosphorylation regulates the binding of a PDZ protein provides a new insight into ephrinB-reverse signaling. We found that GRIP binding to ephrinB ligands was independent of tyrosine phosphorylation *in vivo* and *in vitro* and therefore suggest that tyrosine/serine phosphorylations are two independent events regulating different aspects of ephrinB-reverse signaling. Src family kinases were shown to phosphorylate ephrinB tyrosine residues, but we can only speculate about the identity of the serine kinase for ephrinB ligands. PKC is a promising candidate, as it is located to synapses and is involved in serine phosphorylation events during LTP/LTD, e.g. phosphorylation of ser880 of GluR2. A future challenge will be to identify the serine kinase that phosphorylates ephrinB ligands. Besides the search for such a kinase, it would be interesting to further elucidate the role of serine phosphorylation in ephrinB signaling. It is likely that, besides GRIP, other PDZ-binding partners of ephrinB ligands might be regulated by serine phosphorylation. Furthermore, serine phosphorylation might play an important role in other functions of ephrinB ligands beyond that of AMPA-receptor

trafficking. Moreover, ephrinBs are expressed in various other tissues outside the nervous system and it would be interesting to look at the function of serine phosphorylation in non-neuronal cells. A mouse model would, therefore, provide an excellent tool to study the relevance of ephrinB serine phosphorylation in detail.

### **6.2.5 How does ephrinB2 exert its function during synaptic plasticity?**

Looking at the synapse, the Eph receptors located at the presynaptic side could possibly provide a trans-synaptic signal to the ephrinB molecules to strengthen the synaptic contact, thus stabilizing AMPA receptors at the surface. Indeed, structural studies estimated that the distance between two cell membranes, that still allows Eph receptor-ephrin ligand engagement, is about the size of the synaptic cleft (Himanen et al., 2007). The absence of a presynaptic receptor would then result in a lack of ephrinB2 activation and consequently lead to the impairment of AMPA-receptor stabilization. This might, in part, explain the plasticity defects observed in the synaptic connection of the hippocampal CA3-CA1 region (Schaffer collateral pathway) of mice lacking EphA4 or EphB2 receptors. These mice showed impaired LTP and LTD but the defects turned out to be independent of the receptor's kinase activity. GFP fusion proteins rescued the plasticity phenotype and gave hints to the involvement of ephrinB ligands in plasticity.

Stabilization of AMPA receptors is required during LTP when the number of receptors is increased through the insertion of additional receptors. Increased neuronal activity leads to the potentiation of synaptic contacts and therefore ephrinB2 activation would be activity dependent. We show that ephrinB2 cluster formation can be induced by membrane depolarization, as occurs during neuronal activity. It would be tempting to speculate that Eph receptors, also show activity-dependent clustering, thus enabling the engagement of opposing ephrinB ligands. Interestingly, in the Schaffer collateral pathway, the Eph receptors are expressed both pre and postsynaptically. A potential *cis*-interaction between postsynaptic receptors and ligands might as well contribute to the regulation of AMPA-receptor trafficking and, quite possibly, even counteract the interaction in *trans*. *Cis*-interactions of EphA and ephrinA ligands have been shown to inhibit classical *trans*-

interactions in axon guidance (Hornberger et al., 1999; Marquardt et al., 2005). However, proof of a *cis*-interaction in the B type of Eph receptors and ligands is so far missing.

As mentioned above, ephrinB2 mediated AMPA-receptor stabilization might preferably concern extrasynaptic AMPA receptors. But just how does AMPA-receptor stabilization occur at extrasynaptic site, and where does the Eph receptor input come from in that case? It might be possible that adjacent glia cells, which are found to surround, stabilize and support synaptic contacts and spines, provide Eph-receptor input to extrasynaptic ephrinBs. Astrocytes are found to express various Eph-receptor and ephrin-ligand types and several studies have reported their impact not only in modulating synaptic plasticity, but also in regulating the clearance of neurotransmitters from the synaptic cleft, in releasing factors such as ATP which modulate presynaptic function, and even in releasing neurotransmitters themselves (Nestor et al., 2007; Vernadakis, 1996).

### 6.2.6 Concluding remarks

Here we have elucidated different roles of ephrinB ligands during synaptic plasticity involving both morphological changes and the regulation of synaptic transmission. We describe their impact in spine morphogenesis and synapse formation, as well as their role in the regulation of synaptic strength by controlling AMPA receptor trafficking. We furthermore report a novel regulatory mechanism involving the serine phosphorylation of ephrinB ligands. These findings open a new research perspective which will help to broaden our understanding of how serine phosphorylation contributes to the different functions of Eph and ephrins.



## 7 Material and methods

### 7.1 Material

#### 7.1.1 Chemicals, Reagents, Commercial Kits & Enzymes

Table 7-1: Chemicals, reagents, commercial kits& enzymes

Chemicals	Ordering information	Supplier
(S)- $\alpha$ -Amino-3-hydroxy-5-methylisoxazole-4-propionic acid (AMPA)	#A0326-5MG	Sigma
1- $\alpha$ -D-Arabinofuranosylcytosine (AraC)	#251010	Calbiochem
30 % (w/v) Acryamide/Bis solution 29:1 (3.3 % C)	#161-0157	BioRad
6-Cyano-7-nitroquinoxaline-2,3-dione (CNQX)	#0190	Tocris
Agarose, high	#01280	Biomol
Ammonium persulfate (APS)	# 161-0700	BioRad
BES	#B-6420	Sigma
BioRad DC Protein Assay	#500-116	BioRad
Blotting grade milk powder	#T145.2	Roth
Borax	#B-3545-500G	Sigma
Boric acid	#203667	Merck
Bovine albumin powder	#7906	Sigma
Complete EDTA-free, proteinase inhibitor cocktail tablets	#1873580	Roche
DL-2-Amino-5-phosphonopentanoic acid (APV)	# A5282-10MG	Sigma
DMSO	#41641	Fluka
DNA ladder GeneRuler Ladder mix	#SM0331	Fermentas
ECL Western blot detection reagent	# RPN2134	GE Healthcare
EZ-Link Sulfo-NHS-SS-Biotin	#21331	Pierce
Gel Extraction Kit	#28704	Qiagen
HNO <sub>3</sub> (Salpetersäure) 65%	#84381-1L	Sigma
Human IgG Fc-fragment	#009-000-008	Dianova (Jackson)
Immobilized NeutrAvidin <sup>TM</sup>	#29200	Pierce
Iodoacetamide	#11149-5G	Sigma
Mouse EphB2/Fc chimera	#467-B2-200	R&D

Mouse EphB4/Fc chimera	#446-B4-200	R&D
Mouse ephrinB1	#473-EB-200	R&D
Natural mouse laminin	#23017015	Invitrogen
N-Methyl-D-Aspartic acid (NMDA)	#M3262-100MG	Sigma
Normal donkey serum	#017-00-121	Dianova (Jackson)
Normal goat serum	#005-000-121	Dianova (Jackson)
NucleoSpin Extract II	#740609.250	Macherey & Nagel
OrangeG	#O-1625	Sigma
PCR Purification Kit	#28104	Qiagen
PFA (Paraformaldehyd)	#1.04005.1000	VWR
Pfu Ultra DNA polymerase	#600380	Stratagene
Poly-D-Lysine hydrobromide	#P7886-1G	Sigma
Ponceau S solution	#33427	Serva
Precision plus protein standard	#161-0373	Bio-Rad
ProLong Antifade Kit	#P7481	Invitrogen
Protein A sepharose CL-4B	#17-0780-01	GE Healthcare
Protein G sepharose 4 fast flow	#17-0618-01	GE Healthcare
QIAGEN Plasmid Maxi Kit	#12162	Qiagen
QIAGEN Plasmid Mini Kit	#12125	Qiagen
Restriction enzymes	All from NEB	New England Biolabs
Sodium Fluoride (NaF)	#S-1501-100G	Sigma
Sodium ortho vanadate (NO <sub>3</sub> VO <sub>4</sub> )	#S-6508	Sigma
Sodium Pyrophosphate (NaPP)	#221368-100G	Sigma
Sucrose	#5737	Merck
T4 DNA ligase	#M0202L	New England Biolabs
Taq DNA polymerase	#M0267L	New England Biolabs
TEMED	#161-0801	Bio-Rad
TritonX (TX)-100 solution	#37238	Serva
Tween 20 (Polyoxyethylene sorbitan monolaurate)	#P5927-500ML	Sigma
β-Mercaptoethanol	#M-7522	Sigma

### 7.1.2 Antibodies

Tabelle 7-2: Primary Antibodies

Primary Antibodies		
Anti-ephrinB1 (C-18) , rabbit	#SC-910	Santa Cruz
Anti-ephrinB2, goat	#AF496	R&D Systems
Anti-Flag M2, mouse	#F3165-2MG	Sigma
Anti-GFP JL8, mouse	#632381	Clontech
Anti-GFP, rabbit	#RDI-GRNFP-4ABR	Fitzgerald
Anti-GIT1, GIT2, rabbit	DU139, DU137	Premont et al 1998, Bagrodia et al 1999
Anti-GIT1, goat	#sc-9657	Santa Cruz
Anti-GluR1, rabbit extracell.	#PC246	Calbiochem
Anti-GluR2, mouse extracell.	#MAB397	Upstate
Anti-GluR2, rabbit	#AB1768-25UG	Upstate
Anti-Grb4, rabbit	#07-100	Upstate
Anti-GRIP1 CT, rabbit	#06-986	Upstate
Anti-GRIP1, mouse	#611319	Becton Dickinson
Anti-HA, clone 12CA5, mouse	#1583816	Roche
Anti-Homer, rat	#AB5875	Chemicon
Anti-MAP2, mouse	#MAB3418	Chemicon
Anti-N-Cadherin, mouse	#610921	Becton Dickinson
Anti-NR1, mouse	#114-001	Synaptic Systems
Anti-Phospho-Tyrosine clone 4G10, mouse	#05-321	Upstate
Anti-Phosph-Serine 880 GluR2, rabbit	#07-294	Upstate
Anti-PICK1 (H-100), rabbit IP	#SC-11410	Santa Cruz

Anti-PICK1 (N-18), goat WB	#SC-9539	Santa Cruz
Anti-PICK1, rabbit	#AB3420	Abcam
Anti-PRK2 clone 22, mouse	#610794	BD Bioscience
Anti-PSD-95, mouse	#P246-100UL	Sigma
Anti-Synapsin1, mouse	#106-001	Synaptic Systems
Anti-Synaptophysin1, rabbit	#101002	Synaptic Systems
Anti-Transferrin receptor, mouse	#A11130	Molecular Probes
Anti-V5, mouse	#R960-25	Invitrogen
Anti- $\beta$ PIX, rabbit	DU248	Premont et al 1998, Bagrodia et al 1999

Tabelle 7-3: Secondary Antibodies

<b>Secondary Antibodies</b>		
Donkey anti-mouse minx AMCA	#715-155-150	Dianova (Jackson)
Donkey anti-mouse minx cy2	#715-225-151	Dianova (Jackson)
Donkey anti-mouse minx cy3	#715-165-151	Dianova (Jackson)
Donkey anti-rabbit minx AMCA	#711-155-152	Dianova (Jackson)
Donkey anti-rabbit minx cy2	#711-225-152	Dianova (Jackson)
Donkey anti-rabbit minx cy3	#711-165-152	Dianova (Jackson)
Goat anti-human IgG Fc-fragment	#109-005-098	Dianova (Jackson)
Goat anti-mouse Alexa488	#A11029	Invitrogen
Goat anti-mouse FITC	#81-6511	Invitrogen (Zymed)
Goat anti-mouse HRP	#115-035-146	Dianova (Jackson)
Goat anti-rabbit HRP	#111-035-003	Dianova (Jackson)

## 7.1.3 Consumable Material

Tabelle 7-4: Consumable Material

Material	Type	Supplier
96well PCR plate	#AB-0900	ABgene
Combitips plus	2ml, 5ml, 10ml	Eppendorf
Cover slips 12/13mm Ø	#01-115-30	Marienfeld
CryoTubes, Nunc	#343958 1.5ml	Nunc
Extra thick blot paper Protean XL size	#1703969	BioRad
Faltenfilter Ø 240mm	# 10311651	Schleicher & Schuell
Filtered pipette tips	10µl, 20µl, 200µl, 1000µl	G. Kisker
Gel-saver tips 0.5-10 µl	#GS1025	G. Kisker
Gene Pulser® Cuvette (0.2 cm)	#165-2086	BioRad
Hyperfilm ECL 8x10in	#28-9068-39	GE Healthcare
Latex gloves, powder-free	Size S6-7	Semperguard
Multiwell cell culture plates, Costar	24 well	Corning
Nitril gloves, powder-free	Size S6-7	Semperguard
Parafilm®	“M”laboratory film	Pechiney plastic packaging
Pastuer pipettes, glass	#150.01	Poulsen & Graf
Pipette tips	10µl, 20µl, 200µl, 1000µl	Peske
Plastic pipettes, Cellstar	5ml, 10ml, 50ml	Greiner
Plastic pipettes, Falcon	1ml, 2ml, 5ml, 10ml, 25ml, 50ml	Becton Dickinson
Polypropylene round bottom tube, Falcon	14ml, 5ml	Becton Dickinson

Polystyrene, Polypropylene conical tube, Falcon	15ml, 50ml	Becton Dickinson
Protean extra thick blot paper	#1703969	BioRad
Reaction tube, safelock	1.5ml, 2ml	Eppendorf
Steritop, bottle top filter	250ml, 500ml (0.22 $\mu$ m)	Millipore
Storage box 50 slides	#N953.1	Roth
Strips of 8 domed caps	#AB-0602	ABgene
Syringe	5ml, 10ml, 50ml	Becton Dickinson
Syringe driven filter unit, Millex®GV	0.22 $\mu$ m, 0.45 $\mu$ m	Millipore
Tissue culture plastic dishes, Falcon	10 cm $\varnothing$ , 6cm $\varnothing$	Becton Dickinson
Tissue culture plastic dishes, Nunclon™	10 cm $\varnothing$ , 6cm $\varnothing$	Nunc
Whatman Protran nitrocellulose transfer membrane	#10401196	Schleicher& Schuell

### 7.1.4 Equipment

Tabelle 7-5: Equipment

Equipment	Model	Supplier
+ 4 °C fridge	Premium	Liebherr
-20 °C freezer	Liebherr comfort GS-5203	Liebherr
-80 °C freezer	Ultra low freezer U57085	Labotech
Balance	XT2220M-DR	Precisa
Burner	Fireboy eco	Integra Biosciences
Cell culture Hood	HERAsafe	Kendro
Centrifuge	Sorvall RC 5Bplus	Kendro

## 7 Material and methods

---

Centrifuge	Varifuge 3.0R	Kendro
Centrifuge	Centrifuge 5810	Eppendorf
Centrifuge micro	Table centrifuge	Roth
Centrifuge table	Centrifuge 5415D	Eppendorf
Centrifuge table, refridg.	Centrifuge 5415R	Eppendorf
CO <sub>2</sub> incubator	HERAcell 240	Kendro
Digital camera	SpotRT	Diagnostic Instruments
Electrophoresis chamber	Small, medium, big	homemade
Electrophoresis Power supply	EPS 601, EPS 301	Amersham
Epifluorescence microscope	Zeiss Axioplan	Zeiss
Fine balance	XT2220A-FR	Precisa
Gel documentation system	Herolab E.A.S.Y RH 429K	Herolab
Glas homogenizer	#S1149	B. Braun, Melsungen AG
Heating block	DRI-Block DB2D & 2A	Techne
Hemocytometer	Neubauer improved (depth 0.100mm, 0.0025mm <sup>2</sup> )	Brand
Incubator shaker	Unitron-Pro	Infors
Laminar flow hood	HERAGuard	Kendro
Magnetic stirrer with heating	Heat-stir CB162	Stuart
Magnetic stirring bar	50x8mm, 30x8mm	Brand
Microwave	Severin 700	Severin
Multi channel pipette	0.5-10µl, research	Eppendorf
Multi channel pipette	20-200µl, Transferpette-8	Brand
Multi pipette	Multipipette ®plus	Eppendorf

Oven	Heraeus 0-250 °C	Thermo Fisher
PCR machine	PTC-225 peltier thermal cycler	MJ research
pH meter	Inolab, pH level 1	WTW
Pipette boy	Pipetteboy acu	Integra Biosciences
Pipettes	P2, P20, P200, P1000	Gilson
Rotator	NeoLab rotator 2-1175	NeoLab
Rotor	GSA rotor & type 3	Sorvall
Sequencer	ABI Prism 377 DNA sequencer	Applied Biosystems
Shaker		homemade
Small microscope	Leica DM IL HC Fluo	Leica
Spectrometer	Ultrospec 3000	Amersham
TECAN reader	GENious	Tecan
Thermo mixer	Thermomixer compact & comfort	Eppendorf
Vacuum system	VACUSAFE comfort	Integra Biosciences
Vortex	Top-Mix 11118	Fisher Scientific
Water bath	Type 3043	Koettermann
Water bath	Type 1083	GFL
Water purification system	Milli-Q Biocel A10	Millipore
<b>Western Blot analysis</b>		
Semidry blotting apparatus	Trans-blot SD cell	BioRad
BioRad gel system	Mini PROTEAN® 3 cell	BioRad
<b>Dissection tools:</b>		
Spring scissors strait	#15003-08	Fine Science Tools
Tissue scissors strait	#14028-10	Fine Science Tools

## 7 Material and methods

Biology tip Dumostar 5	#11295-10	Fine Science Tools
Forceps narrow pattern	#11002-13	Fine Science Tools
Dissection microscope	Olympus SZX9	Olympus

### 7.1.5 Oligonucleotides

Tabelle 7-6: Oligonucleotides

Cre1	5'-GCC TGC ATT ACC GGT CGA TGC AAC GA-3'	Genotyping
Cre2	5'-GTG GCA GAT GGC GCG GCA ACA CCA TT-3'	Genotyping
B2Cs1	5'-CTT CAG CAA TAT ACA CAG GAT G-3'	Genotyping
B2Cas1	5'-TGC TTG ATT GAA ACG AAG CCC GA-3'	Genotyping
Ephrinb2YFPS-9>A_for	5'-GCC CCC ACA GGC TCC TGC CAA CAT TC-3'	Mutagenesis
Ephrinb2YFPS-9>A_rev	5'-GAA TGT TGG CAG GAG CCT GTG GGG GC-3'	Mutagenesis
Ephrinb2YFPS-9>E_for	5'-GCC CCC ACA GGA ACC TGC CAA CAT TC-3'	Mutagenesis
Ephrinb2YFPS-9>E_rev	5'-GAA TGT TGG CAG GCT TCT GTG GGG GC-3'	Mutagenesis
CMV_sense-II (pExFP, pcDNA3)	5'-CCA TCC GCA CAT GCC ACC CTC C-3'	Sequencing
pAdlox_afterMCS_rev (pExFP)	5'-GGT TCA GGG GGA GGT GTG GG-3'	
b2 tm_for	5'-AAG TCC CTT TGT GAA GCC-3'	Sequencing
b2 ecto_f	5'-CCC GGA AGC TTG GGG GTC GCT-3'	Sequencing
b2 ecto_r	5'-GAA TAA GGC CAC TTC GGA TCC CAG GAG ATT-3'	Sequencing

pEFCF-N1_clontech	5'-CGT CGC CGT CCA GCT CGA CCA G-3'	Sequencing
pEFCF-C1_clontech	5'-CAT GGT CCT GCT GGA GTT CGT G-3'	Sequencing
PDZ7-hind3_for	5'-GCA GAT ATC AAA GCT TTG TAC AAA- 3'	Cloning
PDZ7-kpn1_rev	5'-CCA CTT TGT ACA AGG TAC CTG GGT G-3'	Cloning
eph-PDZ_WT-for	P5'-TCG AGT GCA GGA GAT GCC CCC ACA GAG TCC TGC CAA CAT TTA CTA CAA GGT CTG AG-3'	Cloning
eph-PDZ_WT-rev	P5'-AAT TCT CAG ACC TTG TAG TAA ATG TTG GCA GGA CTC TGT GGG GGC ATC TCC TGC AC-3'	Cloning
eph-PDZ_SA-for	P5'-TCG AGT GCA GGA GAT GCC CCC ACA GGC TCC TGC CAA CAT TTA CTA CAA GGT CTG AG-3'	Cloning
eph-PDZ_SA-rev	P5'-AAT TCT CAG ACC TTG TAG TAA ATG TTG GCA GGA GCC TGT GGG GGC ATC TCC TGC AC-3'	Cloning
eph-PDZ_SE-for	P5'-TCG AGT GCA GGA GAT GCC CCC ACA GGA TCC TGC CAA CAT TTA CTA CAA GGT CTG AG-3'	Cloning
eph-PDZ_SE-rev	P5'-AAT TCT CAG ACC TTG TAG TAA ATG TTG GCA GGT TCC TGT GGG GGC ATC TCC TGC AC-3'	Cloning

### 7.1.6 Plasmids

#### pECFP and pEYFP

The pExFP-N1 and pExFP-C1 plasmids from Clontech are used as backbone for all the following ExFP fusion protein constructs.

#### GIT1, Grb4 and ephrinB1 peptide constructs

The expression constructs encoding full-length rat GIT1-Flag and GIT2-Flag, kindly provided by R.T. Premont (Premont et al., 1998). GIT1 $\Delta$ SLD-Flag, GIT1-Y392F, SLD-YFP and SLD-CFP and SLD-V5 (GIT1-SLD encoding region 375–596) were generated by Stefan Weinges as described (Segura et al., 2007; Weinges, 2006).

The expression constructs Grb4-YFP, Grb4 SH2-YFP or Grb4 SH3-YFP, and the ephrinB1 peptide YFP-p-313–335 (22 AA long, CPHYEKVSGDYGHPVYIVQEMP) were generated by Stefan Weinges as described (Segura et al., 2007; Weinges, 2006).

#### HA-ephrinB1, HA-ephrinB1- $\Delta$ C and HA-ephrinB1-6F

Expression constructs of HA-ephrinB1, HA-ephrinB1- $\Delta$ C and HA-ephrinB1-6F were generated by subcloning from pJP104, pJP105 (Bruckner et al., 1999) and pKB21, respectively, into pcDNA3.1/Hygro using EcoRI and XhoI restriction sites.

#### EphrinB1 $\Delta$ C-ECFP and EphrinB2-EYFP/ECFP

The ephrinB1 $\Delta$ C-ECFP, the ephrinB2-EYFP and ephrinB2-ECFP plasmids were provided by Jenny Lauterbach (pJK32, pJK36-pJK38) (Lauterbach and Klein, 2006).

#### EphrinB2S>A YFP/CFP

The ephrinB2S>AYFP or ephrinB2S>ACFP plasmid were generated from the plasmids ephrinB2YFP/CFP by site directed mutagenesis PCR (Stratagen) using the primers *Ephrin2YFPS-*

9>A\_for and *Ephrinb2YFPS-9>A\_rev*. The correct sequence was confirmed by sequencing using the primers *CMV\_sense-II*, *b2 tm\_for*, *b2 ecto\_f* and *b2 ecto\_r*.

### **EphrinB2 S>E YFP/CFP**

The ephrinB S>EYFP or ephrinB S>ECFP plasmid was generated as described for the ephrinB2S>AYFP/CFP using the primers *Ephrinb2YFPS-9>E\_for* and *Ephrinb2YFPS-9>E\_rev*.

### **Myc-GRIP and GRIP1-PDZ6 constructs**

The myc-GRIP1 (Bruckner et al., 1999) and the GRIP1-PDZ6 (pJP127) (Bruckner et al., 1999) constructs were provided by the Lab of R. Klein.

### **GRIP1-PDZ6 CFP**

The GRIP1-PDZ6 CFP construct was generated by subcloning the GRIP1-PDZ6 insert of a pGADGH vector (pJP127)(Bruckner et al., 1999) into the pECFP-C1 vector using EcoRI and XhoI restriction enzymes. The correct sequence was confirmed by sequencing using the primer *pECFP-C1\_clontech*.

### **GRIP1-PDZ7 CFP**

The GRIP1-PDZ7 CFP construct was generated by cloning the PCR product of the GRIP1 sequence 988-1112 from myc-GRIP1 (Bruckner et al., 1999) using the primers *PDZ7-hind3\_for* and *PDZ7-kpn1\_rev* with flanking HindIII and KpnI restriction sites into pECFP-C1 (Clontech). The correct sequence was confirmed by sequencing using primer *pECFP-C1\_clontech*.

### **B2-peptideWT-CFP, B2-peptideSA-CFP and B2-peptideSE-CFP**

To generate the B2-peptideWT, SA or SE CFP constructs, oligonucleotides containing the sequence of sense and antisense strands of the last 48pb (16 amino acids) of ephrinB2, ephrinB2SA or ephrinB2SE, with flanking HindIII or KpnI restriction sites, were allowed to anneal and form

## 7 Material and methods

---

double stranded DNA inserts. The inserts were cloned into pECFP-C1 using HindIII and KpnI restriction sites. Correctness of the sequence was confirmed by sequencing using the primer *pECFP-C1\_clontech*.

Expression of all constructs was tested in HeLa cells and checked by immunoblotting.

### 7.1.7 Cell lines and bacteria

Bacteria

Strain	genotype
<b>TOP10</b>	F- <i>mcrA</i> $\Delta$ ( <i>mrr-hsdRMS-mcrBC</i> ) $\Phi$ 80 <i>lacZ</i> $\Delta$ M15 $\Delta$ <i>lacX74</i> <i>recA1</i> <i>ara</i> $\Delta$ 139 $\Delta$ ( <i>ara-leu7697</i> ) <i>galU galK rpsL</i> (Str <sup>r</sup> ) <i>endA1 nupG</i>
<b>DH5<math>\alpha</math></b>	<i>supE44</i> $\Delta$ <i>lacU169</i> ( $\Phi$ 80 <i>lacZ</i> $\Delta$ M15) <i>hsdR17 recA1 endA1</i> <i>gyrA96 thi-1 relA1</i>

Cell lines

Line	Origin	Culture medium
<b>HeLa</b>	Human cervix carcinoma cells	DMEM, FBS
<b>HeLa b1</b>	HeLa stably expressing <i>ephrinB1</i>	DMEM, FBS, Geneticin
<b>293 HEK</b>	Human embryonic kidney cells	DMEM, FBS
<b>293 GluR2 HEK</b>	HEK stably expressing <i>GluR2</i>	DMEM, FBS, Geneticin

### 7.1.8 Primary cells and tissue

Primary cells and animal tissues were obtained from BL/6 mice or Wistar rats (Harlan). EphrinB2 knockout neurons and control cells were isolated from conditional *ephrinB2*<sup>lox/lox</sup> knockout mice

(Grunwald et al., 2004) crossed with Nestin Cre<sup>+</sup> or Nestin Cre<sup>-</sup>. These mice express cre-recombinase under the Nestin-promotor which specifically deletes ephrinB2 in the central nervous system.

### 7.1.9 Media and standard solutions

#### Dulbecco's phosphate-buffered saline (D-PBS)

137 mM NaCl	→	NaCl	8g
2.7 mM KCl	→	KCl	0.2 g
8 mM Na <sub>2</sub> HPO <sub>4</sub>	→	Na <sub>2</sub> HPO <sub>4</sub>	1.15 g
1.5 mM KH <sub>2</sub> PO <sub>4</sub>	→	KH <sub>2</sub> PO <sub>4</sub>	0.24 g

Dissolve ingredients in 800 ml of sterile water. Adjust solution to pH 7.4 with HCl, fill up to 1l total volume and sterilize by autoclaving. Store at room temperature (RT).

#### 10x D-PBS

137 mM NaCl	→	NaCl	80g
2.7 mM KCl	→	KCl	2 g
8 mM Na <sub>2</sub> HPO <sub>4</sub>	→	Na <sub>2</sub> HPO <sub>4</sub>	11.5 g
1.5 mM KH <sub>2</sub> PO <sub>4</sub>	→	KH <sub>2</sub> PO <sub>4</sub>	2.4 g

Dissolve ingredients in 800 ml of sterile water. Adjust solution to pH 7.4 with HCl, fill up to 1l total volume and sterilize by autoclaving. Store at RT.

#### 0.5 M EDTA, pH 8.0

Disodium EDTA·2H <sub>2</sub> O	→	186.1 g
---------------------------------	---	---------

Dissolve disodium EDTA in 800 ml of sterile water. Adjust solution to pH 7.4 with HCl, fill up to 1l total volume and sterilize by autoclaving. Store at RT.

### 1M Tris-HCl, pH 7.4 or 8.0

Tris base	→		121.1 g
pH 7.4	→	HCl	70 ml
pH 8.0	→	HCl	42 ml

Dissolve Tris base in 800 ml of sterile water. Adjust solution to the desired pH with concentrated HCl, fill up to 1l total volume. Sterilize by autoclaving and store at RT.

### Tris-EDTA (TE) buffer, pH 8.0

10 mM Tris-HCl

1 mM EDTA

Adjust to pH 8.0 by adding concentrated HCl and fill up to 1l volume. Sterilize by autoclaving and store at RT.

### 50x Tris-acetate-EDTA (TAE) electrophoresis buffer

Tris base	→		242 g
Glacial acetic acid	→		57.1 ml
0.5 M EDTA (pH 8.0)	→		100 ml

Add distilled water to 1l total volume, the pH should be ~8.3. Store at RT. Dilute stock solution with distilled water to prepare both agarose gels and the electrophoresis buffer.

**6x Agarose gel-loading buffer**

50% Glycerol (v/v)	→	87% Glycerol	57 ml
1x TAE buffer	→	50x TAE buffer	2 ml
0.2% Orange G (w/v)	→	Orange G	0.2 g

Add distilled water to 100 ml total volume and store at RT.

**4% Paraformaldehyde (PFA)**

PFA (w/v)	40 g
10x D-PDS	100 ml
10N NaOH	100 µl

Heat 800 ml of sterile water in the water bath to approximately 70°C, add PFA powder and stir thoroughly. Add NaOH to completely dissolve the PFA and let it cool down to RT. Add 100 ml 10x D-PBS and fill up to 1l total volume with water. Adjust the pH to 7-7.3, filter solution using Whatman paper and store at -20°C in aliquots of adequate volume. Use a freshly thawed aliquot each time.

**7.1.9.1 Media for bacterial culture****Luria-Bertani (LB) medium**

Bacto-Tryptone	10 g
Bacto-Yeast extract	5 g
NaCl	5 g

Dissolve in 1l sterile water and adjust pH to 7.5. Sterilize by autoclaving and store at RT.

### LB plates

LB medium	1 l
Bacto-Agar	15 g

Autoclave, pour into petri-dishes and store at 4°C.

### Antibiotics 1000x stock solution

Ampicillin	100 mg/ml
Kanamycin monosulfate	50 mg/ml

### 7.1.9.2 Media and supplements for cell culture

#### DMEM-FBS growth medium

DMEM (Invitrogen, #61965-059)	500 ml
FBS, heat inactivated (Invitrogen, #10270-106)	50 ml
Penicillin/Streptomycin (5000U/ml, 100µg/ml) (Invitrogen #15070-063)	5 ml
200 mM L-Glutamine (100x) (Invitrogen #25030-024)	5 ml
100 mM Sodium pyruvate (100x) (Invitrogen #11360-039)	5 ml

Store at 4 °C.

#### DMEM-FBS starving medium

Same composition as DMEM growth medium, but with 0.5% FBS instead of 10%.

**293 GluR2 and HeLa b1 growth medium**

DMEM-FBS medium	1 l
Geneticin (Invitrogen, # 10131-027)	4 ml

Store at 4°C.

**293 GluR2 and HeLa b1 starving medium**

Same composition as 293 GluR2 growth medium, but with 0.5% FBS instead of 10%.

**7.1.9.3 Media and supplements for primary cell culture****Borate buffer**

Boric acid	1.55 g
Borax	2.375 g

Dissolve in 500 ml distilled water, adjust to pH 8.5 and store at 4°C. For coating of plates and cover slips, dissolve Poly-D-Lysine (10 mg/ml) in borate buffer and sterilize by filtration.

**Neurobasal medium (NB)**

Neurobasal medium (Invitrogen, #21103-049)	500 ml
B27supplement (Invitrogen, #17504-044)	10 ml
L-Glutamine, stable 200mM (PAA, #M11-004)	1.25 ml

Store at 4°C. For low density and mouse hippocampal neuron cultures add 10% conditioned neurobasal medium.

### Conditioned neurobasal medium (CM)

The supernatant of old cultures (10-17DIV) is sterilized by passing through a 0.22  $\mu\text{m}$ -pore sized filter and stored at 4°C.

### Serum medium (SM)

DMEM 100 ml

FBS, heat inactivated (Invitrogen, #F-7524) 10 ml

Sterilize by passing through a 0.22  $\mu\text{m}$ -pore sized filter and store at 4°C. FBS is kept in aliquots of 10 ml at -20°C.

### Dissection medium

HBSS (Invitrogen, #24020-091) 500 ml

Penicillin/Streptomycin (Invitrogen, #15070-063) 5 ml

1M HEPES (Invitrogen, #15630-056) 3.5 ml

L-Glutamine 200mM (PAA, #M11-004) 5 ml

Store at 4°C and keep on ice during dissection.

### Artificial cerebrospinal fluid (ACSF)

124 mM NaCl

5 mM KCl

1.25 mM  $\text{NaH}_2\text{PO}_4$

2 mM  $\text{MgSO}_4$

10 mM Glucose

Dissolve in distilled  $\text{H}_2\text{O}$ , gas with 5 %  $\text{CO}_2$  / 95 %  $\text{O}_2$ , add 2 mM  $\text{CaCl}_2$  after 5 minutes and finally 26 mM  $\text{NaHCO}_3$  after 10 minutes.

### 7.1.9.4 Media and solutions for cell transfection

#### CaCl<sub>2</sub>

1 M CaCl <sub>2</sub>	CaCl <sub>2</sub> ·2H <sub>2</sub> O	2.94 g
2.5 M CaCl <sub>2</sub>	CaCl <sub>2</sub> ·6H <sub>2</sub> O	11 g

Add 20 ml distilled water, sterilize by passing through a 0.22 µm pore-sized filter and store 1 ml aliquots at -20°C.

#### 2x BES-buffered saline (BBS)

50 mM BES	→BES	1.07 g
280 mM NaCl	→NaCl	1.6 g
1.5 mM Na <sub>2</sub> HPO <sub>4</sub> ·2H <sub>2</sub> O	→ Na <sub>2</sub> HPO <sub>4</sub> ·2H <sub>2</sub> O	0.027 g

Dissolve in 80 ml of distilled water, adjust the pH with NaOH to 6.96- 7.26 (depending on the size and preparation of the plasmid DNA) and fill up to 100 ml total volume. Sterilize by passing through a 0.22 µm filter and store aliquots at -20°C.

#### Washing buffer for hippocampal neurons (HBSS pH 7.3)

	mM	M (g/mol)	2l (g)
NaCl	135	58.44	15.78
KCl	4	74.55	0.6
Na <sub>2</sub> HPO <sub>4</sub> (2xH <sub>2</sub> O)	1	141.96 (177.99)	0.28 (0.355)
CaCl <sub>2</sub> x 2H <sub>2</sub> O	2	147.02	0.59
MgCl <sub>2</sub> x 6H <sub>2</sub> O	1	203.3	0.41
HEPES	20	238.31	9.53
d-Glucose	10	180.16	3.6

## 7 Material and methods

---

d-Glucose x 1H <sub>2</sub> O	10	198.17	3.96
-------------------------------	----	--------	------

Dissolve all ingredients in 1.8 l distilled water, adjust pH to 7.3 and fill up to 2 l total volume.

### 7.1.10 Solutions and buffers for Western Blot analysis

#### 6x sample buffer for reducing and non-reducing conditions

12% SDS	→ SDS	3.6 g
300 mM Tris-HCl, pH 6.8	→ 1.5 mM Tris	6 ml
600 mM DTT	→ DTT	2.77 g
0.6% Bromphenol blue	→ Bromphenol blue	0.18 g
60% Glycerol	→ 99% Glycerol	18 ml

Add distilled water to 30 ml, store aliquots at -20°C. For reducing conditions add 50 µl β-mercaptoethanol to 1 ml of 4x sample buffer, or 25 µl to 1 ml of 2x sample buffer.

#### LBA Lysis buffer

50 mM Tris-HCl, pH 7.5	→ 1M Tris, pH 7.5	25 ml
150 mM NaCl	→ 5 M NaCl	15 ml
0.5-1% Triton X (TX)-100	→ TX-100	2.5-5 ml

Add distilled water to 500ml and store at 4°C.

Add fresh to 50 ml:

1 mM Sodium ortho vanadate (Na <sub>3</sub> VO <sub>4</sub> )	→ 100 mM Na <sub>3</sub> VO <sub>4</sub>	500 µl
10 mM NaPPi	→ NaPPi	0.225 g
20 mM NaF	→ NaF	0.042 g
Proteinase inhibitor cocktail tablet	→ 1 tablet in 500 µl H <sub>2</sub> O	500 µl

**HNTG buffer**

20 mM	HEPES (pH 7.5)
150 mM	NaCl
10 %	Glycerol
0.1 %	Triton-X100

Dissolve all ingredients in distilled water, adjust pH to 7.5 and keep buffer at 4°C. Add 1 mM  $\text{Na}_3\text{VO}_4$  and 1 % complete inhibitor cocktail (Roche) freshly right before use.

**Laemmli separating gel**

Concentration	6%	7.5%	9%	10%
30% (w/v) Acrylamid/bisacrylamid	2 ml	2.5 ml	3 ml	3.3 ml
1.5 M Tris-HCl pH 8.8, 0.4% SDS	2.6 ml	2.6 ml	2.6 ml	2.6 ml
H <sub>2</sub> O	5.35 ml	4.85 ml	4.4 ml	4.05 ml
10% APS	50 µl	50 µl	50 µl	50 µl
TEMED	5 µl	5 µl	5 µl	5 µl

Always prepare fresh, add APS and TEMED just before pouring the gel. Load distilled water on top to smoothen the edge of the polymerizing gel.

### Laemmli stacking gel, 10 ml

30% (w/v) Acryl amid/bisacrylamid	1.3 ml
0.5 M Tris-HCl pH 6.8, 0.4% SDS	2.6 ml
H <sub>2</sub> O	6.1 ml
10% APS	100 µl
TEMED	10 µl

Always prepare fresh, add APS and TEMED just before pouring the gel.

### 5x Laemmli electrophoresis buffer

Tris base	154.5 g
Glycerin	721 g
SDS	50 g

Add distilled water to 10 l total volume, store at RT.

### 10x Transfer buffer

Tris base	60.5 g
Glycin	281.5 g
SDS	25 g

Add distilled water to 2.5l total volume, store at RT. Add 20% methanol to the 1x transfer buffer right before use.

**TBS or PBS-Tween (TBS-T, PBS-T)**

1x D-TBS or PBS

0.1% Tween®20

Store at RT.

**Blocking solution**

Depending on the requirements of the primary antibody use TBS/PBS-T, PBS or TBS with 3-5% milk powder (Roth) or 3-5% BSA (Sigma). Prepare fresh, storage at 4 °C o/n possible.

**Sodium phosphate buffer, pH 7.2**

1 M Na<sub>2</sub>HPO<sub>4</sub>                      68.4 ml

1 M NaH<sub>2</sub>PO<sub>4</sub>                      31.6 ml

2% SDS

Add water to 1 l total volume and store at RT.

**Stripping buffer**

5 mM Sodium phosphate buffer, pH 7-7.4

2 mM β-Mercaptoethanol

25 SDS

Store at RT. Add β-Mercaptoethanol right before use.

## 7.2 Methods

### 7.2.1 Molecular Biology

#### 7.2.1.1 Genomic DNA extraction and genotyping polymerase chain reactions (PCR)

##### DNA preparation

The DNA for genotyping was prepared from mouse tails of about 0.1-0.5 cm length. The tails were boiled at 95°C in 100 µl 50 mM NaOH for 45 min using the PCR machine and thoroughly vortexed afterwards. If necessary, this step was repeated until the tails were properly dissolved. To neutralize the lysates, 10 µl of 1.5 M Tris pH 8.3 was added, mixed by vortexing and centrifuged down for 30''. 2 µl of the samples was used for genotyping.

##### Genotyping PCR

The mice were checked for the presence of homozygous ephrinb2lox alleles and the presence of Cre recombinase under the Nestin-promoter.

PCR- master mix for 50 µl reaction volume (always include a positive and a negative control for the Cre-PCR)

Tabelle 7-7: PCR master mix

Genotype	Cre	B2lox
dNTPs (25 mM each)	0.4 µl	0.4 µl
10x Taq pol buffer (NEB)	5 µl	5 µl
Primer 1 (100 mM)	0.5 µl Cre1	0.5 µl B2cs1
Primer 2 (100 mM)	0.5 µl Cre2	0.5 µl B2cas1
Taq Polymerase (NEB)	0.25 µl	0.5 µl
Distilled H <sub>2</sub> O	41.35 µl	41.1 µl

The DNA samples (2 µl) were placed into 96well PCR reaction tubes, the master mixed was prepared and added, and the tubes were placed into the PCR machine to run the appropriate program:

B2lox PCR program

Tabelle 7-8: B2lox genotyping PCR program

Segment	Cycles	Temperature	Time
1	1	94°C	1 min
2	35	94°C	45 sec
		62°C	45 sec
		72°C	45 sec
3	1	72°C	5 min
4	1	10°C	forever

Cre PCR program (Optimized)

Tabelle 7-9: Cre-Genotyping PCR program

Segment	Cycles	Temperature	Time
1	1	94°C	3 min (2min)
2	35	94°C	1 min (40 sec)
		67°C	1 min (30 sec)
		72°C	1 min (40 sec)
3	1	72°C	5 min
4	1	10°C	forever

### 7.2.1.2 Plasmid DNA preparation

Plasmid DNA was prepared from small-scale (2ml, miniprep) or from large-scale (200 ml, maxiprep) bacterial cultures. These cultures were grown in LB medium containing 100 µg/ml of selective antibiotics (ampicillin or kanamycin) at 37°C over night (o/n) from either a single colony of transformed bacteria picked from an agar plate or from a glycerol stock. Bacteria were harvested by centrifugation at 4000 rpm for 10 min (miniculture) or 20 min (maxiculture) at 4°C and the plasmid DNA purification was carried out using the QIAGEN® DNA purification Maxi/Mini Kit following the protocol described in the QIAGEN handbook including the steps of cell lysis, binding of the plasmid to the column, washing, elution and precipitation of the plasmid DNA (maxiprep). The precipitated DNA was dissolved in distilled water and the DNA concentration determined using a UV spectrometer at 260 nm. (formula dsDNA:  $OD_{260} \times 50 \times \text{dilution factor} = X \text{ µg/ml DNA}$ )

### 7.2.1.3 Enzymatic treatment of DNA

#### DNA cleavage

The recommended reaction volume for digestions is 50 µl. 0.5-2 µg DNA was incubated with 10U (1 µl) restriction enzyme in the appropriate buffer (1x), with 100 µg/ml BSA if required, for 1-2 hours at 37°C. The reaction was stopped by heat-inactivation of the enzyme at 65°C for 20 min. Successful digestion was checked by running 10 µl of the sample in a separating agarose gel. All enzymes used are purchased from New England Biolabs, for maximal success read the enzymes information provided by the company.

#### DNA-fragment dephosphorylation

The treatment of DNA or RNA with antarctic phosphatase results in a removal of the 5' phosphoryl termini, which is required by ligases. It prevents target vectors from self-ligation and is therefore useful to decrease vector background in cloning strategies. The usual reaction volume was 50 µl including 1 µl enzyme and the digested sample in 1x antarctic phosphatase buffer. The reaction takes place at 37°C, the recommended time is 30 min followed by heat inactivation for 5 min at 65°C.

### **Ligation of DNA fragments and target vectors**

The enzyme T4 ligase catalyses the formation of a phosphodiester bond between 5' phosphate and 3' hydroxyl termini in double stranded DNA or RNA and is therefore used to join DNA fragments, inserts, into open vectors. In a 20 µl volume, cleaved vector ( app. 0.1 µg) and DNA inserts of a 1:5 ratio, 1 µl of T4 ligase in 1x T4 ligase buffer was incubated o/n at 16°C or 2 hours at RT, followed by heat inactivation of the enzyme at 65°C for 10min and subsequent transformation of bacteria.

#### **7.2.1.4 Transformation of competent Bacteria**

For each transformation, 50 µl of competent bacteria (TOP10) were gently thaw on ice and placed into the upper corner of a Gene pulser® cuvette. There they were mixed with 1-2 µl ligation product and keep on ice until the electroporation with Gene pulser apparatus (BioRad) (50 µF, 1.8 kV and 200 Ω). To set the electro pulse, bacteria were transferred to the bottom of the cuvette by softly knocking the cuvette onto the table (bubbles should be avoided), and the cuvette placed into the electroporation chamber and pulsed once. Quickly after the pulse, 0.5 ml of RT LB medium was added, the bacterial suspension was transferred to a fresh sterile Eppendorf tube using a fire-sterilized Pasteur pipette and placed into a shaker (250 rpm) at 37°C for 60 min. The transformed bacteria were then plated onto an LB agar plate containing the appropriate selective antibiotic and incubated at 37°C o/n.

#### **7.2.1.5 Gel electrophoresis**

To separate different sized DNA fragments or/and to determine their length and amount, DNA samples were run on agarose gels of 1-2% and separated by electrophoresis. High agarose (Biomol) was dissolved in 1x TAE buffer by microwaving, mixed with 1 µl/100 ml ethidium bromide to visualize the DNA, poured into an electrophoresis gel chamber and cooled to RT while polymerizing. DNA samples were mixed with loading buffer (6:1) loaded into the gel pockets and separated for approximately 30-45 min at 100-200V depending on the gel size. A picture of the gel was taken in the transilluminator on UV light. For preparative gels, the DNA

band of interest was excised from the agarose gel using a clean, sharp blade and purified as described below.

### 7.2.1.6 DNA purification

#### From agarose gels

After excising the DNA band of interest from an agarose gel, the DNA fragments were purified using the Qiagen Gel Extraction Kit (#28704) following the enclosed Qiagen protocol.

#### From enzymatic reactions

After enzymatic reactions, e. g. PCRs, DNA fragment were cleaned from salts, enzymes, and remnant nucleotides using either the PCR Purification Kit (Qiagen, #28104) or the NucleoSpin ExtractII (Macherey&Nagel, #740609.250), following the enclosed protocol of the provider.

### 7.2.1.7 Mutagenesis PCR (plasmids)

All mutagenesis PCRs were done using the Site-directed Mutagenesis Kit (Stratagene) according to the protocol provided by Stratagene. The appropriate base pair changes and reading frame of the product were confirmed by sequencing (ABI Prism 377 DNA sequencer). The PCR program used was the following:

Tabelle 7-10: Mutagenesis PCR

Segment	Cycles	Temperature	Time
1	1	95°C	2'
2	5	95°C	1'
		55°C	1'
		72°C	12' (or 2x kb of the plasmid)
3	25	95°C	1'

---

		65°C	1'
		72°C	12'+10''
4	1	72°C	5'
5	1	10°C	o/n

---

## 7.2.2 Cell culture

### 7.2.2.1 Mammalian cell lines

#### Propagation

293 HEK or 293 GluR2 HEK cells were cultivated in DMEM growth medium at 37°C and 5% CO<sub>2</sub> below total confluency. For splitting, the cells were washed with PBS, treated with trypsin/EDTA (Invitrogen, #25300-054) at 37°C until the cells started to detach from the culture dish, and collected in the appropriate volume of growth medium. The cells were then distributed in the desired dilution onto fresh culture plates with pre-warmed medium.

#### Freezing and thawing

Cells were harvested using trypsin as described above, collected by centrifugation at 800 rpm for 5 min and re-suspended in FBS with 5% DMSO and distributed into cryo-tubes of 1 ml volume, which were immediately after placed into a freezing box to allow slow freezing at -80°C. For long term storage, frozen cells are kept in liquid nitrogen. To thaw frozen cells, the cryo-tube was quickly placed into a 37°C water bath and 10 ml of pre-warmed growth medium was added as soon as its content was thawed. The cells were collected by centrifugation at 800 rpm for 5 min, re-suspended and seeded onto culture plates with pre-warmed growth medium.

### 7.2.2.2 Cultivation of primary hippocampal neurons

#### Coverslip (CVS) treatment

CVS were treated with nitric acid (Fluka) in a glass beaker at RT over night. The next day, the CVS were washed 3-4 times with H<sub>2</sub>O, left with changes of fresh H<sub>2</sub>O on a rocker 4 times for 30 minutes to briefly remove the acid and spread separately on Whatmann paper to dry. Dry CVS were baked to sterilize in the oven at 165°C.

#### Coating of the CVS

The CVS were placed into 24-well plates (Costar) and coated with 1 mg/ml poly-D-lysine (Sigma, #P7886-1G) in Borate-Buffer (400 µl/well), which had been sterilize by passing through a 0.22 µm pore size filter after poly-D-lysine dissolvment, at 37°C for minimum 5 hours. Then the CVS were washed 3x with distilled sterile H<sub>2</sub>O, left in the hood to dry and coated with 5µg/ml laminin in PBS (400µl/well) for minimum 2 hours at 37°C. Excessive laminin was washed off 3x with PBS, the wells were filled with 400 µl NB medium and placed into the incubator for pH and temperature equilibration.

#### Isolation of hippocampal neurons (adapted from Jenny Lauterbach )

4 ml of serum medium (SM) and Neurobasal medium (NB) each was filled in dishes and placed into the incubator; trypsin was put into the water bath to warm up. The embryos of pregnant E18-19 rats or E17 mice were taken, the heads were cut off and collected in a 35mmØ dish filled with chilled dissection medium (DM). Carefully the skulls were opened, the brains removed and transfered into a fresh dish of 35mmØ filled with chilled DM. The two cortices halves of each brain were then separated from the brain steam, the meninges were removed and the hippocampi were cut out of each cortex half. The hippocampi were collected in a 15 ml tube on ice filled with 10 ml DM. When all hippocampi were isolated, the DM was carefully replaced by 1-2 ml prewarmed trypsin and the tube placed into the water bath for 20 min at 37°C. Meanwhile, a Pasteur pipette was flamed to decrease the diameter of the tip. The trypsin was removed after 20 min and the hippocampi washed 3x with prewarmed SM to stop the reaction. The tissue was homogenized in 1.5 ml SM using the fire-polished Pasteur pipette by pipetting up and down 20-

30 times, it was carefully avoided to make bubbles (neurons do not like oxygen). Cells were collected by centrifugation for 5 min at 650 rpm, the supernatant removed and the cells resuspended in warm NB medium using the fire-polished Pasteur pipette. Cell number was determined using a Neubauer counting chamber, thereafter the cells were plated on the CVS in 24-well plates with prewarmed medium at desired density. Low density cultures require 15-25.000 cells/well (24 well plate), high density up to 70.000 cells per well.

### 7.2.2.3 Transfection of cell lines and primary hippocampal neurons

#### CaPO<sub>4</sub>-transfection (general protocol)

24 hour prior transfection cells were splitted to achieve the appropriate density (20-40% confluence) and incubated with growth medium.

Mix for one 10 cm Ø dish:

9 ml fresh growth medium +	1000µl Transfection Mix containing:
	450 µl H <sub>2</sub> O – DNA (10-20µg)
	50 µl 2.5 M CaCl <sub>2</sub>
	500 µl 2x BBS (pH 6.96-7.10)

First, the water was mixed with the DNA in an Eppendorf tube, then 50 µl CaCl<sub>2</sub> was added and finally the BBS. The transfection mix was vortexed shortly and incubated for 15 minutes at RT. The cells were washed with PBS and covered with 9 ml fresh warmed growth medium. The transfection solution was added to the plate by dropping it slowly into the medium. The cells were incubated with the transfection solution for 8 hours, washed briefly with PBS (CaMg) and covered with 10 ml fresh growth medium. 24 hours before performing stimulation assays, the cells were starved by exchanging growth against starving medium.

#### CaPO<sub>4</sub>-transfection primary hippocampal neurons

Mix for 4 wells (24-well plate):

900µl fresh NB medium +	100µl Transfection Mix containing
	37.5 µl H <sub>2</sub> O – DNA (4-7µg)
	12.5 µl 1M CaCl <sub>2</sub>
	50 µl BBS (pH 7.26)

NB medium (900µl per 4 wells) with freshly added B27 was placed into the incubator to warm for at least 30 minutes. Meanwhile, the transfection mix for 4 wells each was prepared in a fresh sterile Eppendorf tube by adding first the H<sub>2</sub>O, then the CaCl<sub>2</sub> and the DNA. 900 µl warm NB medium was transferred into a 5 ml polypropylene round bottom tube (Falcon, #352052) and vortexed. Then 50 µl BBS was added to the first Eppendorf tube and the complete transfection mix added into the NB medium while vortexing by dropping it in slowly. The culture medium on the cells was quickly replaced with 250 µl of the fresh mixed transfection solution per well (100µl transfection mix + 900 µl NB medium), the old culture medium was kept in a separate tube. Always 4 wells were done at a time, these steps were repeated until each well had received transfection solution, and then the plate was put back into the incubator. If needed and to exclude contamination the collected, old culture medium might be sterile filtered by passing through a 45 µm pore filter with a syringe and was kept in the incubator to later replace the transfection solution. Meanwhile, the washing solution (HBSS pH 7.3) was warmed in the water bath at 37°C. After approximately 2 hours, when small precipitates had formed, the wells were washed 2x with pre-warmed washing solution (HBSS pH 7.3) and the old culture medium ( 300 µl per well) was placed back on to the cells. The cells were assayed 2-5 days after transfection.

### 7.2.3 Biochemistry

#### 7.2.3.1 Cell stimulation

##### EphB and ephrin stimulation

For stimulation, recombinant EphB-Fc, ephrinB-Fc, or Fc (Biochemistry: 1 µg/ml (cells) or 4 µg/ml (neurons); Immunocytochemistry: 4 µg/ml) were preclustered with goat anti-human IgG antibodies (1/10) for 1 hour at RT. Cells were washed once with warmed PBS (CaMg) and stimulated in culture medium (3ml for 10 cmØ, 300µl per 24-well plate well) for 10-60 minutes,

depending on the assay conditions. For inhibition of SFKs, the specific inhibitor PP2 was dissolved in DMSO and added to the plates (20 $\mu$ M) 15 minutes prior EphB stimulation.

### **AMPA stimulation**

AMPA (Sigma) was dissolved in artificial cerebrospinal fluid (ACSF) and kept at -80°C in aliquots of 100 mM (1000x). Cells were stimulated in culture medium with 100 $\mu$ M AMPA for 10 minutes at 37°C. In case of double stimulation with EphB4, AMPA was added in for the last 10 minutes of stimulation.

### **NMDA stimulation**

NMDA (Sigma) was dissolved in ACSF and kept in aliquots of 50 mM at -80°C. Cells were stimulated by adding 50  $\mu$ M NMDA for 2 minutes to the culture medium, and leaving the reaction proceed for additional 10 minutes. In case of double stimulation with EphB4, NMDA was added in for 2 minutes during the last 10 minutes of the stimulation.

### **KCl stimulation**

For the KCl stimulation, neurons were treated for 10 minutes with 10 mM KCl in NB medium and assayed for activity-induced ephrinB2 cluster formation. EphrinB2 clusters were visualized indirectly by the binding of soluble EphB4-Fc to surface ephrinB2 and subsequent detection using goat anti- human IgG-cy2 antibodies.

## **7.2.3.2 Cell or tissue lysis and protein concentration measurements**

### **Cell and tissue lysis**

Cells or tissues, that were assayed by immunoprecipitation or/and immunoblotting, were lysed in chilled lysis buffer (containing freshly added vanadate, NaF, NaPPi and kinase inhibitor cocktail(Roche) ). Cells were placed on an ice tray, washed once with cold PBS and collected from the culture dish in the appropriate volume of lysis buffer (e. g. 500  $\mu$ l/ 10 cm  $\varnothing$  dish) using

cell scrapers (Sarsted). Tissue was homogenized in chilled lysis buffer using a glass homogenizer (B. Braun, Melsungen AG). Lysates were collected in tubes on ice and fixed on a spinning wheel at 4°C for minimum 10 minutes to let the lysis proceed. Thereafter, the lysates were cleared from cell debris by centrifugation at 4°C (10 minutes for cell lysates, 45 minutes for homogenized tissue) and the protein content was determined.

### **Protein concentration measurement**

To determine the protein concentration of different lysates, the BioRad DC Protein Assay kit was used. Different BSA concentrations in the range of 0-10 mg/ml (0, 1, 2, 5, 10) served as standard and were assayed at the same time with 2-5 µl of the samples in doublets. The amount of protein of each sample was determined and equal amounts were used for immunoprecipitation and pulldown experiments.

### **7.2.3.3 Immunoprecipitation and pulldown experiments**

#### **Immunoprecipitation**

The agarose beads for immunoprecipitation were kept in suspension (1:1) in PBS with 50% ethanol to avoid contamination. 10 µl of the beads per sample (20 µl of the beads-PBS suspension) were placed into an Eppendorf tube, washed with PBS by centrifugation 3 times at 2.8 rpm for 2.5 minutes and left with approximately 100 µl PBS to dissolve the primary antibody in. First, the beads were incubated with the antibody for 40-60 minutes at RT on a rotating wheel, then loaded with the samples of equal protein content and placed in a spinning wheel at 4°C. After 2 hours, the beads were washed 3 times by centrifugation (3.0 rpm, 3 minutes) with chilled lysis buffer containing vanadate to remove any unbound proteins. After the last wash the liquid was removed completely using extra thin gel saver tips (Kisker), 25 µl 2x sample buffer per tube was added and mixed in briefly by vortexing. The samples were boiled at 95°C for 5 minutes, run on SDS gels to separate the precipitated proteins, and analyzed by immunoblotting.

Table 7-11: Agarose beads and antibody specificity

<b>Product</b>	<b>Specificity</b>
Protein A-Agarose	mouse IgG <sub>2a</sub> , IgG <sub>2b</sub> & IgA, rabbit polyclonal, human IgG <sub>1</sub> , IgG <sub>2</sub> & IgG <sub>4</sub> antibodies
Protein G PLUS-Agarose	mouse IgG <sub>1</sub> , IgG <sub>2a</sub> , IgG <sub>2b</sub> & IgG <sub>3</sub> , rat IgG <sub>1</sub> , IgG <sub>2a</sub> , IgG <sub>2b</sub> & IgG <sub>2c</sub> , rabbit and goat polyclonal, human IgG <sub>1</sub> , IgG <sub>2</sub> , IgG <sub>3</sub> &IgG <sub>4</sub> antibodies
Protein A/G PLUS	All of the above antibodies
Protein L-Agarose	Mouse, rat, human IgG
Glutathione-Agarose	GST fusion proteins

### **Pulldown experiments**

EphrinB molecules (~47 kDa) run at the height of the antibodies' heavy chain in reducing gels and the signal is hidden by non-specific antibody interaction. Therefore, to specifically identify ephrinB molecules, the use of non-reducing SDS-PAGE gels is required. Alternatively, pulldowns that are based on the highly specific ligand-receptor-interaction provide a powerful tool to isolate and to study ephrinB molecules and their interaction partners. To pulldown ephrinB molecules from cell or tissue lysates, the extracellular part of Eph receptors fused to Fc portions of human antibodies (EphB2-Fc) is used (Cowan and Henkemeyer, 2001).

10 µl of G-sepharose beads (20 µl suspension) per sample were taken, washed 3 times with PBS by centrifugation at 2.8 rpm 2.5 minutes, loaded with 5 µg EphB-Fc or Fc (control for unspecific binding) together with the lysates and incubated over night at 4°C on a rotating wheel. (If necessary and to minimize unspecific binding to the beads, lysates can be pre-cleaned by incubation with only beads for 30 minutes at 4°C. The supernatant is then loaded to fresh beads with EphB-Fc or Fc). The beads were washed 3 times with chilled HNPG buffer by centrifugation at 3.0 rpm for 3 minutes, the liquid was removed completely using gel saver tips (Kisker) and 25 µl sample buffer was added. The samples were boiled at 95°C for 5 minutes and then separated on SDS page gels.

### 7.2.3.4 Immunoblotting

For immunoblotting, protein samples in loading buffer were boiled at 95°C for minutes, and separated by 6 %, 7.5 %, 9 % or 10 % SDS page. The separated proteins were transferred using semi-dry blotting chambers (Bio-Rad) in transfer buffer (20% methanol) to a nitrocellulose membrane. If an unstained marker was used, the membrane was incubated in Ponceau S for a few minutes until the marker was visible and drawn over by pencil. The membranes were blocked in blocking solution appropriate for the primary antibody used (3-5% milk in PBS, PBS-T or TBS, or 3-5% BSA in PBS or TBS) for 45 minutes at RT, incubated with the primary antibody in blocking solution for 1 hour at RT, washed 3 times 10 minutes with PBS-T and finally incubated with the secondary antibody in blocking solution (anti-rabbit, anti-mouse or anti-goat HRP). The membranes were washed again 3 times for 10 minutes (if no special treatment necessary) and the signal was visualized using chemiluminescent reagent ECL (Amersham) and captured on films taking different exposure times.

### 7.2.3.5 Immunocytochemistry

After transfection and stimulation, cells and neurons grown on cover slips were fixed with 4 % paraformaldehyde (PFA), 4 % sucrose in PBS for 12 minutes on an ice tray (4°C). The cells were rinsed twice with PBS and incubated with 50 mM NH<sub>4</sub>Cl in PBS for 10 minutes at 4°C to remove excessive PFA. The NH<sub>4</sub>Cl was rinsed off twice with cold PBS before the cells were permeabilized for 5 minutes with ice cold 0.1 % Triton X-100 in PBS. After washing the cells 3 times for 5 minutes with PBS, the cells were blocked for 30 minutes at RT in blocking solution (2 % bovine serum albumin, 4 % donkey and/or 4 % goat serum (Jackson ImmunoResearch)), and thereafter incubated with primary antibodies for 60-90 minutes at RT, or over night at 4°C. The samples were washed thoroughly with PBS 3 times 5 minutes and incubated with secondary antibodies for 60 minutes at RT protected from light. Finally, the cover slips were washed 3 times for 5 minutes with PBS, once with H<sub>2</sub>O by dipping them into a water filled dish, and mounted on slides using the Gel/Mount anti-fading medium (Biomedica corp.). Images were acquired using a digital camera (SpotRT; Diagnostic Instruments) attached to an epifluorescence microscope (Zeiss).

### 7.2.3.6 Internalization assays

#### Biotinylation assay

The biotinylation assay was performed as described (Chung et al., 2000; Lin et al., 2000; Man et al., 2000) with some modifications. Live hippocampal neurons 15-20 DIV or cells were incubated with 1 mg/ml or 300 µg/ml EZ-link NHS-SS-biotin (Pierce) in D-PBS buffer with  $\text{Ca}^{2+}\text{Mg}^{2+}$  for 3 min at 37°C, washed with D-PBS buffer with  $\text{Ca}^{2+}\text{Mg}^{2+}$  and optionally the remaining reactive biotin was quenched by incubating the cells with 200 mM glycine in PBS at 4°C for 20 minutes. After surface biotinylation, the cells were stimulated in culture medium with human Fc or EphB4-Fc (1 µg/ml cells or 4 µg/ml neurons) for 1 hour (neurons) or 30 minutes (cells); 100 µM AMPA was added in for the last 10 minutes. The reaction was stopped by cooling the cells to 4°C on an ice tray. The remaining surface biotin of non-internalized molecules was eliminated by washing the cells with 150 mM of glutathione (Sigma) in 150 mM NaCl for 10 minutes at 4°C. The glutathione was then neutralized by 50 mM iodoacetamide (Sigma) in D-PBS buffer with  $\text{Ca}^{2+}\text{Mg}^{2+}$ . The cells were lysed in LBA lysis buffer, centrifuged at 13.0 rpm for 10 minutes at 4°C and the supernatants with equal amounts of total protein were incubated with streptavidin beads, 100 µl/sample, over night at 4°C to capture internalized biotinylated proteins. The following day, the samples were washed 3 times with LBA buffer by centrifugation at 3 rpm for 3 minutes each at 4°C, the liquid was removed completely using gel saver tips (Kisker), and 25 µl sample buffer was added. The samples were boiled at 95°C for 5 minutes, separated on SDS page gels and analyzed by immunoblotting with the appropriate antibodies.

#### Antibody feeding assay

The antibody feeding assay was performed as described (Lin et al., 2000; Man et al., 2000) with some modifications. Hippocampal neurons from E19 rat or E17 mouse embryos were isolated and plated on coated coverslips Ø13 mm in 24-well plates. Briefly, hippocampal neurons 15-21DIV were blocked at 37°C for 10 minutes in blocking solution, incubated with the primary antibody anti-GluR2 (AA 175-430; 1:500) (Chemicon) or GluR1( AA 271-285; 1:50) (Calbiochem) for 18 minutes at 37°C, and washed with warm D-PBS +  $\text{Ca}^{2+}\text{Mg}^{2+}$ . The antibody-labeled cells were then stimulated with human Fc or EphB4-Fc (1 µg/ml) in 300 µl NB medium at 37°C for 1 hour; 100 µM AMPA was added in the last 10 minutes. For NMDA stimulation 50 µM NMDA was

added to the cells for 2 minutes. The cells were fixed as described under the point immunocytochemistry, and incubated with Alexa Fluor 488- or Cy2- conjugated secondary antibodies for 2 hours at RT protected from light to detect pre-labeled surface remained receptors. After washing 3 times 5 minutes with PBS, the neurons were permeabilized for 4 minutes with ice cold 0.1% Triton X-100 in PBS, blocked again for 30 minutes and finally incubated with Cy3-conjugated secondary antibodies to visualize pre-labeled internalized receptors. For the rescue experiments, hippocampal neurons isolated from NestinCre<sup>+</sup> ephrinB2<sup>lox/lox</sup> were transfected with CFP-ephrinB2 WT, CFP-ephrinB2 S-9>A or CFP-ephrinB2 S-9>E 5 days before performing the antibody feeding assay. For interference experiments hippocampal, neurons 15-17DIV were transfected 2-4 days prior performing the antibody feeding assay with GRIP1-PDZ6-CFP or GRIP1-PDZ7-CFP or the ephrinB peptide constructs ephb2-peptideWT, SA or SE CFP. All neurons transfected with CFP-constructs were incubated additionally with anti-GFP antibodies (RDI) after permeabilization to strengthen the CFP signal. Consequently, these neurons were treated in the last step with AMCA-conjugated and Cy3-conjugated secondary antibodies. Images were acquired using a digital camera (SpotRT; Diagnostic Instruments) attached to an epifluorescence microscope (Zeiss).

### 7.2.4 Postsynaptic density fractionation

PSD fractions were prepared by Stefan Weinges (Weinges, 2006) as described (Cho et al., 1992)

### 7.2.5 Tandem affinity purification (TAP) and mass spectrometry

Grb4-CTAP (C-terminal fusion) was generated as described in Stefan Weinges thesis (Bouwmeester et al., 2004; Weinges, 2006). TAP purification, protein digestion, mass spectrometry and protein identification were done as described in Stefan Weinges thesis (Angrand, 2006; Weinges, 2006).

### 7.2.6 Electrophysiology-patch-clamp recordings

Miniature excitatory postsynaptic currents (mEPSC) were recorded from dissociated hippocampal neurons (15 -19 DIV) at room temperature (20-22°C). The recording chamber was continuously perfused with carbogenated artificial cerebro-spinal fluid (ACSF) that contained (in mM): 119 NaCl; 2.5 KCl; 1.3 MgSO<sub>4</sub>; 2.5 CaCl<sub>2</sub>; 1 NaH<sub>2</sub>PO<sub>4</sub>; 26.2 NaHCO<sub>3</sub> and 11.1 D-glucose supplemented with 100 μM picrotoxin (PTX), 100 μM D(-)-2-Amino-5-phosphonovaleric acid

(APV) and 200 nM tetrodotoxin (TTX). Membrane currents were recorded at a holding potential of -70 mV using a MultiClamp 700B amplifier (Molecular Devices). Patch pipettes (WPI) with a resistance of 3.5-5 M $\Omega$  were filled with an internal solution containing (in mM): 150 CsGluc; 10 HEPES; 2 MgATP; 0.2 EGTA; 5 QX314; 8 NaCl, 290 mosm, pH 7.2. Signals were filtered at 2 kHz and digitized at 5 kHz via a Digidata 1440A digitizer (Axon Instruments, Molecular Devices). Data were collected using Clampex 10.1 and analyzed with Clampfit 10.1 software (Axon Instruments, Molecular Devices). Only cells with a series resistance lower than 25 M $\Omega$  and a noise level lower than 10 pA were analyzed. 80 events per cell were recorded. Cells with very high mEPSC frequencies were excluded. Statistical analysis was performed with Prism (Version 5.00, GraphPad).

## 7.2.7 Data analysis

### Immunofluorescence

Images were acquired using a digital camera (SpotRT; Diagnostic Instruments) attached to an epifluorescence microscope (Zeiss) equipped with a 40x and a 63X objective (Plan-Apochromat; Zeiss). All quantitative measurements were performed using MetaMorph software (Molecular Devices).

Quantification of AMPA-receptor internalization was based on fluorescence intensities. The percentage of internalized GluR2 or GluR1 (red fluorescence intensity) versus total GluR2 or GluR1 (red + green fluorescence intensity) was calculated for dendrite stretches of 100-200  $\mu$ m imaged on at least 10 different transfected or treated neurons (n= 50-100). Student's t tests were used to assess statistical significance of the quantifications (Microsoft Excel).

For the quantification of spine length, spine head area and protrusion number, approximately 100 dendrites from independent transfections were selected randomly. For each construct the number of protrusions on dendrite stretches of proximal 50  $\mu$ m, and the area of the spines heads were quantified. The protrusion length was determined by measuring the distance between the tip and the base (n>500 protrusions). Groups of protrusions were compared using t-test (Microsoft Excel).

Synapse formation and number of mature synapses was analyzed by counting the number of clusters positive for the pre-synaptic protein synapsin1, or the post-synaptic marker PSD-95 along dendrite stretches of approximately 100  $\mu\text{m}$ .

Spine morphogenesis was assayed by analyzing protrusion length and percentage of mature mushroom-like spines relative to total number of protrusions.

### **Electrophysiology**

Data were collected using Clampex 10.1 and analyzed with Clampfit 10.1 software (Axon Instruments, Molecular Devices). Only cells with a series resistance lower than 25  $\text{M}\Omega$  and a noise level lower than 10 pA were analyzed. 80 events per cell were recorded. Cells with very high mEPSC frequencies were excluded. Statistical analysis was performed with Prism (Version 5.00, GraphPad).



## 8 Acknowledgements

Foremost I would like to express my gratitude to Prof. Amparo Acker-Palmer for giving me the opportunity to do my thesis in her group, a great scientific environment. I am very grateful for her support and her trust in me, her constructive suggestions and critical discussions. Her positive energy and scientific enthusiasm created a fruitful environment and a very pleasant working atmosphere and an unforgettable time.

I wish to thank Rüdiger Klein who accepted to be my thesis supervisor and supported my work with critical questions, suggestions and great interest. Moreover I am thankful for numerous memorable events that, in pleasant atmospheres, provided great opportunities to exchange scientific and non-scientific experiences.

Particularly, I would like to thank Inmaculada Segura and Stefan Weinges for effective collaboration and shared work for the first publication.

Furthermore, the second paper would not have been possible without the supportive help from Elsa Martinez and Julia Geiger, the successful collaboration with Valentin Stein and Matthias Traut contributing with electrophysiological data and encouraging discussions, and the experimental contribution from Elsa Martinez and Manuel Zimmer.

I am very grateful to the two external members of my thesis committee, Stefan Sigrist and Valentin Stein, whose interest, critical discussion, suggestions and encouragement supported me throughout my thesis.

Special thanks are dedicated to the members and former members of the Acker-Palmer group, Elsa Martinez, Julia Geiger, Aycan Senturk, Inmaculada Segura, Helge zum Buttel, Suphansa Sawamiphak and Stefan Weinges for the great, continuous assistance, cheerful and friendly working atmosphere providing the perfect conditions for my PhD thesis.

The members of the Klein Lab and the Tavosanis Lab I want to thank for critical suggestions and discussions during the joined lab-meetings and for their technical help when required.

Moreover, I want to thank my colleagues from the institute for the nice and relaxed working atmosphere and their scientific and practical advices, nice conversations and friendships, especially

Jenny Lauterbach, Archana Mishra, Andreas Schaupp, Edward Fellows, Matthias Traut, Ali Erturk, Daniela Röttschke and Aline Lukas.

Finally, I want to thank my parents, my sister and brother, my grandparents, as well as my best friends, who supported and encouraged me during all this time, they deserve my deep gratitude.

## 9 Curriculum Vitae

### Personal data

**Name** Clara Luise Essmann  
**Birth date** 23<sup>rd</sup> of March 1979  
**Birth place** Freiburg im Breisgau, Germany  
**Nationality** German  
**Parents** Prof. Dr. Dr. H.F. und Karin L. Essmann

### Professional appointments

**July 2008-present**    **Postdoc position**  
Goethe-University Frankfurt  
Institute for Cell Biology and Neurosciences  
Laboratory of Prof. Acker-Palmer

### Education

**2004–2008**            **PhD thesis**  
Max-Planck-Institute for Neurobiology, Martinsried  
Department of Molecular Neurobiology  
Junior research group: Signal transduction, Prof. Acker-Palmer

**Dec2003–May2004**    **Diploma thesis**  
Friedrich-Alexander-University of Erlangen Nürnberg  
Experimentellen Medizin I, Nicolaus-Fiebiger Zentrum  
supervised by Prof K. von der Mark and PD H. Schneider  
*“Identification and characterisation of NG2-positive cells in postnatal bone marrow of rats and mice”*

**2001–2004**            **Diploma in Molecular Medicine**  
Friedrich-Alexander-University of Erlangen Nürnberg  
Major subject: Cell Biology  
Minor subject: Neurobiology, Human Genetics, Immunology

- 2000-2001**            **European Exchange Student** (Erasmus/Socrates)  
University of Gothenburg, Sweden
- 1998-2000**            **Basic studies in Biology**  
Albert-Ludwig -University of Freiburg
- 1989-1998**            **Abitur** (17.June 1998)  
Kepler-Gymnasium Freiburg

## 10 Bibliography

- Adams RH, Diella F, Hennig S, Helmbacher F, Deutsch U and Klein R (2001) The cytoplasmic domain of the ligand ephrinB2 is required for vascular morphogenesis but not cranial neural crest migration. *Cell* **104**(1):57-69.
- Akins MR and Biederer T (2006) Cell-cell interactions in synaptogenesis. *Curr Opin Neurobiol* **16**(1):83-89.
- Angrand PO, Segura, I., Volkel, P., Ghidelli, S., Terry, R., Brajenovic, M., Vintersten, K., Klein, R., Superti-Furga, G., Drewes, G., Kuster, B., Bouwmeester, T., Acker-Palmer, A. (2006) Transgenic mouse proteomics identifies new 14-3-3 associated proteins involved in cytoskeletal rearrangements and cell signaling. *Mol Cell Proteomics* **5**:2211-2227.
- Aoto J and Chen L (2007) Bidirectional ephrin/Eph signaling in synaptic functions. *Brain Res* **1184**:72-80.
- Arvanitis D and Davy A (2008) Eph/ephrin signaling: networks. *Genes Dev* **22**(4):416-429.
- Bartley TD, Hunt RW, Welcher AA, Boyle WJ, Parker VP, Lindberg RA, Lu HS, Colombero AM, Elliott RL, Guthrie BA and et al. (1994) B61 is a ligand for the ECK receptor protein-tyrosine kinase. *Nature* **368**(6471):558-560.
- Bear MF and Malenka RC (1994) Synaptic plasticity: LTP and LTD. *Curr Opin Neurobiol* **4**(3):389-399.
- Beattie EC, Carroll RC, Yu X, Morishita W, Yasuda H, von Zastrow M and Malenka RC (2000) Regulation of AMPA receptor endocytosis by a signaling mechanism shared with LTD. *Nat Neurosci* **3**(12):1291-1300.
- Beckmann MP, Cerretti DP, Baum P, Vanden Bos T, James L, Farrah T, Kozlosky C, Hollingsworth T, Shilling H, Maraskovsky E and et al. (1994) Molecular characterization of a family of ligands for eph-related tyrosine kinase receptors. *EMBO J* **13**(16):3757-3762.
- Borgdorff AJ and Choquet D (2002) Regulation of AMPA receptor lateral movements. *Nature* **417**(6889):649-653.
- Bouwmeester T, Bauch A, Ruffner H, Angrand PO, Bergamini G, Croughton K, Cruciat C, Eberhard D, Gagneur J, Ghidelli S, Hopf C, Huhse B, Mangano R, Michon AM, Schirle M, Schlegl J, Schwab M, Stein MA, Bauer A, Casari G, Drewes G, Gavin AC, Jackson DB, Joberty G, Neubauer G, Rick J, Kuster B and Superti-Furga G (2004) A physical and functional map of the human TNF-alpha/NF-kappa B signal transduction pathway. *Nat Cell Biol* **6**:97-105.
- Bredt DS and Nicoll RA (2003) AMPA receptor trafficking at excitatory synapses. *Neuron* **40**(2):361-379.
- Bruckner K, Pablo Labrador J, Scheiffele P, Herb A, Seeburg PH and Klein R (1999) EphrinB ligands recruit GRIP family PDZ adaptor proteins into raft membrane microdomains. *Neuron* **22**(3):511-524.
- Bruckner K, Pasquale EB and Klein R (1997) Tyrosine phosphorylation of transmembrane ligands for Eph receptors. *Science* **275**(5306):1640-1643.
- Burnashev N, Monyer H, Seeburg PH and Sakmann B (1992) Divalent ion permeability of AMPA receptor channels is dominated by the edited form of a single subunit. *Neuron* **8**(1):189-198.

- Cai C, Coleman SK, Niemi K and Keinanen K (2002) Selective binding of synapse-associated protein 97 to GluR-A alpha-amino-5-hydroxy-3-methyl-4-isoxazole propionate receptor subunit is determined by a novel sequence motif. *J Biol Chem* **277**(35):31484-31490.
- Carroll RC, Lissin DV, von Zastrow M, Nicoll RA and Malenka RC (1999) Rapid redistribution of glutamate receptors contributes to long-term depression in hippocampal cultures. *Nat Neurosci* **2**(5):454-460.
- Carvalho RF, Beutler M, Marler KJ, Knoll B, Becker-Barroso E, Heintzmann R, Ng T and Drescher U (2006) Silencing of EphA3 through a cis interaction with ephrinA5. *Nat Neurosci* **9**(3):322-330.
- Cheng HJ and Flanagan JG (1994) Identification and cloning of ELF-1, a developmentally expressed ligand for the Mek4 and Sek receptor tyrosine kinases. *Cell* **79**(1):157-168.
- Cho KO, Hunt CA and Kennedy MB (1992) The rat brain postsynaptic density fraction contains a homolog of the Drosophila discs-large tumor suppressor protein. *Neuron* **9**(5):929-942.
- Chung HJ, Xia J, Scannevin RH, Zhang X and Haganir RL (2000) Phosphorylation of the AMPA receptor subunit GluR2 differentially regulates its interaction with PDZ domain-containing proteins. *J Neurosci* **20**(19):7258-7267.
- Coleman SK, Moykkynen T, Cai C, von Ossowski L, Kuismanen E, Korpi ER and Keinanen K (2006) Isoform-specific early trafficking of AMPA receptor flip and flop variants. *J Neurosci* **26**(43):11220-11229.
- Constantine-Paton M and Cline HT (1998) LTP and activity-dependent synaptogenesis: the more alike they are, the more different they become. *Curr Opin Neurobiol* **8**(1):139-148.
- Contractor A, Rogers C, Maron C, Henkemeyer M, Swanson GT and Heinemann SF (2002) Trans-synaptic Eph receptor-ephrin signaling in hippocampal mossy fiber LTP. *Science* **296**(5574):1864-1869.
- Cowan CA and Henkemeyer M (2001) The SH2/SH3 adaptor Grb4 transduces B-ephrin reverse signals. *Nature* **413**(6852):174-179.
- Cuppen E, Gerrits H, Pepers B, Wieringa B and Hendriks W (1998) PDZ motifs in PTP-BL and RIL bind to internal protein segments in the LIM domain protein RIL. *Mol Biol Cell* **9**(3):671-683.
- Dailey ME and Smith SJ (1996) The dynamics of dendritic structure in developing hippocampal slices. *J Neurosci* **16**(9):2983-2994.
- Dalva MB, Takasu MA, Lin MZ, Shamah SM, Hu L, Gale NW and Greenberg ME (2000) EphB receptors interact with NMDA receptors and regulate excitatory synapse formation. *Cell* **103**(6):945-956.
- Davy A, Gale NW, Murray EW, Klinghoffer RA, Soriano P, Feuerstein C and Robbins SM (1999) Compartmentalized signaling by GPI-anchored ephrin-A5 requires the Fyn tyrosine kinase to regulate cellular adhesion. *Genes Dev* **13**(23):3125-3135.
- Davy A and Robbins SM (2000) Ephrin-A5 modulates cell adhesion and morphology in an integrin-dependent manner. *EMBO J* **19**(20):5396-5405.
- Dong H, O'Brien RJ, Fung ET, Lanahan AA, Worley PF and Haganir RL (1997) GRIP: a synaptic PDZ domain-containing protein that interacts with AMPA receptors. *Nature* **386**(6622):279-284.
- Egea J and Klein R (2007) Bidirectional Eph-ephrin signaling during axon guidance. *Trends Cell Biol* **17**(5):230-238.
- Engert F and Bonhoeffer T (1999) Dendritic spine changes associated with hippocampal long-term synaptic plasticity. *Nature* **399**(6731):66-70.
- Ethell IM, Irie F, Kalo MS, Couchman JR, Pasquale EB and Yamaguchi Y (2001) EphB/syndecan-2 signaling in dendritic spine morphogenesis. *Neuron* **31**(6):1001-1013.

- Fiala JC, Feinberg M, Popov V and Harris KM (1998) Synaptogenesis via dendritic filopodia in developing hippocampal area CA1. *J Neurosci* **18**(21):8900-8911.
- Fu J, deSouza S and Ziff EB (2003) Intracellular membrane targeting and suppression of Ser880 phosphorylation of glutamate receptor 2 by the linker I-set II domain of AMPA receptor-binding protein. *J Neurosci* **23**(20):7592-7601.
- Geinisman Y, Disterhoft JF, Gundersen HJ, McEchron MD, Persina IS, Power JM, van der Zee EA and West MJ (2000) Remodeling of hippocampal synapses after hippocampus-dependent associative learning. *J Comp Neurol* **417**(1):49-59.
- Greger IH, Khatri L, Kong X and Ziff EB (2003) AMPA receptor tetramerization is mediated by Q/R editing. *Neuron* **40**(4):763-774.
- Grunwald IC, Korte M, Adelmann G, Plueck A, Kullander K, Adams RH, Frotscher M, Bonhoeffer T and Klein R (2004) Hippocampal plasticity requires postsynaptic ephrins. *Nat Neurosci* **7**(1):33-40.
- Grunwald IC, Korte M, Wolfer D, Wilkinson GA, Unsicker K, Lipp HP, Bonhoeffer T and Klein R (2001) Kinase-independent requirement of EphB2 receptors in hippocampal synaptic plasticity. *Neuron* **32**(6):1027-1040.
- Grutzendler J, Kasthuri N and Gan WB (2002) Long-term dendritic spine stability in the adult cortex. *Nature* **420**(6917):812-816.
- Hanley JG (2008) PICK1: a multi-talented modulator of AMPA receptor trafficking. *Pharmacol Ther* **118**(1):152-160.
- Hanley JG and Henley JM (2005) PICK1 is a calcium-sensor for NMDA-induced AMPA receptor trafficking. *Embo J* **24**(18):3266-3278.
- Hanley JG, Khatri L, Hanson PI and Ziff EB (2002) NSF ATPase and alpha-/beta-SNAPs disassemble the AMPA receptor-PICK1 complex. *Neuron* **34**(1):53-67.
- Harms KJ and Dunaevsky A (2007) Dendritic spine plasticity: looking beyond development. *Brain Res* **1184**:65-71.
- Hattori M, Osterfield M and Flanagan JG (2000) Regulated cleavage of a contact-mediated axon repellent. *Science* **289**(5483):1360-1365.
- Hayashi Y, Shi SH, Esteban JA, Piccini A, Poncer JC and Malinow R (2000) Driving AMPA receptors into synapses by LTP and CaMKII: requirement for GluR1 and PDZ domain interaction. *Science* **287**(5461):2262-2267.
- Henkemeyer M, Itkis OS, Ngo M, Hickmott PW and Ethell IM (2003) Multiple EphB receptor tyrosine kinases shape dendritic spines in the hippocampus. *J Cell Biol* **163**(6):1313-1326.
- Heynen AJ, Quinlan EM, Bae DC and Bear MF (2000) Bidirectional, activity-dependent regulation of glutamate receptors in the adult hippocampus in vivo. *Neuron* **28**(2):527-536.
- Himanen JP and Nikolov DB (2002) Purification, crystallization and preliminary characterization of an Eph-B2/ephrin-B2 complex. *Acta Crystallogr D Biol Crystallogr* **58**(Pt 3):533-535.
- Himanen JP and Nikolov DB (2003) Eph signaling: a structural view. *Trends Neurosci* **26**(1):46-51.
- Himanen JP, Rajashankar KR, Lackmann M, Cowan CA, Henkemeyer M and Nikolov DB (2001) Crystal structure of an Eph receptor-ephrin complex. *Nature* **414**(6866):933-938.
- Himanen JP, Saha N and Nikolov DB (2007) Cell-cell signaling via Eph receptors and ephrins. *Curr Opin Cell Biol* **19**(5):534-542.
- Hirai H, Maru Y, Hagiwara K, Nishida J and Takaku F (1987) A novel putative tyrosine kinase receptor encoded by the eph gene. *Science* **238**(4834):1717-1720.
- Hollmann M, Hartley M and Heinemann S (1991) Ca<sup>2+</sup> permeability of KA-AMPA-gated glutamate receptor channels depends on subunit composition. *Science* **252**(5007):851-853.

- Holtmaat A, Wilbrecht L, Knott GW, Welker E and Svoboda K (2006) Experience-dependent and cell-type-specific spine growth in the neocortex. *Nature* **441**(7096):979-983.
- Hoogenraad CC, Milstein AD, Ethell IM, Henkemeyer M and Sheng M (2005) GRIP1 controls dendrite morphogenesis by regulating EphB receptor trafficking. *Nat Neurosci* **8**(7):906-915.
- Hornberger MR, Dutting D, Ciossek T, Yamada T, Handwerker C, Lang S, Weth F, Huf J, Wessel R, Logan C, Tanaka H and Drescher U (1999) Modulation of EphA receptor function by coexpressed ephrinA ligands on retinal ganglion cell axons. *Neuron* **22**(4):731-742.
- Huai J and Drescher U (2001) An ephrin-A-dependent signaling pathway controls integrin function and is linked to the tyrosine phosphorylation of a 120-kDa protein. *J Biol Chem* **276**(9):6689-6694.
- Hung AY and Sheng M (2002) PDZ domains: structural modules for protein complex assembly. *J Biol Chem* **277**(8):5699-5702.
- Irie F and Yamaguchi Y (2002) EphB receptors regulate dendritic spine development via intersectin, Cdc42 and N-WASP. *Nat Neurosci* **5**(11):1117-1118.
- Janes PW, Saha N, Barton WA, Kolev MV, Wimmer-Kleikamp SH, Nievergall E, Blobel CP, Himanen JP, Lackmann M and Nikolov DB (2005) Adam meets Eph: an ADAM substrate recognition module acts as a molecular switch for ephrin cleavage in trans. *Cell* **123**(2):291-304.
- Kalo MS, Yu HH and Pasquale EB (2001) In vivo tyrosine phosphorylation sites of activated ephrin-B1 and ephB2 from neural tissue. *J Biol Chem* **276**(42):38940-38948.
- Kayser MS, McClelland AC, Hughes EG and Dalva MB (2006) Intracellular and trans-synaptic regulation of glutamatergic synaptogenesis by EphB receptors. *J Neurosci* **26**(47):12152-12164.
- Kayser MS, Nolt MJ and Dalva MB (2008) EphB receptors couple dendritic filopodia motility to synapse formation. *Neuron* **59**(1):56-69.
- Kim CH, Chung HJ, Lee HK and Haganir RL (2001) Interaction of the AMPA receptor subunit GluR2/3 with PDZ domains regulates hippocampal long-term depression. *Proc Natl Acad Sci U S A* **98**(20):11725-11730.
- Kim E and Sheng M (2004) PDZ domain proteins of synapses. *Nat Rev Neurosci* **5**(10):771-781.
- Kleim JA, Barbay S and Nudo RJ (1998) Functional reorganization of the rat motor cortex following motor skill learning. *J Neurophysiol* **80**(6):3321-3325.
- Klein R (2004) Eph/ephrin signaling in morphogenesis, neural development and plasticity. *Curr Opin Cell Biol* **16**(5):580-589.
- Knott GW, Holtmaat A, Wilbrecht L, Welker E and Svoboda K (2006) Spine growth precedes synapse formation in the adult neocortex in vivo. *Nat Neurosci* **9**(9):1117-1124.
- Knott GW, Quairiaux C, Genoud C and Welker E (2002) Formation of dendritic spines with GABAergic synapses induced by whisker stimulation in adult mice. *Neuron* **34**(2):265-273.
- Kullander K and Klein R (2002) Mechanisms and functions of Eph and ephrin signalling. *Nat Rev Mol Cell Biol* **3**(7):475-486.
- Labrador JP, Brambilla R and Klein R (1997) The N-terminal globular domain of Eph receptors is sufficient for ligand binding and receptor signaling. *EMBO J* **16**(13):3889-3897.
- Lauterbach J and Klein R (2006) Release of full-length EphB2 receptors from hippocampal neurons to cocultured glial cells. *J Neurosci* **26**(45):11575-11581.

- Lee SH, Liu L, Wang YT and Sheng M (2002) Clathrin adaptor AP2 and NSF interact with overlapping sites of GluR2 and play distinct roles in AMPA receptor trafficking and hippocampal LTD. *Neuron* **36**(4):661-674.
- Leonard AS, Davare MA, Horne MC, Garner CC and Hell JW (1998) SAP97 is associated with the alpha-amino-3-hydroxy-5-methylisoxazole-4-propionic acid receptor GluR1 subunit. *J Biol Chem* **273**(31):19518-19524.
- Lerma J (2006) Kainate receptor physiology. *Curr Opin Pharmacol* **6**(1):89-97.
- Lim YS, McLaughlin T, Sung TC, Santiago A, Lee KF and O'Leary DD (2008) p75(NTR) mediates ephrin-A reverse signaling required for axon repulsion and mapping. *Neuron* **59**(5):746-758.
- Lin D, Gish GD, Songyang Z and Pawson T (1999) The carboxyl terminus of B class ephrins constitutes a PDZ domain binding motif. *J Biol Chem* **274**(6):3726-3733.
- Lin JW, Ju W, Foster K, Lee SH, Ahmadian G, Wyszynski M, Wang YT and Sheng M (2000) Distinct molecular mechanisms and divergent endocytotic pathways of AMPA receptor internalization. *Nat Neurosci* **3**(12):1282-1290.
- Lippman J and Dunaevsky A (2005) Dendritic spine morphogenesis and plasticity. *J Neurobiol* **64**(1):47-57.
- Lu Q, Sun EE, Klein RS and Flanagan JG (2001a) Ephrin-B reverse signaling is mediated by a novel PDZ-RGS protein and selectively inhibits G protein-coupled chemoattraction. *Cell* **105**(1):69-79.
- Lu W, Man H, Ju W, Trimble WS, MacDonald JF and Wang YT (2001b) Activation of synaptic NMDA receptors induces membrane insertion of new AMPA receptors and LTP in cultured hippocampal neurons. *Neuron* **29**(1):243-254.
- Lucic V, Yang T, Schweikert G, Forster F and Baumeister W (2005) Morphological characterization of molecular complexes present in the synaptic cleft. *Structure* **13**(3):423-434.
- Luo L (2000) Rho GTPases in neuronal morphogenesis. *Nat Rev Neurosci* **1**(3):173-180.
- Maciver MB (2005) <http://www.stanford.edu/group/maciverlab/hippocampal.html>.
- Maekawa K, Imagawa N, Naito A, Harada S, Yoshie O and Takagi S (1999) Association of protein-tyrosine phosphatase PTP-BAS with the transcription-factor-inhibitory protein IkappaBalpha through interaction between the PDZ1 domain and ankyrin repeats. *Biochem J* **337** ( Pt 2):179-184.
- Majewska AK, Newton JR and Sur M (2006) Remodeling of synaptic structure in sensory cortical areas in vivo. *J Neurosci* **26**(11):3021-3029.
- Malenka RC (1994) Synaptic plasticity in the hippocampus: LTP and LTD. *Cell* **78**(4):535-538.
- Malinow R, Mainen ZF and Hayashi Y (2000) LTP mechanisms: from silence to four-lane traffic. *Curr Opin Neurobiol* **10**(3):352-357.
- Man HY, Lin JW, Ju WH, Ahmadian G, Liu L, Becker LE, Sheng M and Wang YT (2000) Regulation of AMPA receptor-mediated synaptic transmission by clathrin-dependent receptor internalization. *Neuron* **25**(3):649-662.
- Marquardt T, Shirasaki R, Ghosh S, Andrews SE, Carter N, Hunter T and Pfaff SL (2005) Coexpressed EphA receptors and ephrin-A ligands mediate opposing actions on growth cone navigation from distinct membrane domains. *Cell* **121**(1):127-139.
- Marston DJ, Dickinson S and Nobes CD (2003) Rac-dependent trans-endocytosis of ephrinBs regulates Eph-ephrin contact repulsion. *Nat Cell Biol* **5**(10):879-888.
- Matsuda S, Mikawa S and Hirai H (1999) Phosphorylation of serine-880 in GluR2 by protein kinase C prevents its C terminus from binding with glutamate receptor-interacting protein. *J Neurochem* **73**(4):1765-1768.

- Monyer H, Burnashev N, Laurie DJ, Sakmann B and Seeburg PH (1994) Developmental and regional expression in the rat brain and functional properties of four NMDA receptors. *Neuron* **12**(3):529-540.
- Moser MB, Trommald M and Andersen P (1994) An increase in dendritic spine density on hippocampal CA1 pyramidal cells following spatial learning in adult rats suggests the formation of new synapses. *Proc Natl Acad Sci U S A* **91**(26):12673-12675.
- Murai KK and Pasquale EB (2003) 'Eph'ective signaling: forward, reverse and crosstalk. *J Cell Sci* **116**(Pt 14):2823-2832.
- Murai KK and Pasquale EB (2005) New exchanges in eph-dependent growth cone dynamics. *Neuron* **46**(2):161-163.
- Nakanishi S (1992) Molecular diversity of glutamate receptors and implications for brain function. *Science* **258**(5082):597-603.
- Nestor MW, Mok LP, Tulapurkar ME and Thompson SM (2007) Plasticity of neuron-glia interactions mediated by astrocytic EphARs. *J Neurosci* **27**(47):12817-12828.
- Niethammer M, Valtschanoff JG, Kapoor TM, Allison DW, Weinberg RJ, Craig AM and Sheng M (1998) CRIPT, a novel postsynaptic protein that binds to the third PDZ domain of PSD-95/SAP90. *Neuron* **20**(4):693-707.
- Nishimune A, Isaac JT, Molnar E, Noel J, Nash SR, Tagaya M, Collingridge GL, Nakanishi S and Henley JM (1998) NSF binding to GluR2 regulates synaptic transmission. *Neuron* **21**(1):87-97.
- Nobes CD and Hall A (1995) Rho, rac, and cdc42 GTPases regulate the assembly of multimolecular focal complexes associated with actin stress fibers, lamellipodia, and filopodia. *Cell* **81**(1):53-62.
- Osten P, Khatri L, Perez JL, Kohr G, Giese G, Daly C, Schulz TW, Wensky A, Lee LM and Ziff EB (2000) Mutagenesis reveals a role for ABP/GRIP binding to GluR2 in synaptic surface accumulation of the AMPA receptor. *Neuron* **27**(2):313-325.
- Palmer A and Klein R (2003) Multiple roles of ephrins in morphogenesis, neuronal networking, and brain function. *Genes Dev* **17**(12):1429-1450.
- Palmer A, Zimmer M, Erdmann KS, Eulenburg V, Porthin A, Heumann R, Deutsch U and Klein R (2002) EphrinB phosphorylation and reverse signaling: regulation by Src kinases and PTP-BL phosphatase. *Mol Cell* **9**(4):725-737.
- Parnass Z, Tashiro A and Yuste R (2000) Analysis of spine morphological plasticity in developing hippocampal pyramidal neurons. *Hippocampus* **10**(5):561-568.
- Penzes P, Beeser A, Chernoff J, Schiller MR, Eipper BA, Mains RE and Haganir RL (2003) Rapid induction of dendritic spine morphogenesis by trans-synaptic ephrinB-EphB receptor activation of the Rho-GEF kalirin. *Neuron* **37**(2):263-274.
- Peter BJ, Kent HM, Mills IG, Vallis Y, Butler PJ, Evans PR and McMahon HT (2004) BAR domains as sensors of membrane curvature: the amphiphysin BAR structure. *Science* **303**(5657):495-499.
- Pickard L, Noel J, Duckworth JK, Fitzjohn SM, Henley JM, Collingridge GL and Molnar E (2001) Transient synaptic activation of NMDA receptors leads to the insertion of native AMPA receptors at hippocampal neuronal plasma membranes. *Neuropharmacology* **41**(6):700-713.
- Plant K, Pelkey KA, Bortolotto ZA, Morita D, Terashima A, McBain CJ, Collingridge GL and Isaac JT (2006) Transient incorporation of native GluR2-lacking AMPA receptors during hippocampal long-term potentiation. *Nat Neurosci* **9**(5):602-604.
- Poliakov A, Cotrina M and Wilkinson DG (2004) Diverse roles of eph receptors and ephrins in the regulation of cell migration and tissue assembly. *Dev Cell* **7**(4):465-480.

- Premont RT, Claing A, Vitale N, Freeman JL, Pitcher JA, Patton WA, Moss J, Vaughan M and Lefkowitz RJ (1998) beta2-Adrenergic receptor regulation by GIT1, a G protein-coupled receptor kinase-associated ADP ribosylation factor GTPase-activating protein. *Proc Natl Acad Sci U S A* **95**(24):14082-14087.
- Rodenas-Ruano A, Perez-Pinzon MA, Green EJ, Henkemeyer M and Liebl DJ (2006) Distinct roles for ephrinB3 in the formation and function of hippocampal synapses. *Dev Biol* **292**(1):34-45.
- Rouach N, Byrd K, Petralia RS, Elias GM, Adesnik H, Tomita S, Karimzadegan S, Kealey C, Brecht DS and Nicoll RA (2005) TARP gamma-8 controls hippocampal AMPA receptor number, distribution and synaptic plasticity. *Nat Neurosci* **8**(11):1525-1533.
- Sans N, Racca C, Petralia RS, Wang YX, McCallum J and Wenthold RJ (2001) Synapse-associated protein 97 selectively associates with a subset of AMPA receptors early in their biosynthetic pathway. *J Neurosci* **21**(19):7506-7516.
- Schulz TW, Nakagawa T, Licznarski P, Pawlak V, Kollekter A, Rozov A, Kim J, Dittgen T, Kohr G, Sheng M, Seeburg PH and Osten P (2004) Actin/alpha-actinin-dependent transport of AMPA receptors in dendritic spines: role of the PDZ-LIM protein RIL. *J Neurosci* **24**(39):8584-8594.
- Segura I, Essmann CL, Weinges S and Acker-Palmer A (2007) Grb4 and GIT1 transduce ephrinB reverse signals modulating spine morphogenesis and synapse formation. *Nat Neurosci* **10**(3):301-310.
- Shamah SM, Lin MZ, Goldberg JL, Estrach S, Sahin M, Hu L, Bazalakova M, Neve RL, Corfas G, Debant A and Greenberg ME (2001) EphA receptors regulate growth cone dynamics through the novel guanine nucleotide exchange factor ephexin. *Cell* **105**(2):233-244.
- Shen L, Liang F, Walensky LD and Huganir RL (2000) Regulation of AMPA receptor GluR1 subunit surface expression by a 4. 1N-linked actin cytoskeletal association. *J Neurosci* **20**(21):7932-7940.
- Shepherd JD and Huganir RL (2007) The cell biology of synaptic plasticity: AMPA receptor trafficking. *Annu Rev Cell Dev Biol* **23**:613-643.
- Shi S, Hayashi Y, Esteban JA and Malinow R (2001) Subunit-specific rules governing AMPA receptor trafficking to synapses in hippocampal pyramidal neurons. *Cell* **105**(3):331-343.
- Smith FM, Vearing C, Lackmann M, Treutlein H, Himanen J, Chen K, Saul A, Nikolov D and Boyd AW (2004) Dissecting the EphA3/Ephrin-A5 interactions using a novel functional mutagenesis screen. *J Biol Chem* **279**(10):9522-9531.
- Sommer B, Keinänen K, Verdoorn TA, Wisden W, Burnashev N, Herb A, Kohler M, Takagi T, Sakmann B and Seeburg PH (1990) Flip and flop: a cell-specific functional switch in glutamate-operated channels of the CNS. *Science* **249**(4976):1580-1585.
- Sommer B, Kohler M, Sprengel R and Seeburg PH (1991) RNA editing in brain controls a determinant of ion flow in glutamate-gated channels. *Cell* **67**(1):11-19.
- Songyang Z, Fanning AS, Fu C, Xu J, Marfatia SM, Chishti AH, Crompton A, Chan AC, Anderson JM and Cantley LC (1997) Recognition of unique carboxyl-terminal motifs by distinct PDZ domains. *Science* **275**(5296):73-77.
- Steiner P, Alberi S, Kulangara K, Yersin A, Sarria JC, Regulier E, Kasas S, Dietler G, Muller D, Catsicas S and Hirling H (2005) Interactions between NEEP21, GRIP1 and GluR2 regulate sorting and recycling of the glutamate receptor subunit GluR2. *Embo J* **24**(16):2873-2884.
- Takamiya K, Kostourou V, Adams S, Jadeja S, Chalepakis G, Scambler PJ, Huganir RL and Adams RH (2004) A direct functional link between the multi-PDZ domain protein GRIP1 and the Fraser syndrome protein Fras1. *Nat Genet* **36**(2):172-177.

- Takasu MA, Dalva MB, Zigmond RE and Greenberg ME (2002) Modulation of NMDA receptor-dependent calcium influx and gene expression through EphB receptors. *Science* **295**(5554):491-495.
- Tanaka M, Ohashi R, Nakamura R, Shinmura K, Kamo T, Sakai R and Sugimura H (2004) Tiam1 mediates neurite outgrowth induced by ephrin-B1 and EphA2. *EMBO J* **23**(5):1075-1088.
- Thomas CG, Miller AJ and Westbrook GL (2006) Synaptic and extrasynaptic NMDA receptor NR2 subunits in cultured hippocampal neurons. *J Neurophysiol* **95**(3):1727-1734.
- Tomita S, Adesnik H, Sekiguchi M, Zhang W, Wada K, Howe JR, Nicoll RA and Brecht DS (2005) Stargazin modulates AMPA receptor gating and trafficking by distinct domains. *Nature* **435**(7045):1052-1058.
- Tomita S, Chen L, Kawasaki Y, Petralia RS, Wenthold RJ, Nicoll RA and Brecht DS (2003) Functional studies and distribution define a family of transmembrane AMPA receptor regulatory proteins. *J Cell Biol* **161**(4):805-816.
- Torres R, Firestein BL, Dong H, Staudinger J, Olson EN, Haganir RL, Brecht DS, Gale NW and Yancopoulos GD (1998) PDZ proteins bind, cluster, and synaptically colocalize with Eph receptors and their ephrin ligands. *Neuron* **21**(6):1453-1463.
- Trachtenberg JT, Chen BE, Knott GW, Feng G, Sanes JR, Welker E and Svoboda K (2002) Long-term in vivo imaging of experience-dependent synaptic plasticity in adult cortex. *Nature* **420**(6917):788-794.
- Triller A and Choquet D (2005) Surface trafficking of receptors between synaptic and extrasynaptic membranes: and yet they do move! *Trends Neurosci* **28**(3):133-139.
- Tsay D and Yuste R (2004) On the electrical function of dendritic spines. *Trends Neurosci* **27**(2):77-83.
- van Ham M and Hendriks W (2003) PDZ domains-glue and guide. *Mol Biol Rep* **30**(2):69-82.
- Verhage M, Maia AS, Plomp JJ, Brussaard AB, Heeroma JH, Vermeer H, Toonen RF, Hammer RE, van den Berg TK, Missler M, Geuze HJ and Sudhof TC (2000) Synaptic assembly of the brain in the absence of neurotransmitter secretion. *Science* **287**(5454):864-869.
- Vernadakis A (1996) Glia-neuron intercommunications and synaptic plasticity. *Prog Neurobiol* **49**(3):185-214.
- Wahl S, Barth H, Ciossek T, Aktories K and Mueller BK (2000) Ephrin-A5 induces collapse of growth cones by activating Rho and Rho kinase. *J Cell Biol* **149**(2):263-270.
- Wallace W and Bear MF (2004) A morphological correlate of synaptic scaling in visual cortex. *J Neurosci* **24**(31):6928-6938.
- Wang HU, Chen ZF and Anderson DJ (1998) Molecular distinction and angiogenic interaction between embryonic arteries and veins revealed by ephrin-B2 and its receptor Eph-B4. *Cell* **93**(5):741-753.
- Wang X, Roy PJ, Holland SJ, Zhang LW, Culotti JG and Pawson T (1999) Multiple ephrins control cell organization in *C. elegans* using kinase-dependent and -independent functions of the VAB-1 Eph receptor. *Mol Cell* **4**(6):903-913.
- Weinges S (2006) Molecular dissection of ephrinB reverse signaling. *Dissertation*.
- Wenthold RJ, Petralia RS, Blahos J, II and Niedzielski AS (1996) Evidence for multiple AMPA receptor complexes in hippocampal CA1/CA2 neurons. *J Neurosci* **16**(6):1982-1989.
- Wiesner S, Wybenga-Groot LE, Warner N, Lin H, Pawson T, Forman-Kay JD and Sicheri F (2006) A change in conformational dynamics underlies the activation of Eph receptor tyrosine kinases. *EMBO J* **25**(19):4686-4696.
- Wybenga-Groot LE, Baskin B, Ong SH, Tong J, Pawson T and Sicheri F (2001) Structural basis for autoinhibition of the EphB2 receptor tyrosine kinase by the unphosphorylated juxtamembrane region. *Cell* **106**(6):745-757.

- Wyszynski M, Kim E, Dunah AW, Passafaro M, Valtschanoff JG, Serra-Pages C, Streuli M, Weinberg RJ and Sheng M (2002) Interaction between GRIP and liprin-alpha/SYD2 is required for AMPA receptor targeting. *Neuron* **34**(1):39-52.
- Xia H, Winokur ST, Kuo WL, Altherr MR and Brecht DS (1997) Actinin-associated LIM protein: identification of a domain interaction between PDZ and spectrin-like repeat motifs. *J Cell Biol* **139**(2):507-515.
- Xia J, Zhang X, Staudinger J and Huganir RL (1999) Clustering of AMPA receptors by the synaptic PDZ domain-containing protein PICK1. *Neuron* **22**(1):179-187.
- Ye B, Liao D, Zhang X, Zhang P, Dong H and Huganir RL (2000) GRASP-1: a neuronal RasGEF associated with the AMPA receptor/GRIP complex. *Neuron* **26**(3):603-617.
- Yin Y, Yamashita Y, Noda H, Okafuji T, Go MJ and Tanaka H (2004) EphA receptor tyrosine kinases interact with co-expressed ephrin-A ligands in cis. *Neurosci Res* **48**(3):285-296.
- Yuste R and Bonhoeffer T (2001) Morphological changes in dendritic spines associated with long-term synaptic plasticity. *Annu Rev Neurosci* **24**:1071-1089.
- Zamanillo D, Sprengel R, Hvalby O, Jensen V, Burnashev N, Rozov A, Kaiser KM, Koster HJ, Borchardt T, Worley P, Lubke J, Frotscher M, Kelly PH, Sommer B, Andersen P, Seeburg PH and Sakmann B (1999) Importance of AMPA receptors for hippocampal synaptic plasticity but not for spatial learning. *Science* **284**(5421):1805-1811.
- Zhang H, Webb DJ, Asmussen H and Horwitz AF (2003) Synapse formation is regulated by the signaling adaptor GIT1. *J Cell Biol* **161**(1):131-142.
- Zhang H, Webb DJ, Asmussen H, Niu S and Horwitz AF (2005) A GIT1/PIX/Rac/PAK signaling module regulates spine morphogenesis and synapse formation through MLC. *J Neurosci* **25**(13):3379-3388.
- Zhu JJ, Esteban JA, Hayashi Y and Malinow R (2000) Postnatal synaptic potentiation: delivery of GluR4-containing AMPA receptors by spontaneous activity. *Nat Neurosci* **3**(11):1098-1106.
- Ziff EB (2007) TARPS and the AMPA receptor trafficking paradox. *Neuron* **53**:627-633.
- Zimmer M, Palmer A, Kohler J and Klein R (2003) EphB-ephrinB bi-directional endocytosis terminates adhesion allowing contact mediated repulsion. *Nat Cell Biol* **5**(10):869-878.
- Ziv NE and Smith SJ (1996) Evidence for a role of dendritic filopodia in synaptogenesis and spine formation. *Neuron* **17**(1):91-102.
- Zuo Y, Lin A, Chang P and Gan WB (2005) Development of long-term dendritic spine stability in diverse regions of cerebral cortex. *Neuron* **46**(2):181-189.